

DEPOSITIONAL ENVIRONMENT, MINERALOGY, AND SEQUENCE
STRATIGRAPHY OF THE LATE DEVONIAN SANISH MEMBER
(UPPER THREE FORKS FORMATION), WILLISTON BASIN,
NORTH DAKOTA

by

Brian Berwick

Copyright by Brian Berwick

All Rights Reserved

ABSTRACT

Sixteen Late Devonian Upper Three Forks and Lower Bakken Shale cores were described in a selected area in North Dakota. Five lithofacies were identified in the Upper Three Forks and one lithofacies in the Lower Bakken Shale. Beds in the upper part of the Upper Three Forks Formation were informally named the Sanish member.

Locally, the base of the Upper Three Forks is red shale and siltstone that were deposited in continental sabkha environments (Facies A). In the study area, Facies B is commonly at the base of the Upper Three Forks and is dolomitic shale with rip up clasts created by very shallow marine reworking. The Sanish member consists of three facies. Facies C is highly deformed and brecciated silty dolomite that was deposited in tidal mud flat and sabkha environments. Facies D is silty dolomite, dolomitic siltstone, and shale that was deposited in tidal flat and sabkha environments. Locally, Facies E caps the Sanish member and is burrowed dolomitic and silty shale. Deposition was in shallow subtidal environments. The Lower Bakken shale unconformably caps the Sanish member and is black, organic-rich shale that was deposited in a water-stratified marine basin.

X-ray diffraction, scanning electron microscopy, and thin-sections analyses were performed on representative samples from all facies. In order of abundance, Sanish detrital mineralogy consists of quartz, potassium feldspar, illite, dolomite, muscovite, and biotite. Authigenic minerals include potassium feldspar, dolomite, chlorite, quartz, biotite, calcite, and pyrite. The clay-sized fraction contains potassium feldspar, dolomite, illite, and chlorite. The Sanish member has fair to poor porosity, and bedding plane and cross-cutting microfractures enhanced permeability.

Bathymetric shifts occurred during late Devonian and Early Mississippian time creating flooding at the base of the Upper Three Forks, periodic exposure of Facies C and D of the Sanish, local flooding at the top of the Sanish (Facies E), and finally transgression of the Lower Bakken Sea across the Sanish member.

Construction of a cross-section in the study area indicates that the top of Facies D and Facies E is at an angular unconformity. The top of the Sanish member was subaerially exposed and this surface was inundated by the Lower Bakken Sea. The

unconformity and transgression clearly separated the Three Forks and Sanish depositional systems from the Lower Bakken system.

TABLE OF CONTENTS

ABSTRACT	iii
LIST OF FIGURES	ix
LIST OF TABLES	xv
ACKNOWLEDGEMENT.	xvi
CHAPTER 1 INTRODUCTION	1
1.1 Purpose and Scope	1
1.2 Location of Study Area	4
1.3 Research Objective	4
1.4 Research Contributions	4
1.5 Data and Methods.....	5
CHAPTER 2 GEOLOGICAL SETTING	7
2.1 Early Basin History	7
2.2 Devonian Basin History	10
2.3 Late Devonian Sanish Member	10
2.4 Petroleum Geology	11
2.5 Previous Work	17
CHAPTER 3 CORE DESCRIPTIONS AND DEFINITION OF FACIES.....	18
3.1 Methods	18
3.2 Core Descriptions	19
3.3 Facies Descriptions	19
3.3.1 Facies A – Dolomitic and Slightly Silty Shale.....	22
3.3.2 Facies B – Calcareous and Very Slightly Silty Dolomite.....	22

3.3.3	Facies C – Highly Deformed and Brecciated Silty Dolomite.....	22
3.3.4	Facies D – Silty Dolomite and Shale.....	22
3.3.5	Facies E – Burrowed and Slightly Silty Dolomite.....	27
3.3.6	Facies LBS – Dark Black Shale	27
3.4	Facies Occurrences in Core Samples.....	37
3.5	Single and Additional Diagnostic Criteria.....	38
3.6	Facies Associations	38
3.7	Lithological Chart and Facies Related to Open-Hole Logs	41
3.8	Interpretation of Depositional Environments	47
3.8.1	Facies A	47
3.8.2	Facies B	47
3.8.3	Facies C	50
3.8.4	Facies D	58
3.8.5	Facies E	59
3.8.6	Facies LBS	59
3.9	Summary of the Depositional Environment Interpretation.....	59
CHAPTER 4 FACIES MINERALOGY.....		61
4.1	Introduction	61
4.2	X-Ray Diffraction (XRD) Methods.....	61
4.3	X-Ray Diffraction (XRD) Results.....	62
4.4	Scanning Electron Microscopy with Energy Dispersive X-Ray Spectroscopy (SEM-EDS) Methods.....	62

4.5	Scanning Electron Microscopy with Energy Dispersive X-Ray Spectroscopy (SEM-EDS) Results.....	62
4.6	Thin Section Methods	62
4.7	Thin Section Descriptions	65
4.7.1	Facies: A	65
4.7.2	Facies: B	65
4.7.3	Facies: C	66
4.7.4	Facies: D	66
4.7.5	Facies: E	67
4.7.6	Facies: LBS	67
4.8	Comparison of XRD, SEM-EDS and Thin Section Results	68
4.8.1	Illite Problem	68
4.8.2	Kaolinite Problem	68
4.9	Interpretation of the Mineralogical Results	68
4.9.1	Sheet Silicate Minerals – Biotite and Muscovite	69
4.9.2	Silicate Minerals with Framework Structures – Feldspar.....	69
4.9.3	Smectite/Illite – Smectite Illitization	70
4.9.4	Sheet Silicate Mineral – Chlorite	70
4.9.5	Quartz	72
4.9.6	Dolomite	73
4.9.7	Pyrite	74
4.10	Provenance.....	74

CHAPTER 5	SIGNIFICANT SURFACES AND SEQUENCE STRATIGRAPHY OF THE UPPER THREE FORKS FORMATION (SANISH MEMBER).....	75
5.1	Methods	75
5.2	Previous Sequence Stratigraphic Interpretation	75
5.3	Significant Surfaces	77
5.4	Depositional Systems	80
5.5	Sequence Stratigraphy of the Sanish Member and Associated Facies ...	80
5.6	Stratigraphic Placement of the Sanish Member	88
CHAPTER 6	CONCLUSIONS AND RECOMMENDATIONS.....	95
6.1	Conclusions.....	95
6.1.1	Core Lithofacies.....	95
6.1.2	Mineralogy.....	96
6.1.3	Depositional Environments.....	97
6.1.4	Sequence Stratigraphy.....	97
6.2	Recommendations for Further Study.....	98
REFERENCES CITED	100
LIST OF APPENDICES	104
APPENDIX A	105
APPENDIX B	158
APPENDIX C	199
APPENDIX D	248
APPENDIX E	262
CD/DVD	Pocket

LIST OF FIGURES

- Figure 1.1. Study area outline and extent of the Bakken Formation in the United States portion of the Williston Basin. The study area includes the following North Dakota counties: Divide, McKenzie, Mountrail, and Williams. Modified from Pitman et al. (2001).....2
- Figure 1.2. Stratigraphic chart of the Williston basin. Sequences are from Sloss (1963). Modified from <http://en.wikipedia.org/wiki/Image:WillistonStratCol.jpg>.....3
- Figure 1.3. Subsurface core location map. Appendix E contains the core listing. Modified from Pitman et al. (2001).....6
- Figure 2.1. Structural features in the U. S. Williston Basin. The major structural boundaries that surround the Williston basin are highlighted in red. Modified from Gerhard et al. (1990).....8
- Figure 2.2. Sloss's (1963) sequences are shown on this stratigraphic column of the U.S. Williston Basin. The Bakken and Three Forks formations are shaded in red. Oil and gas symbols represent major reservoirs. Blue outline represents carbonate deposition. Red outline represents clastic deposition. Green bars represent source rocks (see text for the identification of source rocks), and Roman numerals represent the three types of source rocks. Modified from Gerhard et al. (1990). Note the Birdbear Formation is also known as the Nisku Formation.9
- Figure 2.3. Late Devonian reconstruction map displaying the continuous connection between the Alberta and Williston basin. Modified from Smith et al. (1995).....12
- Figure 2.4. Paleogeographic map of the Late Devonian (360Ma). Subduction zones and associated orogenic belts (dashed red) surround and separated the North American craton from the Devonian ocean. The North American craton was open to the southwest (yellow arrow). The Williston Basin and the Alberta Basin were connected at that time (W-A). Modified from <http://jan.ucc.nau.edu/rcb7-namD360.jpg>.....13
- Figure 2.5. Paleogeographic map of the Early Mississippian (345Ma). The Alberta Basin (AB) and the Williston (WB) Basin were separated by the Sweetgrass Arch (SA). The Williston Basin was shielded from the Devonian ocean by orogenic belts that surrounded the North American craton and the Transcontinental Arch to the southeast (TA). Modified from <http://jan.ucc.nau.edu/rcb7-namM345.jpg>...14

Figure 2.6. Isopach map of the Upper Kaskaskia sequence (Bakken through the Otter formations). Uplift of the Sweetgrass Arch (SA) to the west and northwest closed the Williston Basin from the Alberta Basin. A regional unconformity developed at the base of the Kibbey Formation, and this map shows preserved Upper Kaskaskia strata (Figure 1.2; 2.2). Thinning is evident over the Nesson Anticline (NA). Classic intracratonic sag is evident (250' contours).15

Figure 2.7. Comparison of the sequence stratigraphy of the Exshaw-Bakken Formation between the Foreland Basin of Canada and the Williston Basin of the United States. From Smith et al.(2000).....16

Figure 3.1. General stratigraphic column for individual facies derived from 15 of the 16 core descriptions for the Upper Three Forks and Lower Bakken Shale. Thickness of each facies varies throughout the study area. The Upper Three Forks Formation includes facies B. Facies C, D and E are included in the Sanish. Facies E only occurred in core #9. The Lower Bakken Shale is labeled LBS.20

Figure 3.2. Stratigraphic column for facies in core #2. Upper Three Forks Formation facies are labeled A and D. Facies D is included in the Sanish. The Lower Bakken Facies is label LBS.....21

Figure 3.3. Facies A. Core #2. 10,701 feet. Facies A consists of moderate red (5 R 4/6) to pale red (5 R 6/2) dolomitic shale with white dolomite clasts.....23

Figure 3.4. Facies B. Core #3. 10,051.1 feet. Facies B is a dark greenish-gray (5 GY 4/1) to medium dark gray (N4) dolomite with rip-up clasts.....24

Figure 3.5. Facies C. Core #1. 10,333 feet. Facies C is dominated by soft-sediment deformation and brecciation. Facies Q is a light green (5 G 8/1) to greenish-gray (5 G 6/1) shale mixed with light gray silty dolomite (N8).25

Figure 3.6. Facies D. Core #2. 10,689.1 feet. Facies D is comprised of 2 lithologies:
1) light green (5 G 8/1) to greenish-gray (5 G 6/1) shale and 2) very light gray,
2) silty dolomite (N8).....26

Figure 3.7. Facies D. Core #7. 10,965 feet. Siltstone grains at the top of this cored interval are coarser than commonly observed for Facies D.28

Figure 3.8. Core #11, 10,981 feet. Sedimentary structures present in Facies D are: parallel-laminations (PL), cross-laminations (CL), soft sediment deformation (SSD), flaser- bedding (FB), and rip-up clasts (RU).....29

Figure 3.9. Facies D. Core #2. 10,315 feet. Soft-sediment deformation (SSD) is common in Facies D. Desiccation cracks, syneresis cracks and exposure surfaces are also identified in this sample.....	30
Figure 3.10. Facies D. Core #5, 11,758 feet. Uni-directional and bi-directional flow (UBDF), parallel laminations (PL), desiccation cracks (DC), soft-sediment deformation (SSD), and brecciation (B) are shown in this sample.....	31
Figure 3.11. Facies D. Core #2. 10,698.8 feet. Brecciation (B) and uni-directional and bi-directional flow (UBDF) are shown in this Sanish sample.....	31
Figure 3.12. Facies D. Core #11. 10,977.5 feet. Mud drapes (MD), type 1 flame structures (FS1), fining upwards cycles (dashed black arrows), desiccation cracks, scour surfaces, exposure surfaces, and uni-directional and bi-directional reactivation surfaces (UBDRS) are all identified in this core sample.....	32
Figure 3.13. Facies D. Core #2. 10,690 feet. Examples of sedimentary structures in Facies D: syneresis cracks (SC), flaser-bedding (FB), herringbone cross-stratification (HB) and type II flame structures (FS2).....	33
Figure 3.14. Facies D. Core #2. 10,695 feet. Examples of syneresis cracks (SC) are shown in this core sample.....	34
Figure 3.15. Facies E. Core #9. 10,757 feet. Extensive burrowing and bioturbation in Facies E.....	35
Figure 3.16. Facies LBS. Core # 12. 10,214 feet. Facies LBS is a grayish black (N2) to dark black (N1) shale, with parallel-laminations, very thin sandstone and calcite stringers, pyrite nodules.....	36
Figure 3.17 Core #1. Core to Log Presentation.....	42
Figure 3.18 Core #5. Core to Log Presentation.....	43
Figure 3.19 Core #11. Core to Log Presentation.....	44
Figure 3.20 Core #12. Core to Log Presentation.....	45
Figure 3.21 Core #14. Core to Log Presentation.....	46
Figure 3.22. An isopach map of the Late Devonian Three Forks Formation shows that most of the cores in this evaluation lie within the thicker portions of the formation. The contour interval is 50 feet. Modified from Pitman et al. (2001)...	48
Figure 3.23. Facies B. Core #16., 8,370.5 to 8735.5 feet. Facies B in northern portion of the study area exhibits large rip-up clasts. Used with the permission of Samson Resources.....	49

Figure 3.24. Core #16. 8,726.5 to 8729.5 feet. Facies C in northern North Dakota. Used with the permission of Samson Resources.....51

Figure 3.25. Supratidal flat environment at Fisherman Bay, Spencer Gulf Australia. Tee-pee structures are created at the surface from the lithified polygonal crusts being thrust up by the episodic groundwater recharge. From Kendall (1992).....52

Figure 3.26. Large, 0.5m, upthrown polygons and tee-pee structures. Devil’s Golf Course, Death Valley, U.S.A. From Kendall (1992).....53

Figure 3.27. Example of desiccation cracks that show buckling effect of polygon edges due to the shriveling of the original microbial (cyanobacteria) mats from prolonged exposure. Hammer is 30 cm long; East Arm Formation, Upper Cambrian, Bonne Bay, western Newfoundland. From Kendall (1992).....54

Figure 3.28. Cyanobacteria (microbial) mats are wrinkled, shriveled, and are 1-2mm long. These are encrusted with gypsum crystals that are later dissolved. Hyeres salt lagoons, Southern France. From Kendall (1992).55

Figure 3.29. Preserved desiccation cracks in a microbial (cyanobacteria) parallel-laminated dolomite. Providence Island Dolomite, Middle Ordovician, Lake Champlain, New York State. From Kendall (1992).56

Figure 3.30. Deposited as a laminated silty dolomite, internal sedimentary structures have been destroyed by the repeated growth and dissolution of evaporites and desiccation. Paradox Formation (Pennsylvanian), Utah. From Kendall (1992)..57

Figure 3.31. Diagram illustrating the typical depositional environments of the Sanish member and associated facies of the Upper Three Forks Formation.....60

Figure 4.1. During the process of smectite illitization, potassium is liberated from K-spar. This “freeing” of potassium from K-spar enables the conversion of smectite to illite. Other free silicates are liberated from k-spar and these aid in the creation of secondary minerals such as chlorite and quartz. From Moore et al.(1997, p. 176).....72

Figure 5.1. Sequence stratigraphic interpretation of the Bakken and Exshaw Formations with associated significant surfaces and interpreted facies in Canada and the United States. From Smith et al. (1995).....76

Figure 5.2. Significant surfaces and associated facies of the Upper Three Forks, Sanish member, and Lower Bakken Shale for 15 of the 16 cores.....78

Figure 5.3. Significant surfaces and associated facies of the of the Upper Three Forks, Sanish member, and Lower Bakken Shale for core # 2 only.....79

Figure 5.4. Isopach map of the Devonian Ashern through Nisku formations (lower Kaskaskia) prior to Three Forks Formation deposition, U. S. Williston Basin. This isopach map shows the continuous thickening to the north into Saskatchewan, Canada. Well spots indicate study cores and assigned numbers. Contour interval is 200 feet.81

Figure 5.5. Isopach map of the Three Forks Formation (including the Sanish member). The basin center shifted from Burke and Mountrail counties, ND, to McKenzie County, ND. Late Devonian thinning between Burke and Mountrail counties, which were previously within the basin center, indicates early separation of the Alberta Basin from the Williston Basin. Well spots are study cores and assigned numbers. Contour interval is 50 feet.....82

Figure 5.6. Shifting depositional centers during the Devonian and Early Mississippian are shown in this map. The shift occurred from north to south across western North Dakota. The blue outline is the Devonian Basin center (Ashern through Nisku formations). The purple outline is the Late Devonian Three Forks Basin center, and the green outline is the Late Devonian and Early Mississippian Bakken Formation Basin center.....84

Figure 5.7. Isopach map of the Lower Bakken Shale. Thinning near the United States and Canadian borders that was present during Three Forks deposition continued during Lower Bakken Shale deposition. C.I.= 10 feet.....85

Figure 5.8. Isopach map of Facies D. Thickness values are from cores interpretations which indicate thinning to the north. The northward thinning is associated with the unconformity at the top of the Sanish member. Contour interval is 5 feet. Note cores 2, 4, 5, 6, 7, 8, 11, 12 and 15 did not penetrate Facies D entirely are not used in the creation of the isopach.....86

Figure 5.9. Core #17 - 8710.5 – 8,711.5. The contact (yellow arrow) between Facies D (top of Sanish member) and facies LBS (Lower Bakken Shale) is shown. Rip-up clasts and lag deposits occur at the contact, and the contact is interpreted to be an unconformity and a marine flooding surface.....87

Figure 5.10. Location map of cross-section A-A'. Cores used in this study are identified by numbers.....89

Figure 5.11. Cross section A-A' showing the erosional unconformity that exists at the top of Facies D and possibly Facies C. This unconformity occurs across the study area. The thickness of Facies D increases toward present day basin-center and is truncated along the basin-edges. Location map for the cross-section is figure 5.11. Note the Three Forks Formation includes both Facies A and B. The Lower 5.12. Bakken Shale is Facies LBS.....90

Figure 5.12. General stratigraphic column for the individual facies derived from 15 of the 16 core descriptions within the study area. This stratigraphic column includes depositional environment and significant surface interpretations. Thickness of each facies varies throughout the study area.....91

Figure 5.13. The stratigraphic column of facies observed in core #2; includes the depositional environment and significant surfaces.....92

Figure 5.14. Sequence stratigraphic placement of the Sanish member with associated facies and significant surfaces.....93

Figure 5.15. Sequence stratigraphic placement of the Sanish member with associated facies and significant surfaces within core #2.....94

LIST OF TABLES

Table 3.5.1. Facies identified in cores. The percentage of each facies relative to all facies is shown at the bottom of each column.....37

Table 3.5.2. Sedimentary structures found in the Upper Three Forks Formation that could occur in several depositional environments.....39

Table 3.5.3. Sedimentary structures found in the Upper Three Forks and Sanish member that are diagnostic for intertidal depositional environments.....40

Table 3.5.4. Facies associations with specific criteria for depositional environments.....41

Table 4.3.1. XRD Data: Lithofacies and corresponding mineral assemblages for the different XRD procedures. Explanation: I – illite, PI – pure illite, Kspar – potassium feldspar, D – dolomite, Qz – quartz, Kao – kaolinite, Chl – chlorite, Ortho – orthoclase, Ca – calcite, Musc – muscovite, Py – pyrite, and (Kao?) – questionable kaolinite. Heating at 550 °C for one hour makes the kaolinite family of minerals amorphous to x-rays.....63

Table 4.5.1. SEM Data: Lithofacies with corresponding detrital grains, authigenic minerals and authigenic clay, and depositional clay. If minerals were not found through SEM/EDS but identified in XRD, they are listed in the identified by XRD category. Explanation: I – illite, PI – pure illite, Kspar – potassium feldspar, D – dolomite, Qz – quartz, Kao – kaolinite, Chl – chlorite, Ortho – orthoclase, Ca – calcite, Musc – muscovite, Bio – biotite, Py – pyrite, O – overgrowths, and GC – grain coating.....64

ACKNOWLEDGEMENTS

First, I would like to thank God for an answer to a prayer. I would like to thank everyone at Samson Resources for their encouragement and making graduate school a reality. I would like to thank both Rich Frommer and Jay Smith for the support and encouragement throughout this process. I would like to thank Greg Anderson for his help, support and encouragement. I would like to thank Ken Tompkins for his mentorship and friendship. Without all of you, none of this would have been possible.

Next, I would like to thank Dr. Piret Plink-Bjorklund at the Colorado School of Mines for the help and guidance on every aspect of my thesis. To Dr. Mike Hendricks, you truly made this thesis what it was meant to be. I thank you for all of your time, mentorship, and friendship. I would like to thank Dr. John Curtis at the Colorado School of Mines for your incredible mentorship, editing and friendship. You made this whole experience truly special and I am honored and privileged to have had you as an advisor.

I would like to thank my parents for the continued love and support throughout my lifetime of education. Finally, I would like to thank my wife Carrie, and sons Lukas and Ethan, for everything. Your love, encouragement and support allowed me to start and complete this program. I could not have done any of this without all of you. This is truly our families Masters Degree and not mine individually. I thank and love you.

CHAPTER 1

INTRODUCTION

High oil prices and the application of horizontal drilling have rejuvenated drilling in the Williston Basin (Figure 1.1). Some current exploration and development efforts have targeted the Late Devonian-Early Mississippian Bakken Formation and the Late Devonian Three Forks Formation. The availability of new cores and wireline logs, along with access to cores and logs taken decades ago, provide an opportunity to gain insights into these sedimentary rocks.

The Upper Three Forks Formation contains a subinterval or member informally named the Sanish member (Figure 1.2). This member is the focus of this evaluation. The age of the Three Forks Formation and Lower Bakken Shale is Late Devonian or Famennian (Smith et al. 1995).

Both the Lower and Upper Bakken Shale beds are prolific source rocks that have been widely studied. The Lower Bakken Shale unconformably caps the Upper Three Forks (Sanish member) in the study area. Despite its proximity to the Lower Bakken Shale, the Sanish member is not well-characterized or understood. To date, only a few papers about the Sanish member have been published. Bakken literature is abundant, but workers have elected not to concentrate on the Upper Three Forks. The author is only aware of one major study on the Sanish member conducted by Murray (1968).

1.1 Purpose and Scope

The purpose of this thesis is to provide an interpretation of the depositional environment, mineralogy, and stratigraphy of the Sanish member. By understanding these stratigraphic components, an overall sequence stratigraphic model can be developed. This understanding, in turn, can aid in defining new petroleum concepts that can ultimately be applied toward future exploration and development efforts.

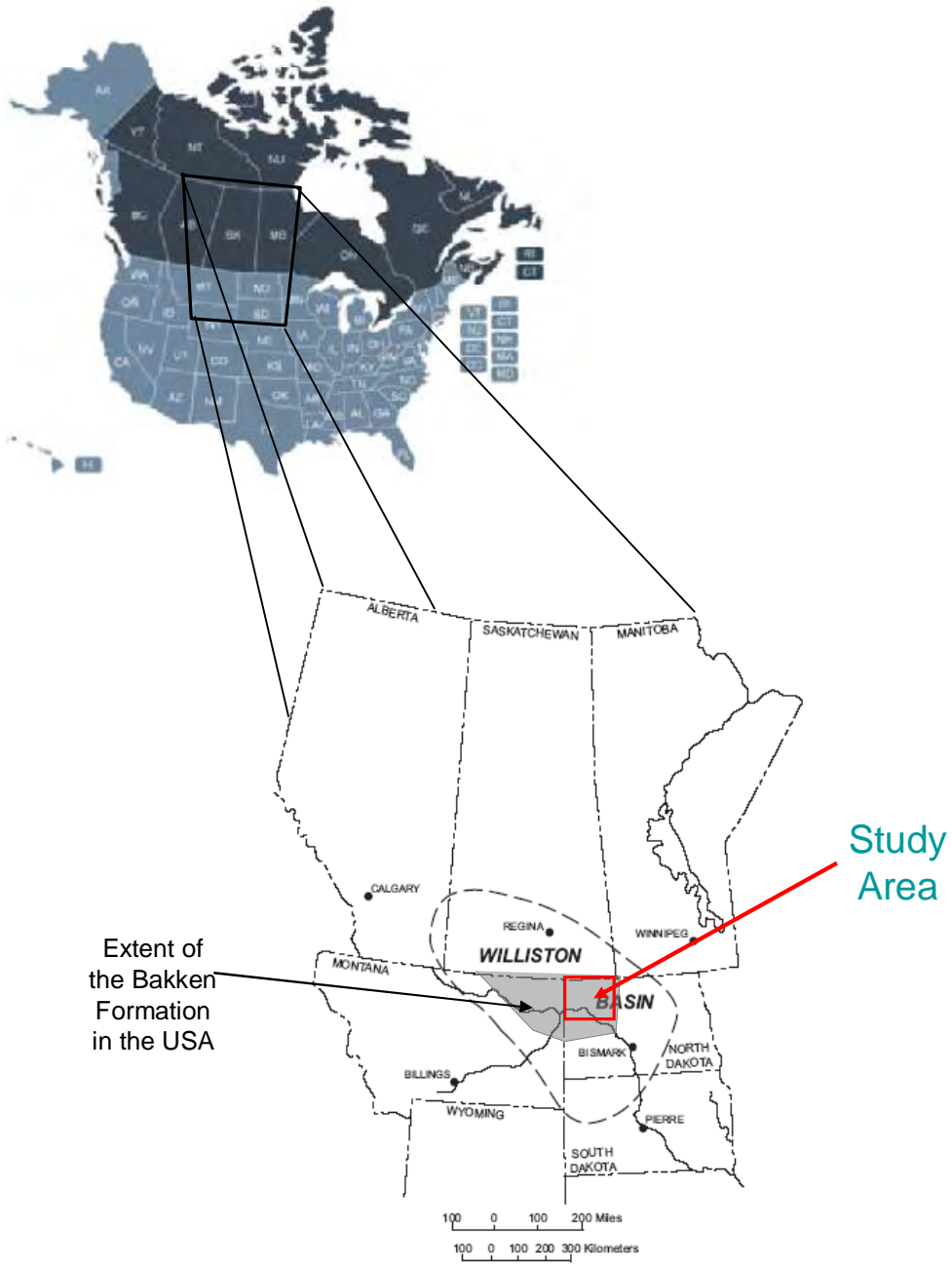


Figure 1.1. Study area outline and extent of the Bakken Formation in the United States portion of the Williston Basin. The study area includes the following North Dakota counties: Divide, McKenzie, Mountrail, and Williams. Modified from Pitman et al. (2001).

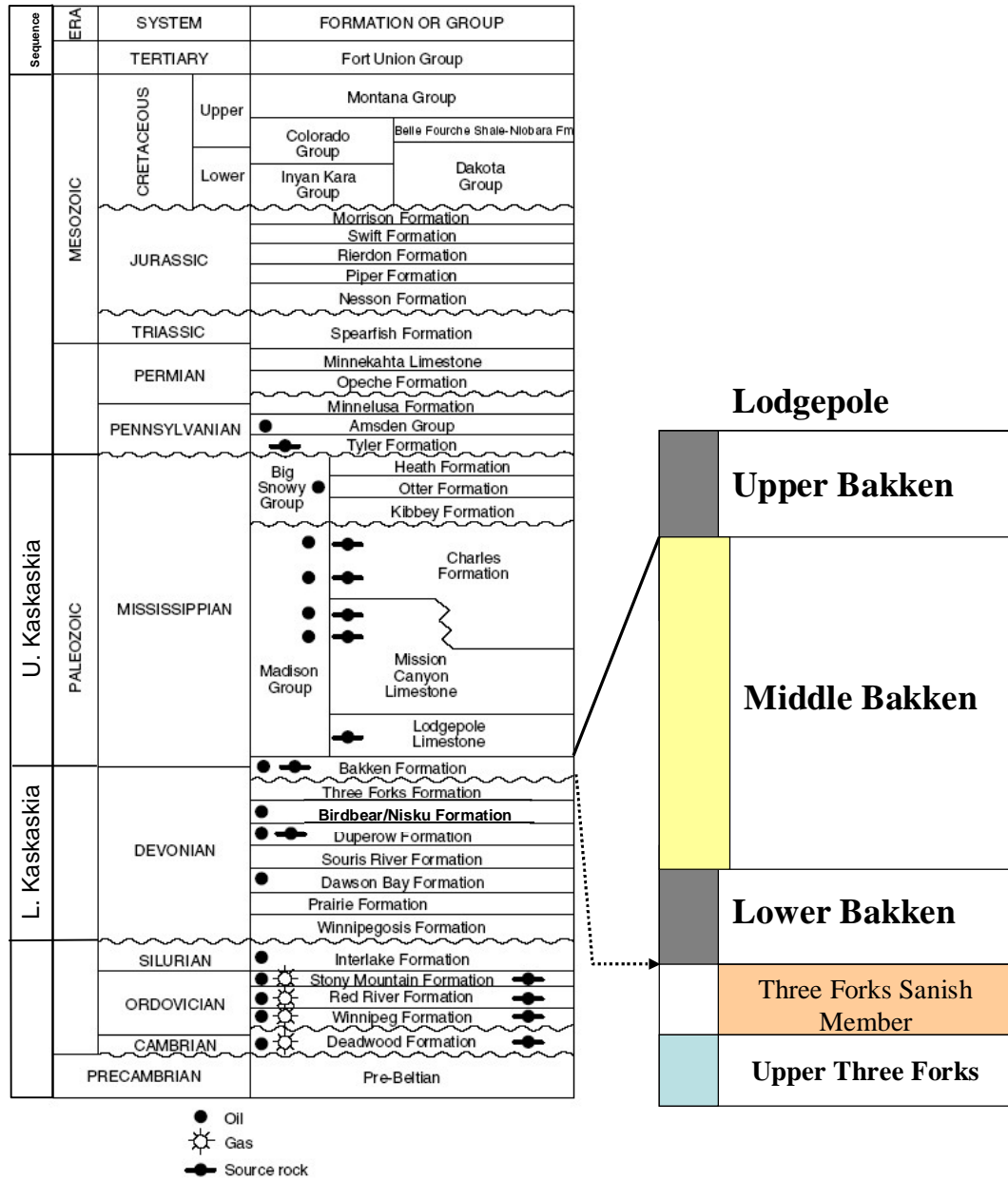


Figure 1.2. Stratigraphic chart of the Williston Basin. Sequences are from Sloss (1963). Modified from <http://en.wikipedia.org/wiki/Image:WillistonStratCol.jpg>.

1.2 Location of Study Area

The study area for the Sanish member is located in the following counties of North Dakota: Divide, McKenzie, Mountrail, and Williams (Figure 1.1). The study interval includes the Late Devonian Three Forks Formation and the Late Devonian-Early Mississippian Bakken Formation (Figure 1.2). These rocks are petroleum targets in the deeper portions of the Williston Basin (Pitman et al. 2001). The Sanish member does not crop out along the flanks of the Basin, so the use of subsurface cores and cutting samples are the only means of acquiring litho-stratigraphic data.

1.3 Research Objectives

The goals of this study are to describe the depositional environment, mineralogy, and stratigraphy of the Sanish member of the Three Forks Formation. To provide such an interpretation, the following research objectives were completed:

- 1) Description and interpretation of 16 subsurface cores from the study area;
- 2) Description of lithofacies and significant depositional and erosional surfaces from subsurface cores;
- 3) Collection and categorization of data from X-ray diffraction (XRD), scanning electron microscopy with energy dispersive X-ray spectroscopy (SEM-EDS), and thin section analysis of lithofacies; and
- 4) Interpretation of the sequence stratigraphic framework of the Sanish member

1.4 Research Contributions

The main contributions of this study are:

- 1) The development of a detailed stratigraphic model of the Upper Three Forks Formation (Sanish member); and
- 2) The description of the erosional contact and unconformity between the Three Forks Formation and the Lower Bakken Shale and the sub-regional distribution of this unconformity

1.5 Data and Methods

This study included 16 Upper Three Forks (Sanish member) cores. The core descriptions were incorporated into Petra[®], Smart-Section[®], and Powerlog[®] software for further interpretation (all software licensed and used by permission of Samson Resources). Fifteen cores are public data that were borrowed from the North Dakota Geological Survey. One core was provided by Samson Resources (Figure 1.3; Appendix E). The open-hole logs are the property of Samson Resources. Samson Resources data and cores are now public. Formation tops used for correlation that are not the author's own are IHS Energy[®] data and are licensed and used by permission of Samson Resources.

Lithofacies identified in core descriptions were further described and analyzed with XRD, SEM-EDS, and thin-sections. Significant stratigraphic surfaces were identified and characterized, and with lithofacies data, these surfaces were used to construct a sequence stratigraphic framework for the Upper Three Forks (Sanish).

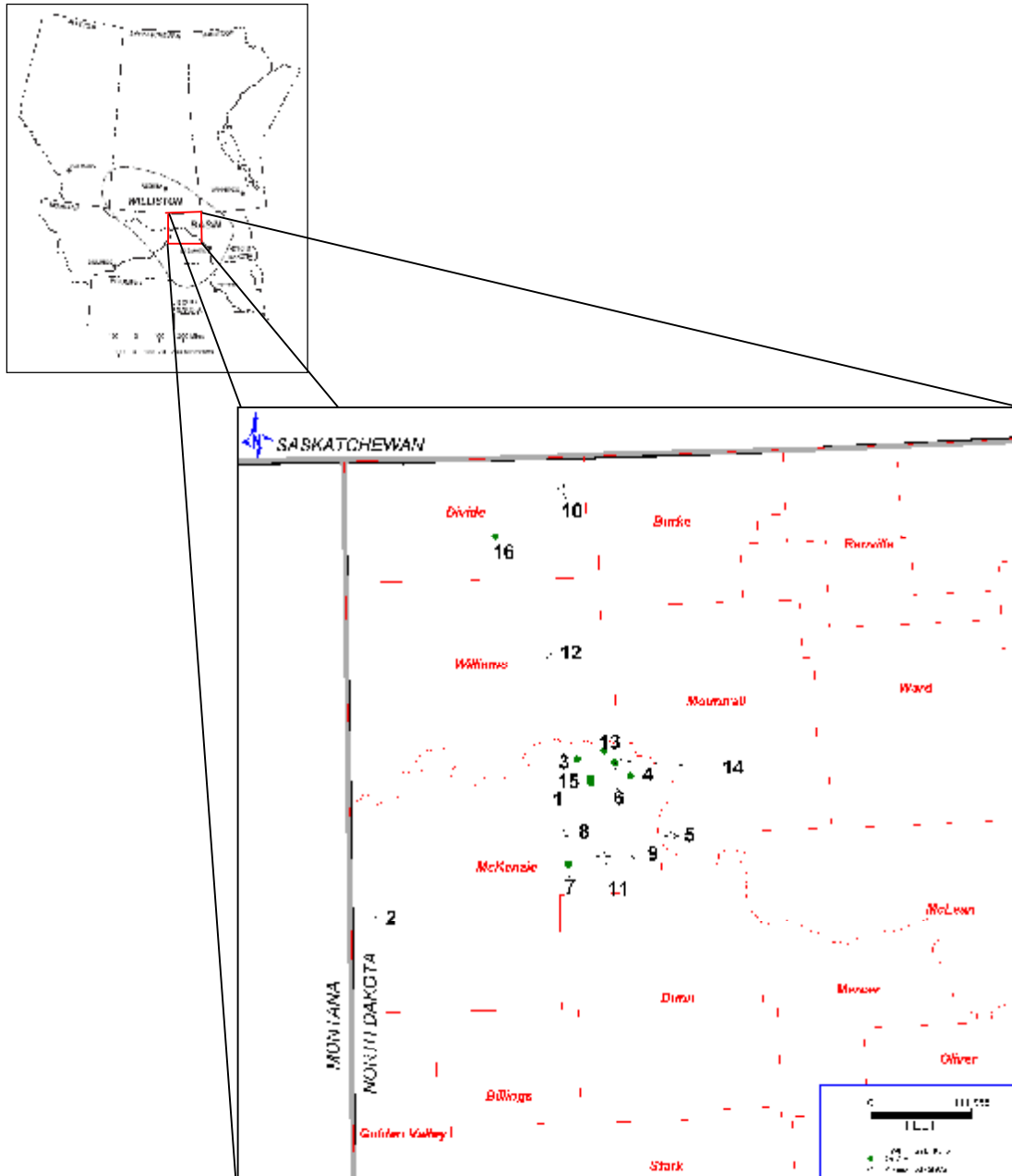


Figure 1.3. Subsurface core location map. Appendix E contains the core listing. Modified from Pitman et al. (2001).

CHAPTER 2

GEOLOGIC SETTING

The Williston Basin is a near-circular, intracratonic sag that underlies most of western North Dakota, eastern Montana, and portions of Alberta, Saskatchewan, and Manitoba (Figure 1.1) (Kerr, 1988; Pitman et al. 2001). Tectonic features define the boundaries of the Williston Basin. Along the northeast flank of the basin, sediments thin onto the Meadow Lake Escarpment. The Cedar Creek Anticline flanks the southwestern edges of the Basin, and along the northwest flank of the basin, the Sweetgrass-Battle River Arch separates the Williston Basin from the Alberta Foreland Basin (Figure 2.1).

2.1 **Early Basin History**

Core and geophysical data indicate that two Archean terranes underlie most of the Williston Basin. The Superior Province is present in eastern North Dakota, eastern South Dakota, and western Manitoba. The Wyoming Province occurs in western North Dakota, western Saskatchewan, western South Dakota, and eastern Montana. Rifting between these two Archean provinces occurred in Precambrian time. Emplacement of complex oceanic and volcanic terranes occurred within the rift, and these rocks comprise the Trans Hudson Orogenic Belt (Green et al. 1985; Gerhard et al. 1990).

At basin-center, nearly 15,000 feet (5000 meters) of sedimentary rocks are present. These sediments range in age from Cambrian to Quaternary. Sloss (1963) divided this accumulation of rocks into sequences bounded by unconformities (Figure 2.2). Sloss's six major sequences are: the Sauk, Tippecanoe, Kaskaskia, Absaroka, Zuni, and Tejas (Bally, 1989; Gerhard et al. 1990). The contact between the Bakken Formation and the Three Forks Formation is the boundary between the lower Kaskaskia and upper Kaskaskia sequence.

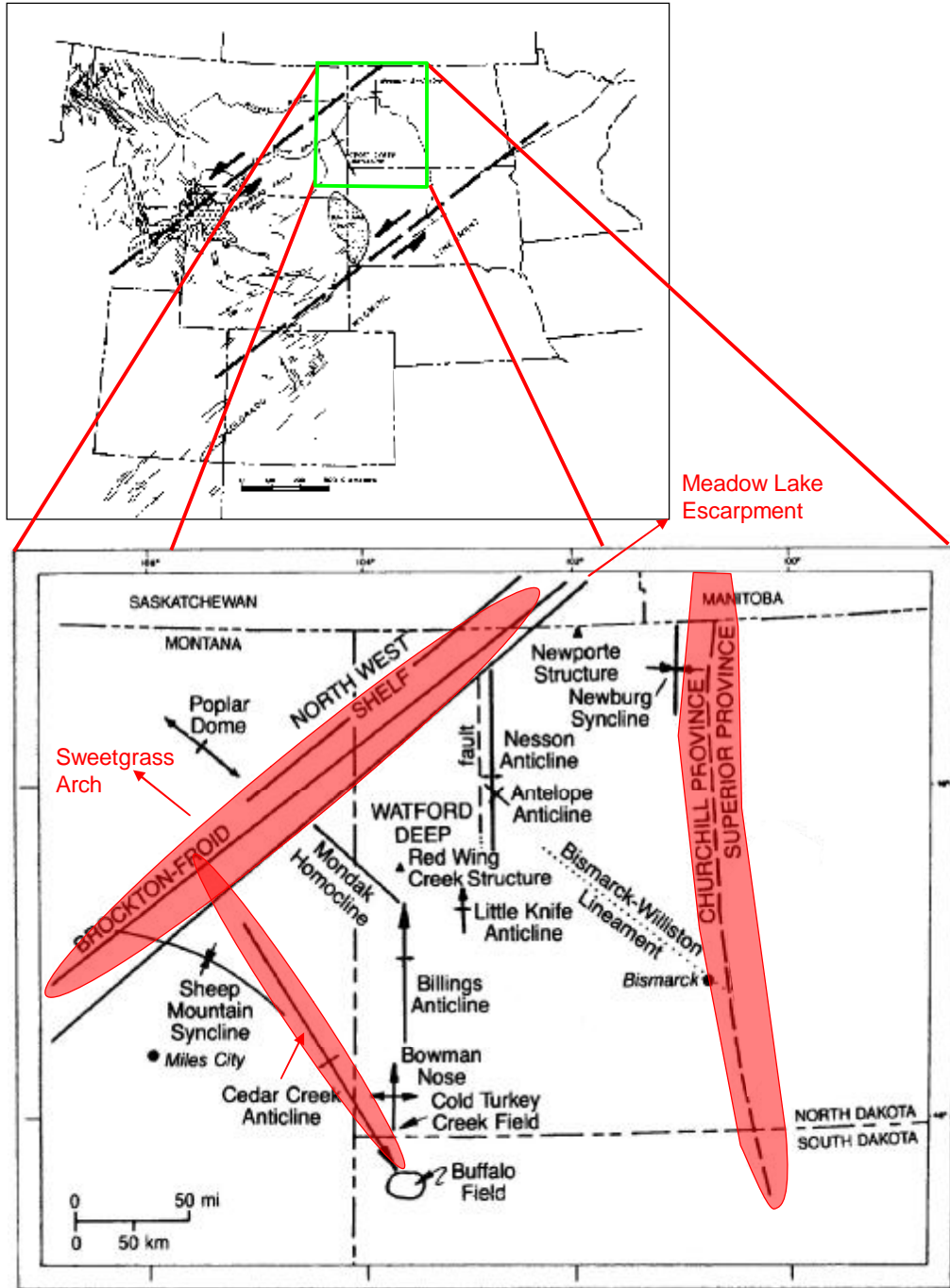


Figure 2.1. Structural features in the U. S. Williston Basin. The major structural boundaries that surround the Williston Basin are highlighted in red. Modified from Gerhard et al. (1990).

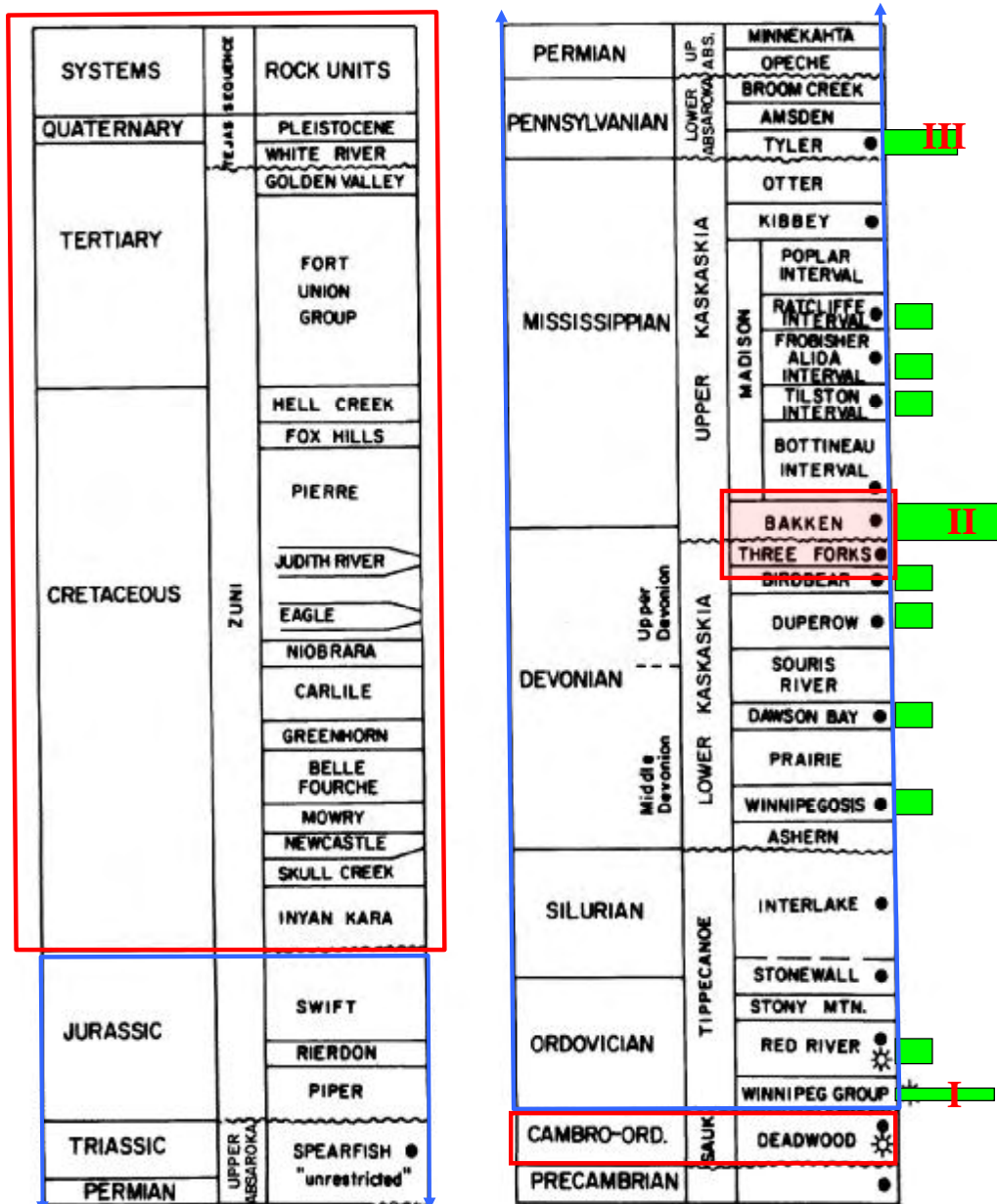


Figure 2.2. Sloss's (1963) sequences are shown on this stratigraphic column of the U.S. Williston Basin. The Bakken and Three Forks formations are shaded in red. Oil and gas symbols represent major reservoirs. Blue outline represents carbonate deposition. Red outline represents clastic deposition. Green bars represent source rocks (see text for the identification of source rocks), and Roman numerals represent the three types of source rocks. Modified from Gerhard et al. (1990). Note the Birdbear Formation is also known as the Nisku Formation.

☼ Gas symbol ● Oil Symbol

2.2 Devonian Basin History

During the Devonian (417 Ma to 360 Ma), the North American craton was connected to open oceanic environments along the southwestern edge of the current continent. The eastern and western edges of the North American craton were rimmed by orogenic belts and associated subduction zones. The Williston and Alberta foreland basins were adjoining and intermittent carbonate reef growth at the western edge of the Alberta Basin restricted flow across the narrow and shallow Elk Point Basin shelf. Evaporites of the Prairie Formation and platform carbonates of the Duperow and Nisku formations are deposits associated with intermittent waning of reef growth and restriction across the shallow Williston shelf (Figures 2.3; 2.4) (Bally, 1989; Gerhard et al.1990).

Following deposition of the Nisku platform carbonates, mixed carbonate and clastic pulses of the Three Forks Formation were deposited. The unconformity at the top of the Three Forks Formation is related to either prolonged exposure and erosion, or down cutting (erosion) during transgression of the Lower Bakken Shale. Basin subsidence and-or sea level rise produced the Lower Bakken flooding event and deposition of marine, organic-rich, black shale of Late Devonian age.

The orientation of the late Devonian Williston Basin changed during early Mississippian time. Early development of the Montana Trough changed the orientation of the Basin (Figure 2.5). Late in Mississippian time the Williston was essentially a closed basin (Figure 2.6) because of the unconformity at the base of the Kibbey Formation (Pitman et al. 2001).

2.3 Late Devonian Sanish Member

The Sanish member is deposited at the top of the Late Devonian Three Forks Formation (lower Kaskaskia). The Late Devonian-Early Mississippian Bakken Formation (upper Kaskaskia) caps the Sanish member (Figure 1.2) (Gerhard et al.1990). Bally (1989) separated the Kaskaskia into the Kaskaskia I subsequence (mid-early Devonian (401 Ma) to latest Devonian (362 Ma)) and the Kaskaskia II subsequence (latest Devonian (362 Ma) to late Mississippian (330 Ma)). The separation of these two subsequences is based on an unconformity that occurs across most of North America. It

is this unconformity that probably occurs in the study area at the top of the Sanish member and at the base of the Lower Bakken Shale. In Canada, Smith et al. (1995) interpret this unconformity to be a sequence boundary that separates the Big Valley-Torquay members of the Upper Three Forks Formation (Western Sedimentary Canadian Basin) from the Canadian equivalent, Late Devonian-Early Mississippian Bakken Formation (Exshaw Formation) (Figure 2.7). At this unconformity, the Upper Three Forks Formation (Big Valley-Torquay member) experienced widespread exposure and erosion. A flooding event of the Canadian Lower Bakken Shale equivalent (Exshaw Formation) capped the Upper Three Forks (Torquay) Formation. Because of this exposure and flooding, Smith et al. (1995) interpreted this boundary to be a sequence boundary that separates the Three Forks Formation (Torquay) and the Bakken-Exshaw Formation.

This study focuses on the United States equivalent Three Forks and Bakken formations. This evaluation characterizes Upper Three Forks stratigraphy and describes the unconformable boundary at Three Forks-Lower Bakken contact.

2.4 Petroleum Geology

The Williston Basin hosts three main types of source rocks: 1) Type I – lacustrine lipid-rich algae, bacteria and sporopollenin (oil-prone): Winnipeg Formation (Ordovician); 2) Type II – marine phytoplankton, zooplankton, and bacteria (oil and gas-prone): Bakken Formation (Late Devonian-Early Mississippian); and 3) Type III – terrestrial vascular plants (gas-prone): Tyler Formation (Pennsylvanian). Organic-rich beds found in the Ordovician Red River and Madison formations are also secondary contributors to hydrocarbons in the overall petroleum system (Figure 2.2) (Meissner, 1979; Gerhard et al.1990). Of the source rocks in the Williston Basin, the Bakken shales are considered to be the most prolific. These highly organic-rich source rocks lie directly above the Sanish member. Petroleum generation and migration from the Bakken Formation has been studied and well documented (Burres et al.1996; Dow, 1974; Hunt, 1996; Meissner, 1979; Murray, 1968, Webster 1982; Webster 1984). The close proximity of the Upper Three Forks Formation to thermally mature Lower Bakken Shale could produce source and trap configurations for petroleum production.

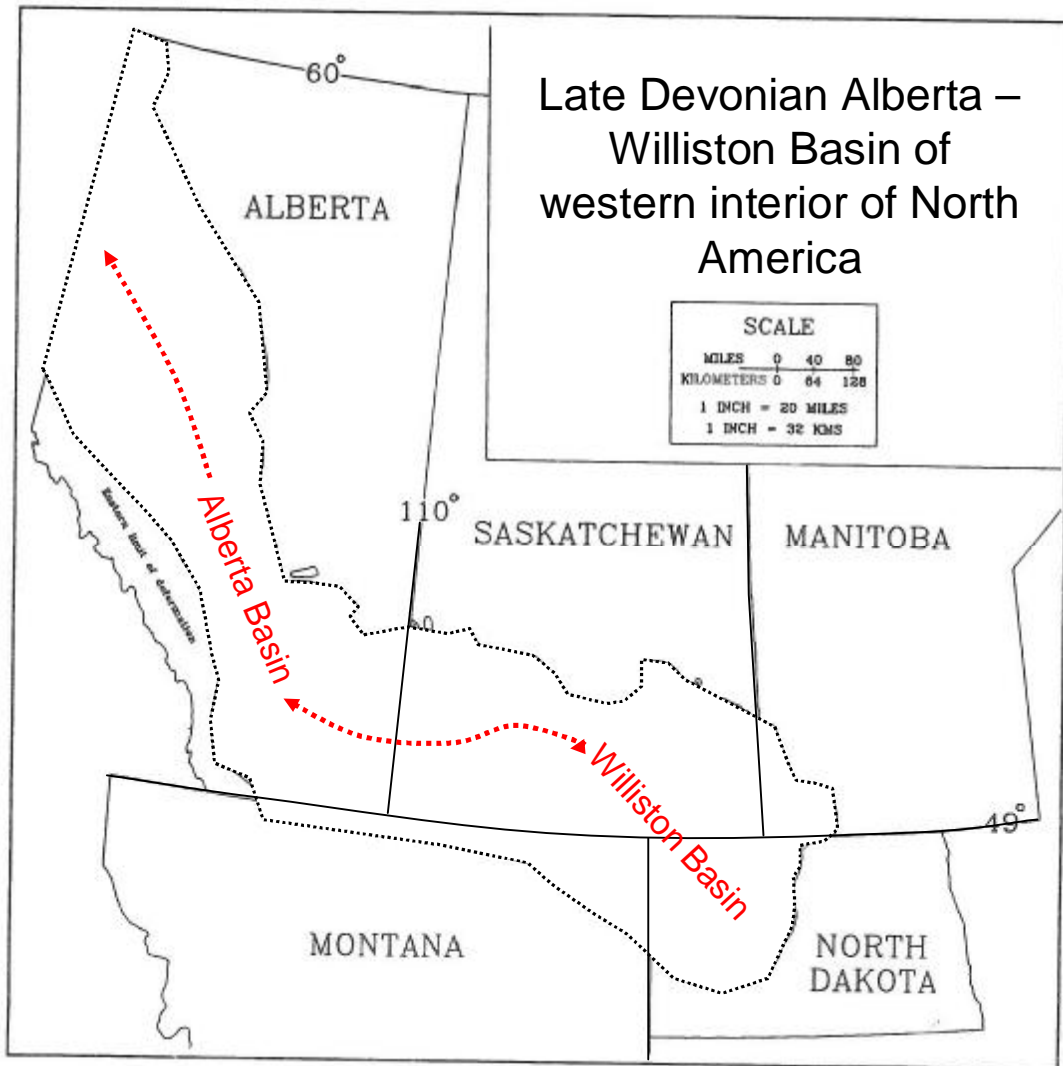


Figure 2.3. Late Devonian reconstruction map displaying the continuous connection between the Alberta and Williston Basin. Modified from Smith et al. (1995).



Figure 2.4. Paleogeographic map of the Late Devonian (360Ma). Subduction zones and associated orogenic belts (dashed red) surround and separated the North American craton from the Devonian ocean. The North American craton was open to the southwest (yellow arrow). The Williston Basin and the Alberta Basin were connected at that time (W-A). Modified from <http://-jan.ucc.nau.edu/rcb7-namD360.jpg>.

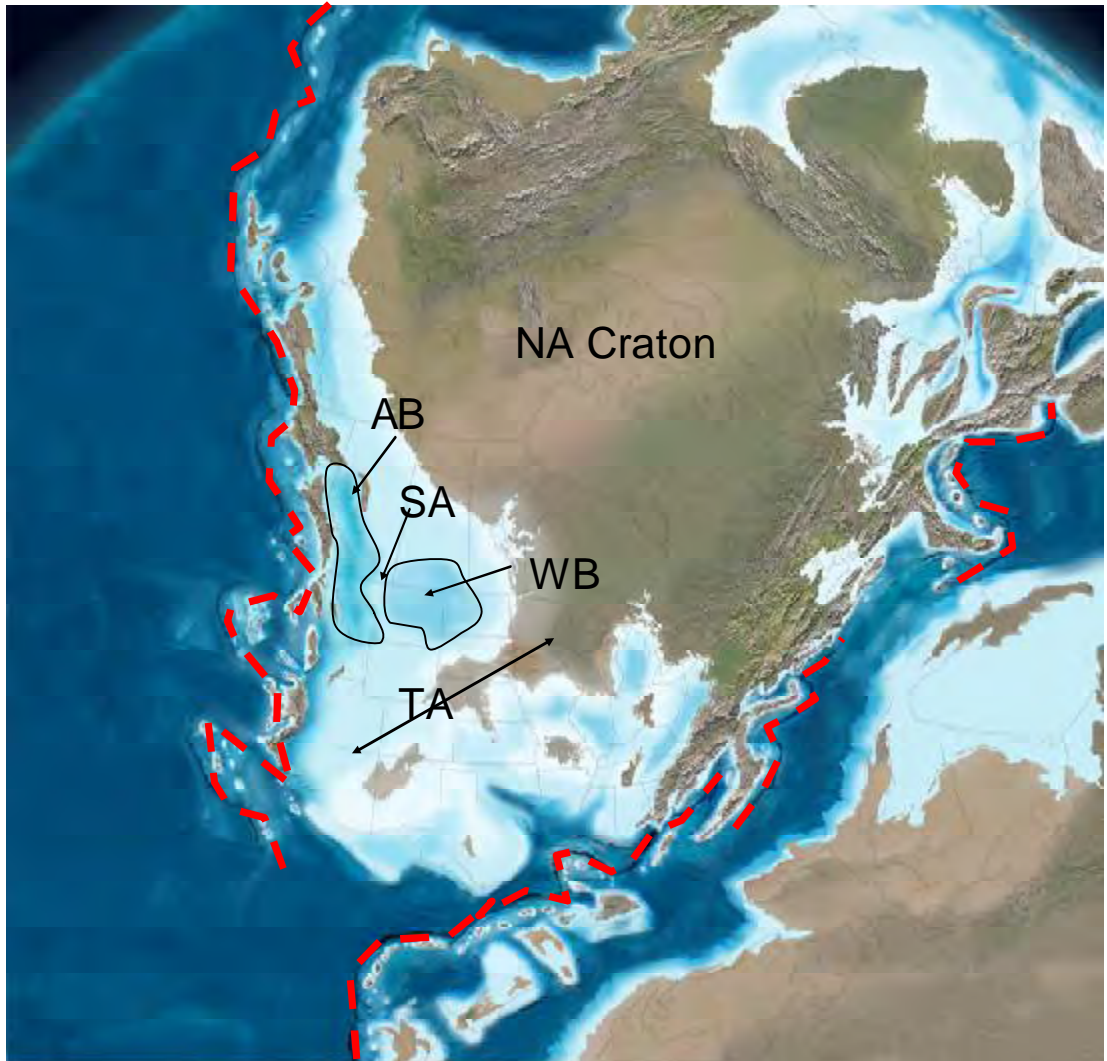


Figure 2.5. Paleogeographic map of the Early Mississippian (345Ma). The Alberta Basin (AB) and the Williston (WB) Basin were separated by the Sweetgrass Arch (SA). The Williston Basin was shielded from the Devonian ocean by orogenic belts that surrounded the North American craton and the Transcontinental Arch to the southeast (TA). Modified from <http://jan.ucc.nau.edu/rcb7-namM345.jpg>.

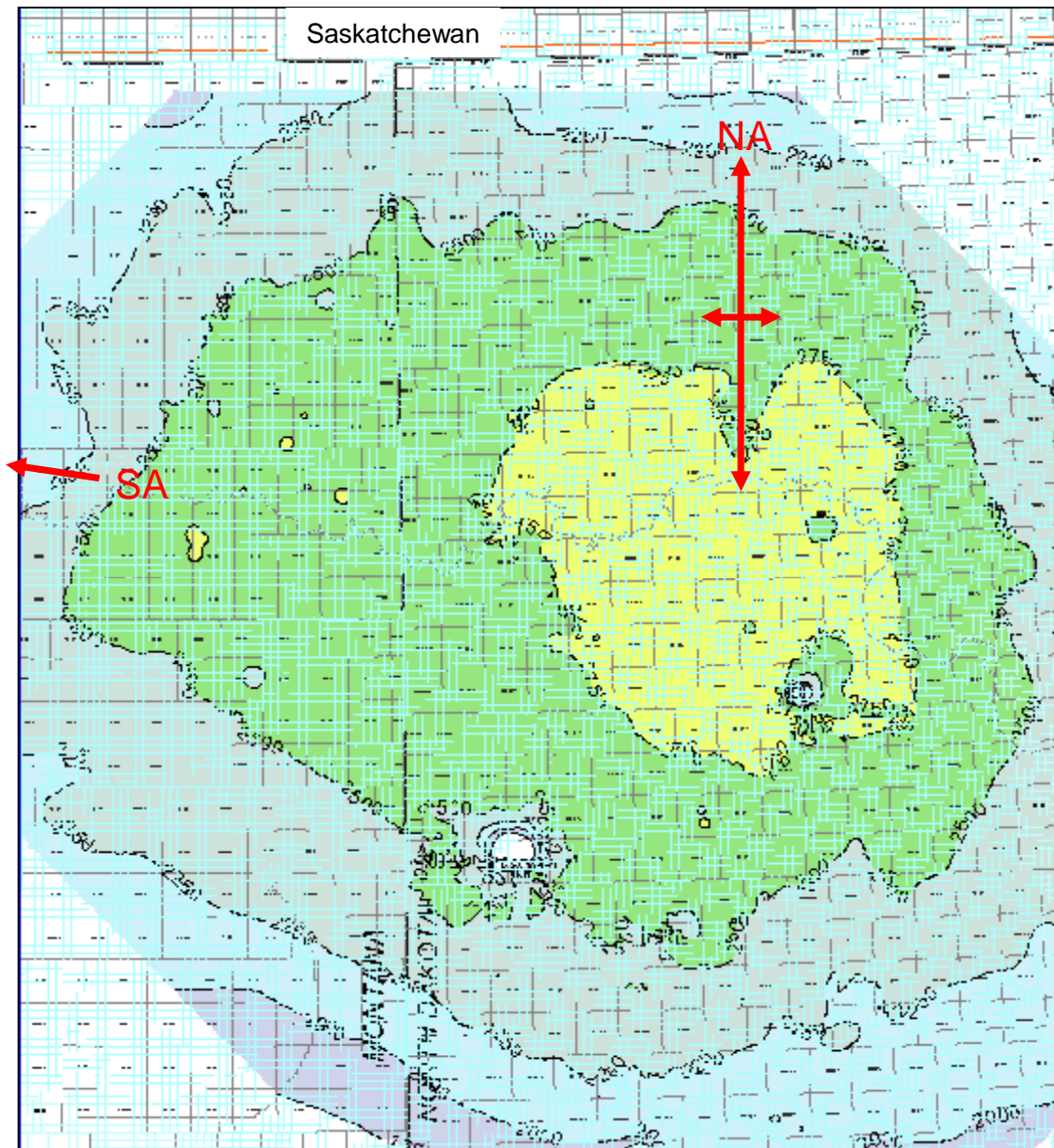


Figure 2.6. Isopach map of the Upper Kaskaskia sequence (Bakken through the Otter formations). Uplift of the Sweetgrass Arch (SA) to the west and northwest closed the Williston Basin from the Alberta Basin. A regional unconformity developed at the base of the Kibbey Formation, and this map shows preserved Upper Kaskaskia strata (Figure 1.2; 2.2). Thinning is evident over the Nesson Anticline (NA). Classic intracratonic sag is evident (250' contours).

Banff Fm.	Banff carbonates		Highstand Systems Tract (partial)	Lodgepole Formation		
	basal Banff black shale		Maximum flooding surface	Upper Member		
Exshaw Formation	Siltstone Member	Sub-unit B-ex	Transgressive Systems Tract	Sub-unit C-bk	Bakken Formation	
		Sub-unit A-ex		Marine flooding surface		Sub-unit B-bk
	Black Shale Member	Mb-2	Lowstand Systems Tract	Sub-unit A-bk		Middle Member
		Mb-1				
Palliser/Big Valley Formations		Transgressive Systems Tract	Lower Member	Big Valley/Torquay Lyleton/Threeforks Formations		

Figure 2.7. Comparison of the sequence stratigraphy of the Exshaw-Bakken Formation between the Foreland Basin of Canada and the Williston Basin of the United States. From Smith et al.(2000).

2.5 Previous Work

Only a few publications on the Bakken and Three Forks formations mention the Sanish member. Murray's (1968) *Quantitative Fracture Study – Sanish Pool, McKenzie County, North Dakota* discussed the role of fractures in the Upper Three Forks (Sanish). In his study, Murray looked at lithological and reservoir characteristics of the Sanish member, the role of fracturing, production history of the field, the significance of reservoir pressure, and the Bakken Shale as a source of oil. Murray's contributions indicate the role fractures play in oil storage and production.

Meissner's (1978) *Petroleum Geology of the Bakken Formation Williston Basin, North Dakota and Montana* discussed the petroleum geochemistry of the Bakken Formation. Meissner described the stratigraphy, reservoir properties, geochemical (source rock) properties, petrophysical properties, and theories on localized fracturing of the Bakken Formation and associated units. Meissner's theories of localized fracturing from expulsion of hydrocarbons are important to this thesis because these relate to the Sanish member's fracturing, mineralogy, and diagenetic history.

Kerr (1988) and Gerhard et al. (1990) wrote overviews of the geology of the Williston Basin. Both papers give a brief, yet useful, description of the Three Forks and Bakken formations.

Smith et al. (1995) defined the sequence stratigraphy of the Bakken Formation in their study entitled *Sequence Stratigraphy of the Bakken and Exshaw Formations: A Continuum of Black Shale Formations in the Western Canadian Sedimentary Basin*. This work interprets the base of the Bakken Formation to be a sequence boundary (marine flooding surface). Their findings show the Lower Bakken Shale rests unconformably on the truncated surface of the Three Forks Formation. Their interpretation of the sequence boundary between the Bakken Formation and the Three Forks Formation is extremely relevant to the depositional and Basin history of the Sanish member.

CHAPTER 3

CORE DESCRIPTIONS AND DEFINITION OF FACIES

The first steps in determining the depositional environments of the Sanish member involved detailed core descriptions and facies interpretations. A facies is a “body of rock that is characterized by a particular combination of lithology, physical, and biological structures that exhibit an aspect different from the bodies of rock above, below, and laterally adjacent” (Walker et al. 1992). Individual lithofacies and significant sedimentary surfaces were identified and described and depositional environments were then inferred.

3.1 **Methods**

Sixteen Upper Three Forks and Lower Bakken cores covering 4 counties in North Dakota (Figure 1.3) were described as part of this evaluation. Lithology and primary and secondary sedimentary structures were identified. Fifteen cores are public data and were shipped from the North Dakota Geological Survey to Triple O Slabbing in Denver, Colorado. One core during the course of data gathering was proprietary to Samson Resources. This core is now public and is stored at the State of North Dakota’s core depository.

Lithology and primary and secondary structures were described in cores. Primary and secondary sedimentary structures were placed into two categories; 1) *single diagnostic criteria* that are unique to a particular depositional environment and 2) *additional diagnostic criteria* that can be ascribed to other depositional environments (Nio et al. 1989). A grain-size chart and a 10X hand lens were used to aid in the identification of lithology. Hydrochloric acid was employed to determine the types of carbonate matrix and cement. Rock color was matched to the Geological Society of America color chart (Goddard et al., 1970). Facies descriptions in this work include data from this chart. Images of individual facies were taken from the North Dakota Geological Survey’s web site that can be referenced with a small subscription price from the following link: <https://www.dmr.nd.gov-oilgas/>.

Six facies were defined in the Upper Three Forks Formation (Sanish) and the Lower Bakken Shale. A representative sample of each facies was prepared for thin-section analysis, X-ray diffraction, and SEM-EDS. These data are discussed in Chapter 4.

3.2 Core Descriptions

Data from core descriptions were categorized and correlated from one core to the next. This process was used to construct a general stratigraphic column showing typical stacking patterns for Upper Three Forks sediments (Figure 3.1). Core #2 was the only core that differed in facies associations. A stratigraphic column was created to show this difference (Figure 3.2). A detailed description of each of the cores is found in Appendix A.

3.3 Facies Descriptions

The only significant variation in Upper Three Forks strata was in thickness of individual facies. Figure 3.1 is a generalized stratigraphic column created from 15 cores that represents the Upper Three Forks and entire Sanish member in the study area. The westernmost core, core # 2, has a different facies association and its stacking pattern is shown in Figure 3.2.

The following facies descriptions start in the Upper Three Forks, continue in the Sanish member, and finish in the Lower Bakken Shale.

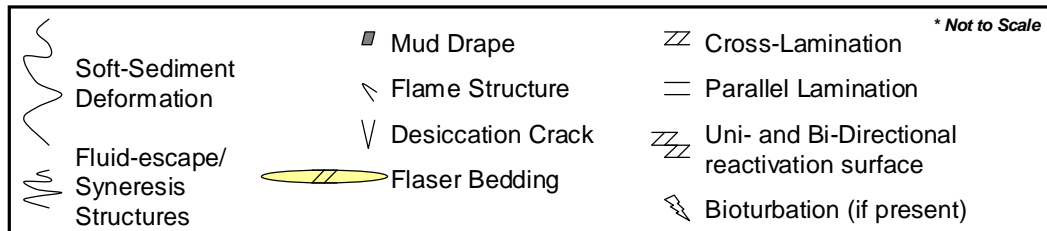
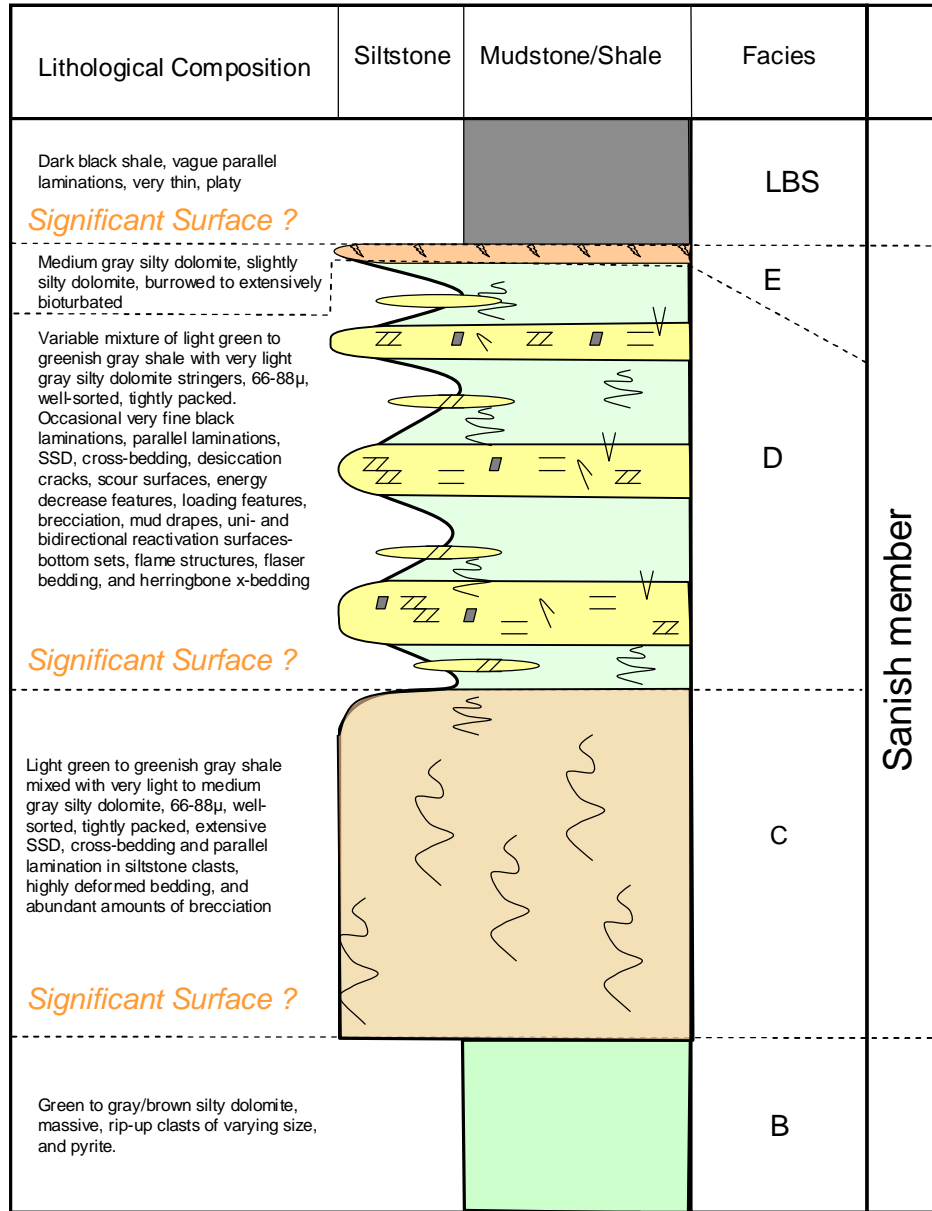


Figure 3.1. General stratigraphic column for individual facies derived from 15 of the 16 core descriptions for the Upper Three Forks and Lower Bakken Shale. Thickness of each facies varies throughout the study area. The Upper Three Forks Formation includes facies B. Facies C, D and E are included in the Sanish. Facies E only occurred in core #9. The Lower Bakken Shale is labeled LBS.

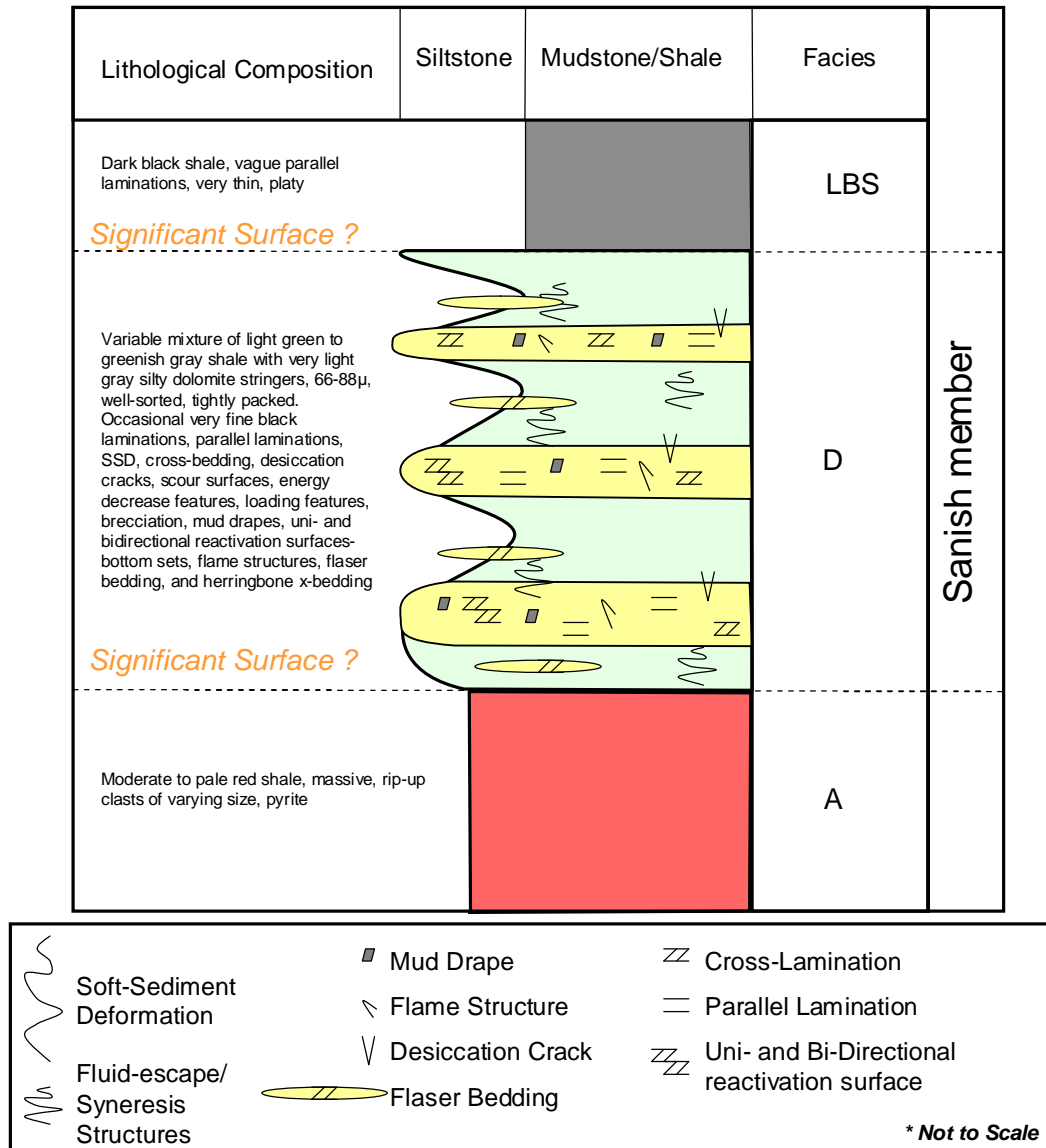


Figure 3.2. Stratigraphic column for facies in core #2. Upper Three Forks Formation facies are labeled A and D. Facies D is included in the Sanish. The Lower Bakken Facies is labeled LBS.

3.3.1 **Facies A – Dolomitic and Slightly Silty Shale**

Facies A is moderate red (5 R 4-6) to pale red (5 R 6-2) dolomitic shale with common shale clasts and discontinuous lenses of very fine to fine-crystalline dolomite and very fine to fine-grained sand. The red color suggests probable oxidation (Figure 3.3). Primary and secondary sedimentary structures are sparse to absent. Facies A occurred in the westernmost portion of the study area where this facies had small shale clasts and pyrite nodules.

3.3.2 **Facies B – Calcareous and Very Slightly Silty Dolomite**

Facies B is calcareous (limey) and silty dolomite. The rock is dark greenish-gray (5 GY 4-1) to medium dark gray (N4) (Figure 3.4). In the northern part of the study area, Facies B has larger rip-up clasts than in the southern part of the study area. Primary and secondary sedimentary structures are rare to absent.

Both Facies A and B can be correlated to wireline logs and are widespread in the study area.

3.3.3 **Facies C – Highly Deformed and Brecciated Silty Dolomite**

Facies C is the lower lithofacies of the Sanish member and was identified in every core that penetrated the entire member, except in core #2 where Facies C is absent. This facies is silty dolomite and gray-green shale. Detritus is 66-88 microns (siltstone to very fine-grained sandstone). Abundant soft-sediment deformation and brecciation partly homogenized light green (5 G 8-1) to greenish gray (5 G 6-1) shale and very light gray (N8) to medium gray (N5) silty dolomite (Figure 3.5). Soft-sediment deformation and brecciation made identification of primary and secondary structures nearly impossible. Even with this sediment deformation and homogenization, Facies C is a petroleum reservoir in parts of the study area.

3.3.4 **Facies D – Silty Dolomite and Shale**

Facies D occurs in the middle and upper Sanish and was observed in every core. Facies D includes two lithologies: 1) light green (5 G 8-1) to greenish gray (5 G 6-1) slightly dolomitic shale and 2) very light gray, silty dolomite (N8) (Figure 3.6).



Figure 3.3. Facies A. Core #2. 10,701 feet. Facies A consists of moderate red (5 R 4-6) to pale red (5 R 6-2) dolomitic shale with white dolomite clasts.



Figure 3.4. Facies B. Core #3. 10,051.1 feet. Facies B is a dark greenish-gray (5 GY 4-1) to medium dark gray (N4) dolomite with rip-up clasts.



Figure 3.5. Facies C. Core #1. 10,333 feet. Facies C is dominated by soft-sediment deformation and brecciation. Facies C is a light green (5 G 8-1) to greenish-gray (5 G 6-1) shale mixed with light gray silty dolomite (N8).

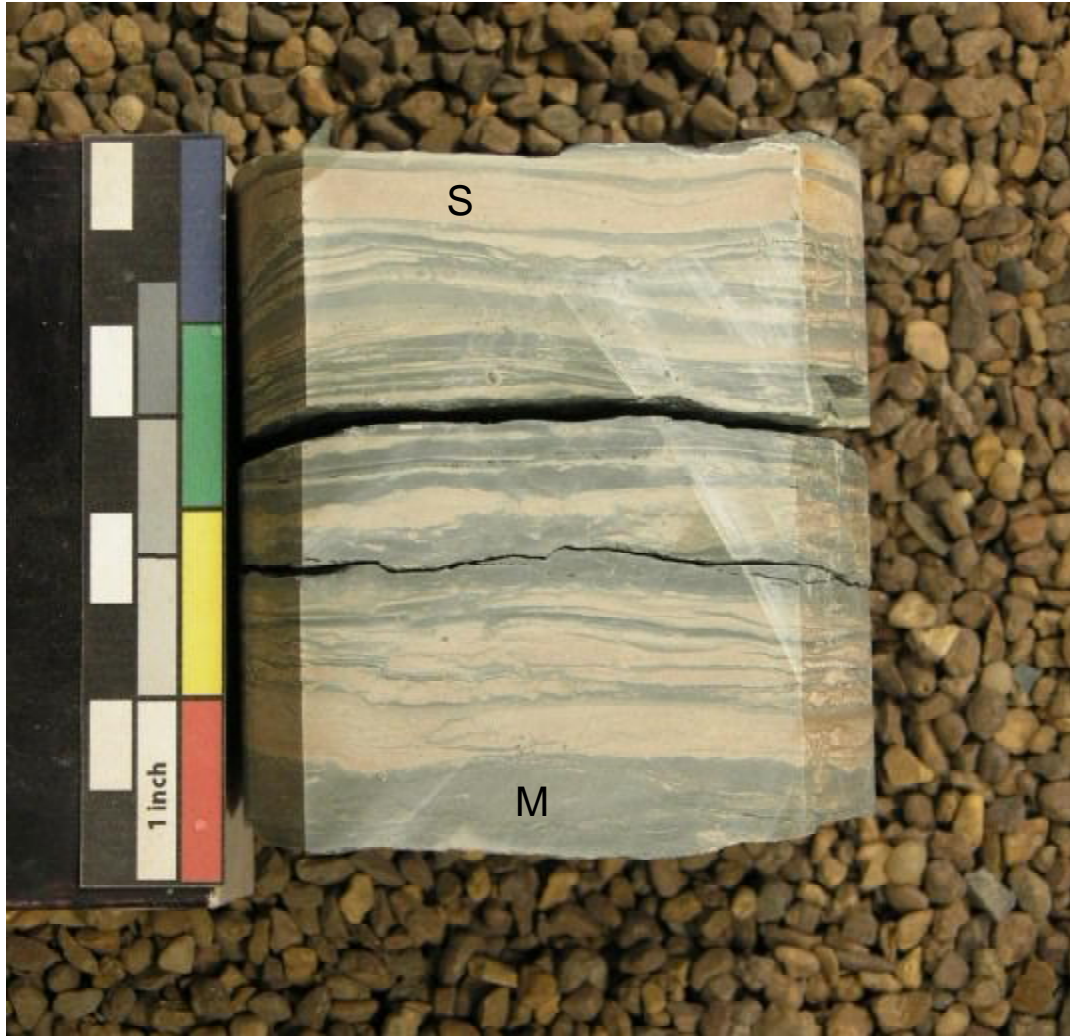


Figure 3.6. Facies D. Core #2. 10,689.1 feet. Facies D is comprised of 2 lithologies: 1) light green (5 G 8-1) to greenish-gray (5 G 6-1) shale and 2) very light gray, silty dolomite (N8).

The percentage of silty dolomite and shale vary in every core. The siltstone ranges in size from 66-88 microns (siltstone to very fine sandstone). Core # 8 has grains that range from 66-125 microns (Figure 3.7).

Silt detritus is moderate to well-sorted and angular to subrounded. Primary sedimentary structures include parallel-laminations, ripple and mega-ripple cross-laminations and soft-sediment deformation. (Figure 3.8). Soft-sediment deformation ranges from partly to almost totally deformed. (Figure 3.9). This facies also includes desiccation cracks, scour surfaces, energy decrease features (siltstone fining upwards to clay), loading features, and brecciation (Figures 3.10; 3.11). Critical components that were used for environmental interpretation include: mud drapes, uni-directional and bi-directional reactivation surfaces, bottom sets associated with the cross-laminations, desiccation cracks, desiccation polygons, cyanobacteria laminations, and flame structures (Figures 3.10; 3.11; 3.12). Additionally, flaser bedding (varying energy regimes) and syneresis cracks are also important environmental indicators (Figures 3.13; 3.14).

3.3.5 Facies E – Burrowed and Slightly Silty Dolomite

Facies E is medium gray (N5) silty dolomite that is burrowed to extensively bioturbated. Where present, this facies occurs at the top of the Sanish member. Bioturbation was extensive in core #9 and original sedimentary structures were obscured (Figure 3.15).

3.3.6 Facies LBS – Dark Black Shale

Facies LBS is the Lower Bakken Shale and it is ubiquitous in the study area (Figure 3.16). Facies LBS lies unconformably on top of the Sanish member. The Lower Bakken Shale is grayish black (N2) to dark black (N1), pyritic shale with parallel-laminations, very thin, very fine-grained sandstone and siltstone laminations, disseminated calcite and dolomite crystals, possible bioturbation, pyrite nodules, and compaction features. Smith et al. (1995) describe this Bakken Formation facies as a “finely laminated, organic-rich, hemi-pelagic, black marine mudstone in which body fossils and bioturbation are rare”.

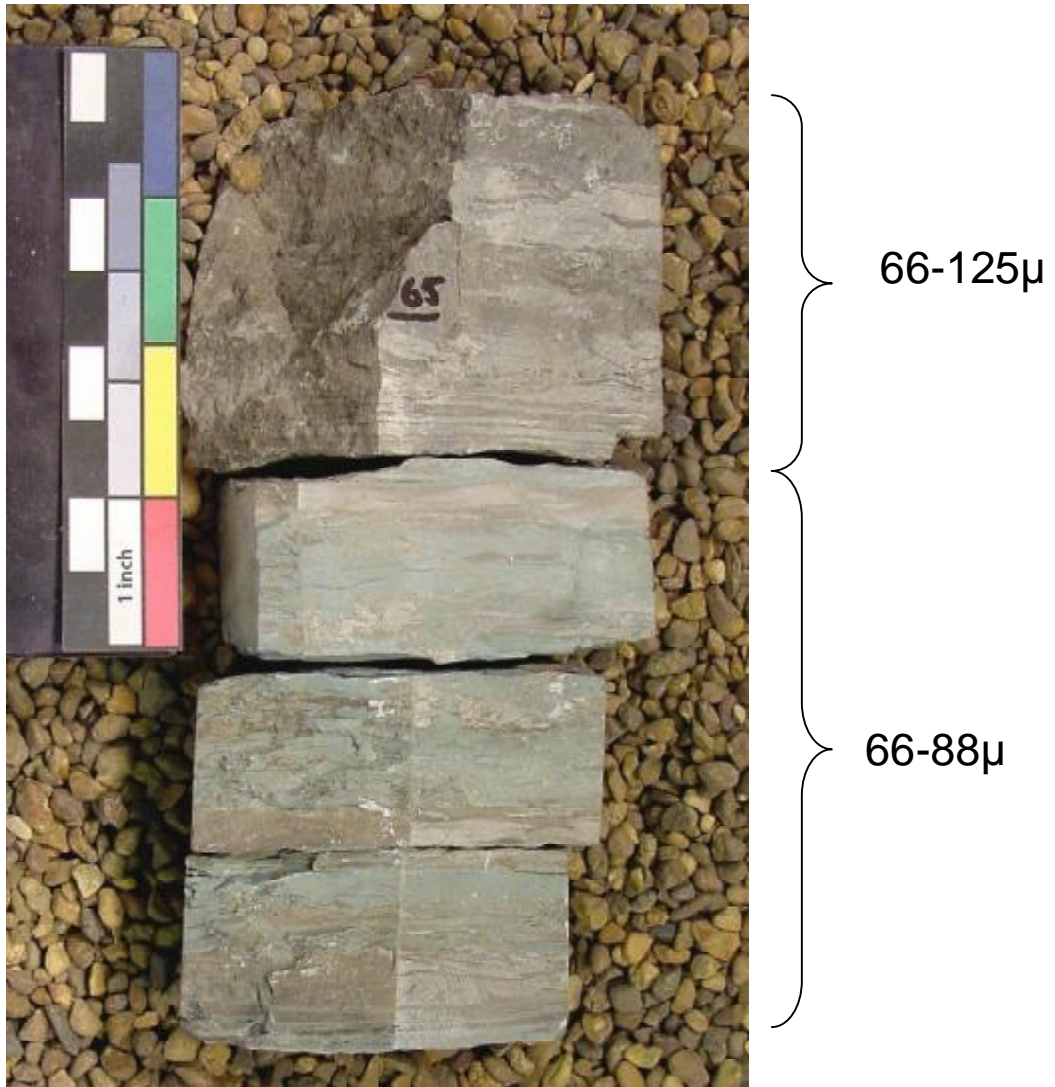


Figure 3.7. Facies D. Core #7. 10,965 feet. Siltstone grains at the top of this cored interval are coarser than commonly observed for Facies D.

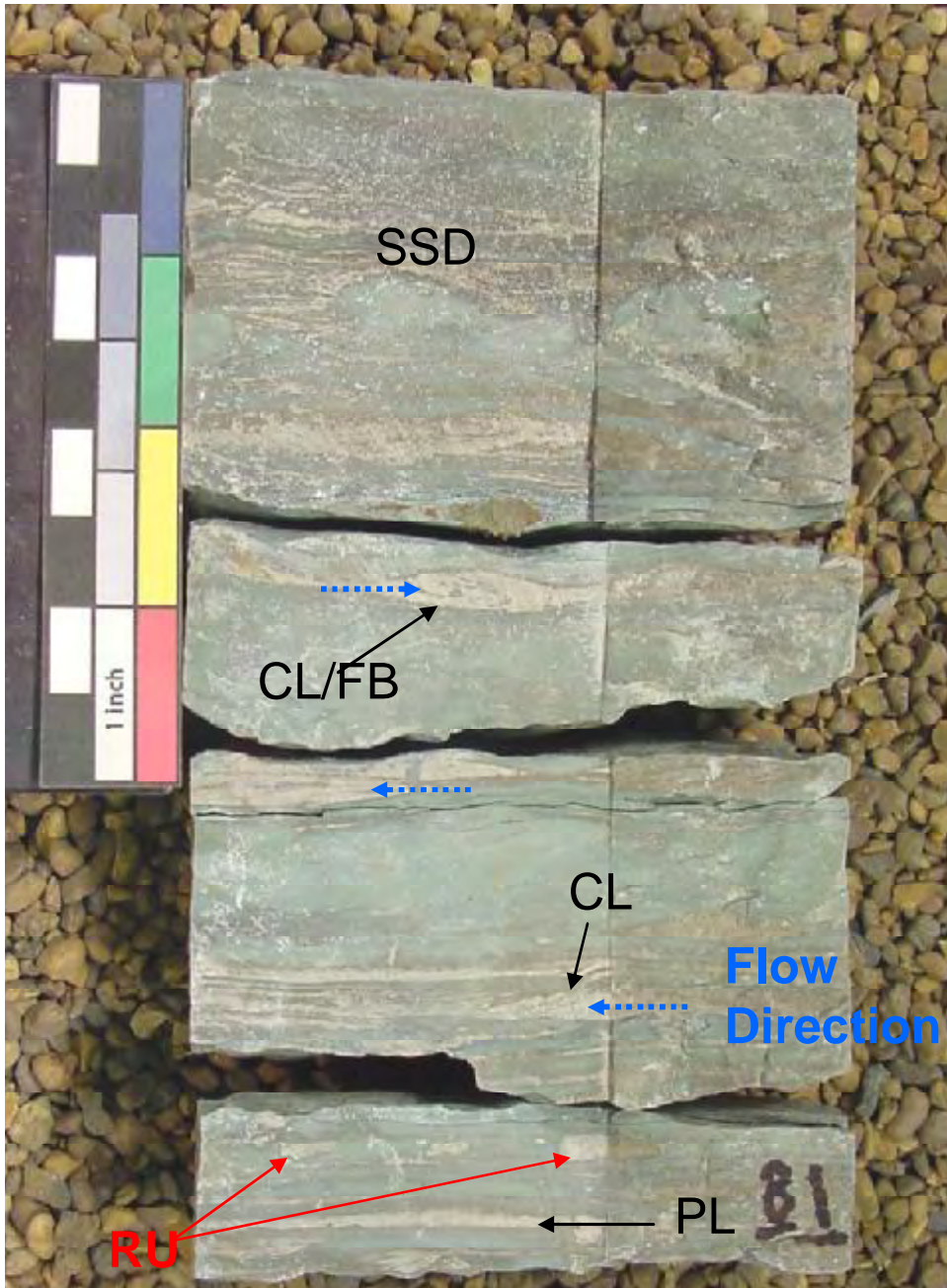


Figure 3.8. Core #11, 10,981 feet. Sedimentary structures present in Facies D are: parallel-laminations (PL), cross-laminations (CL), soft sediment deformation (SSD), flaser- bedding (FB), and rip-up clasts (RU).

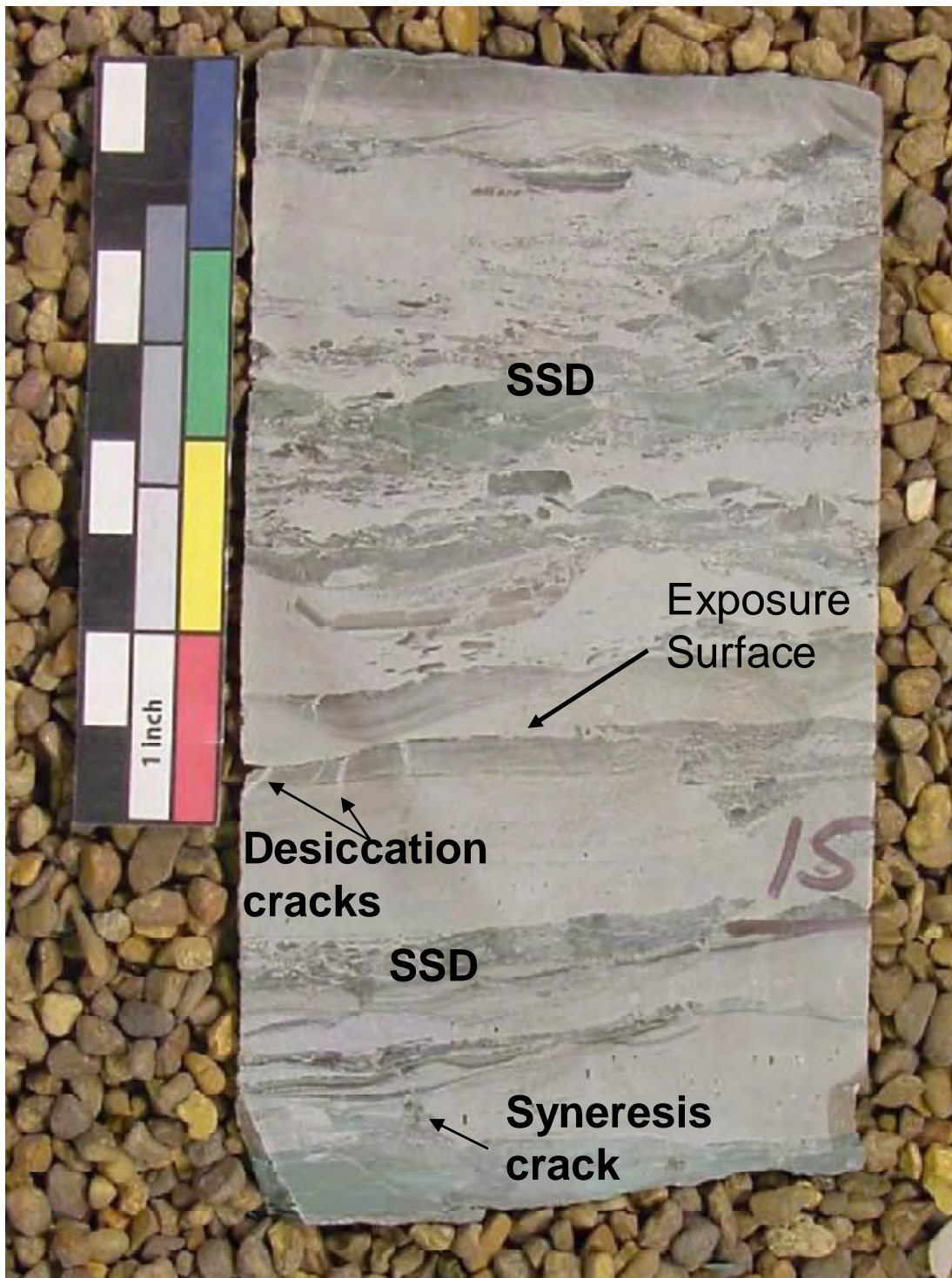


Figure 3.9. Facies D. Core #2. 10,315 feet. Soft-sediment deformation (SSD) is common in Facies D. Desiccation cracks, syneresis cracks and exposure surfaces are also identified in this sample.

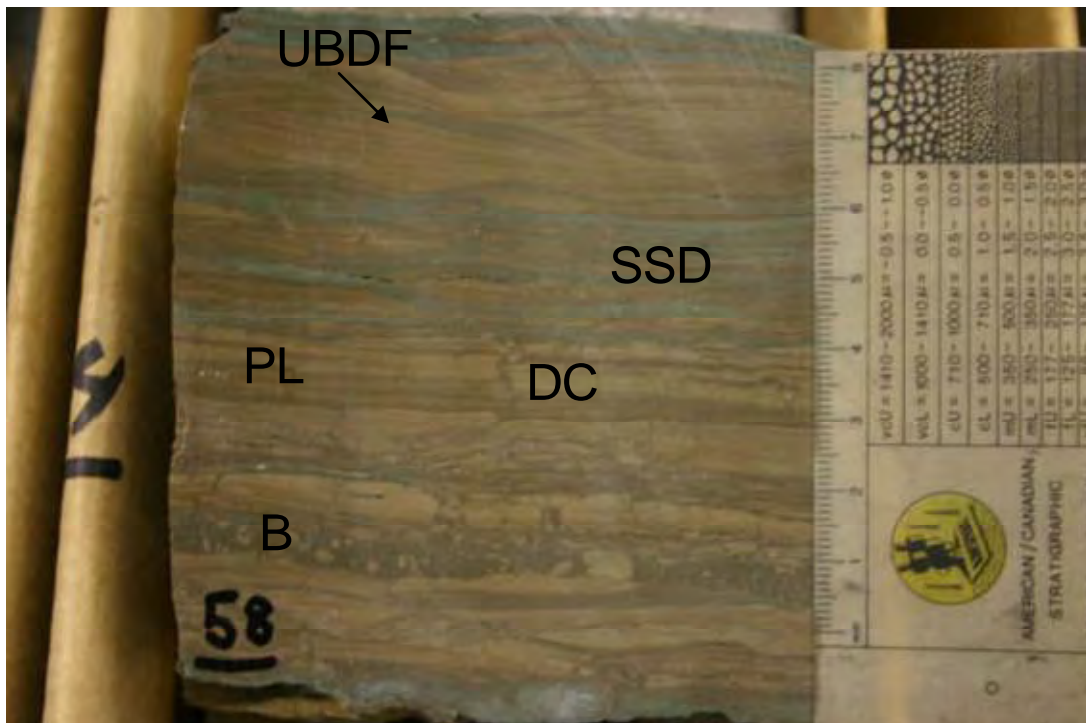


Figure 3.10. Facies D. Core #5, 11,758 feet. Uni-directional and bi-directional flow (UBDF), parallel laminations (PL), desiccation cracks (DC), soft-sediment deformation (SSD), and brecciation (B) are shown in this sample.

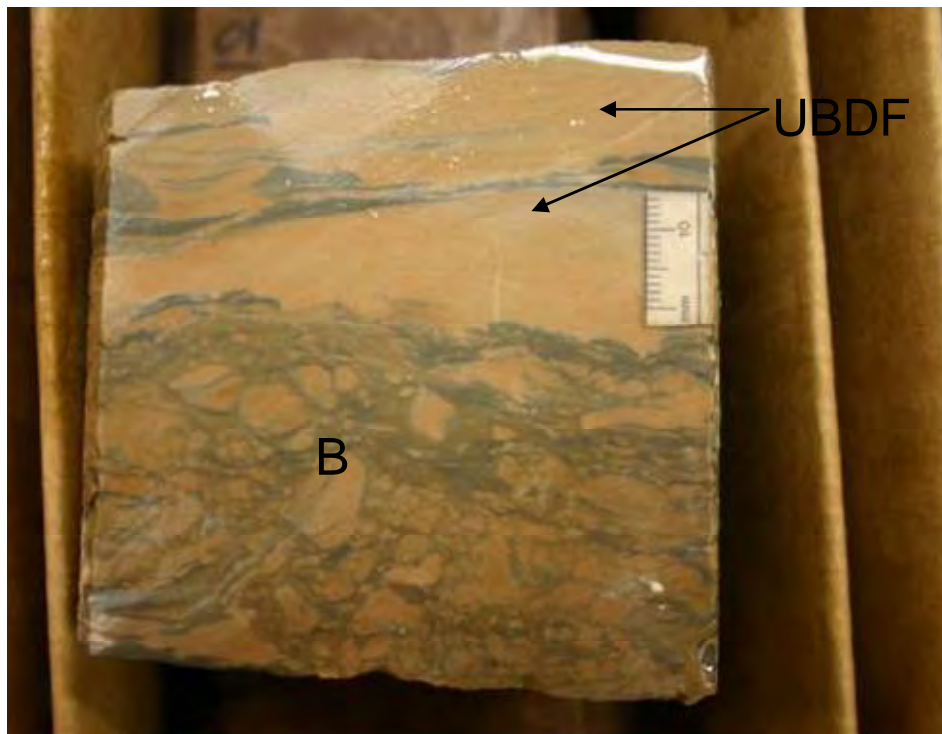


Figure 3.11. Facies D. Core #2. 10,698.8 feet. Brecciation (B) and uni-directional and bi-directional flow (UBDF) are shown in this Sanish sample.

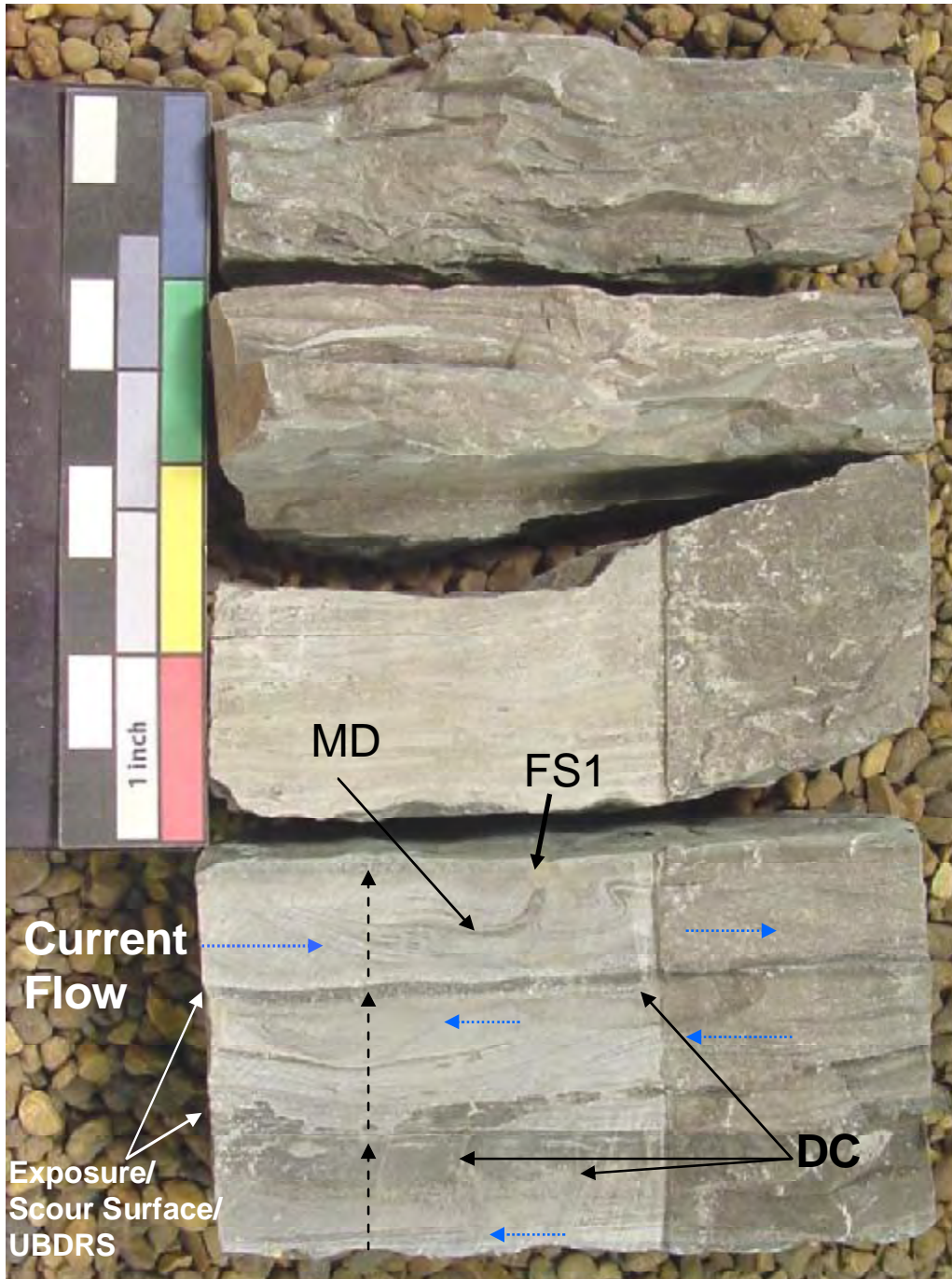


Figure 3.12. Facies D. Core #11. 10,977.5 feet. Mud drapes (MD), type 1 flame structures (FS1), fining upwards cycles (dashed black arrows), desiccation cracks, scour surfaces, exposure surfaces, and uni-directional and bi-directional reactivation surfaces (UBDRS) are all identified in this core sample.

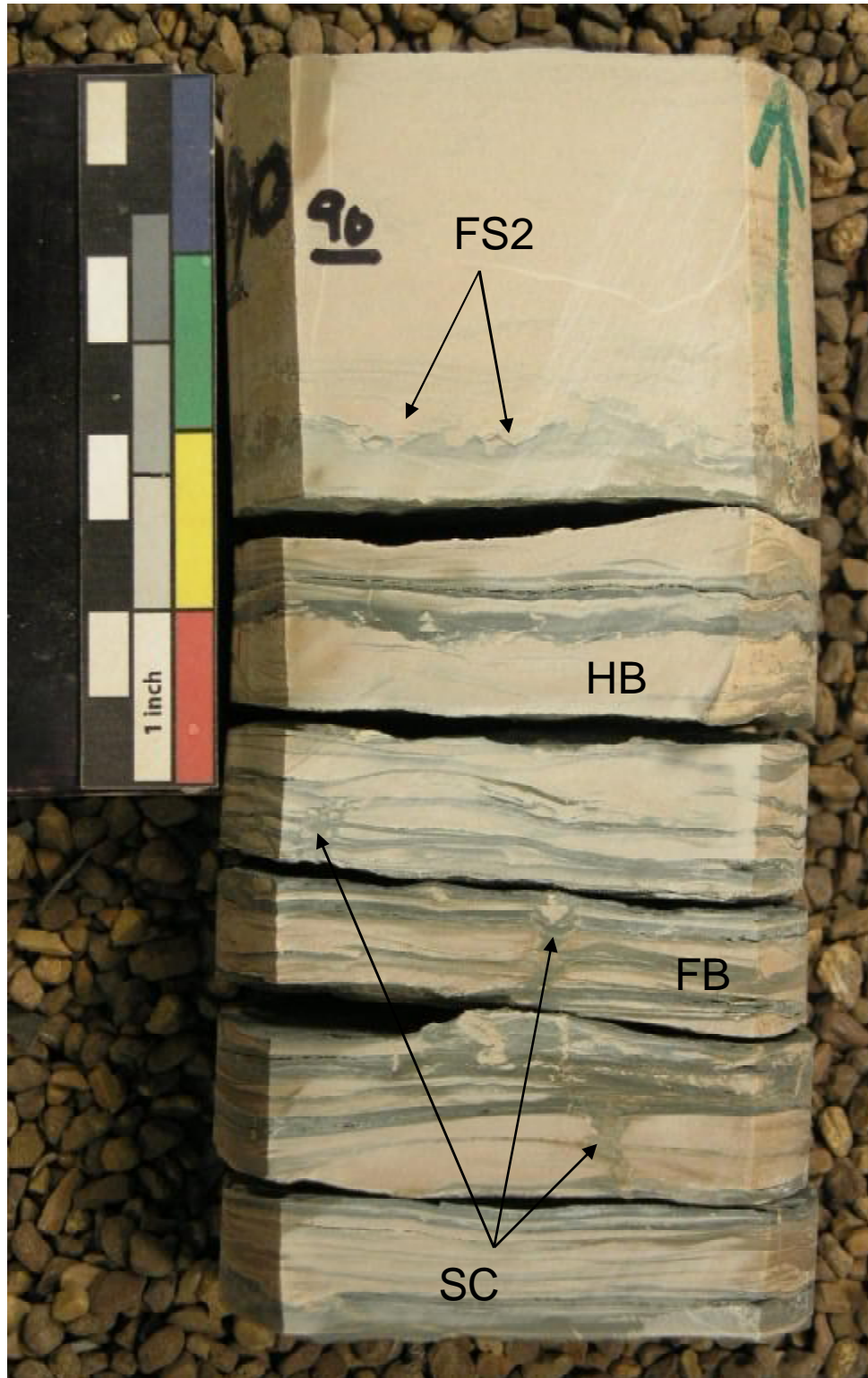


Figure 3.13. Facies D. Core #2. 10,690 feet. Examples of sedimentary structures in Facies D: syneresis cracks (SC), flaser-bedding (FB), herringbone cross-stratification (HB) and type II flame structures (FS2).

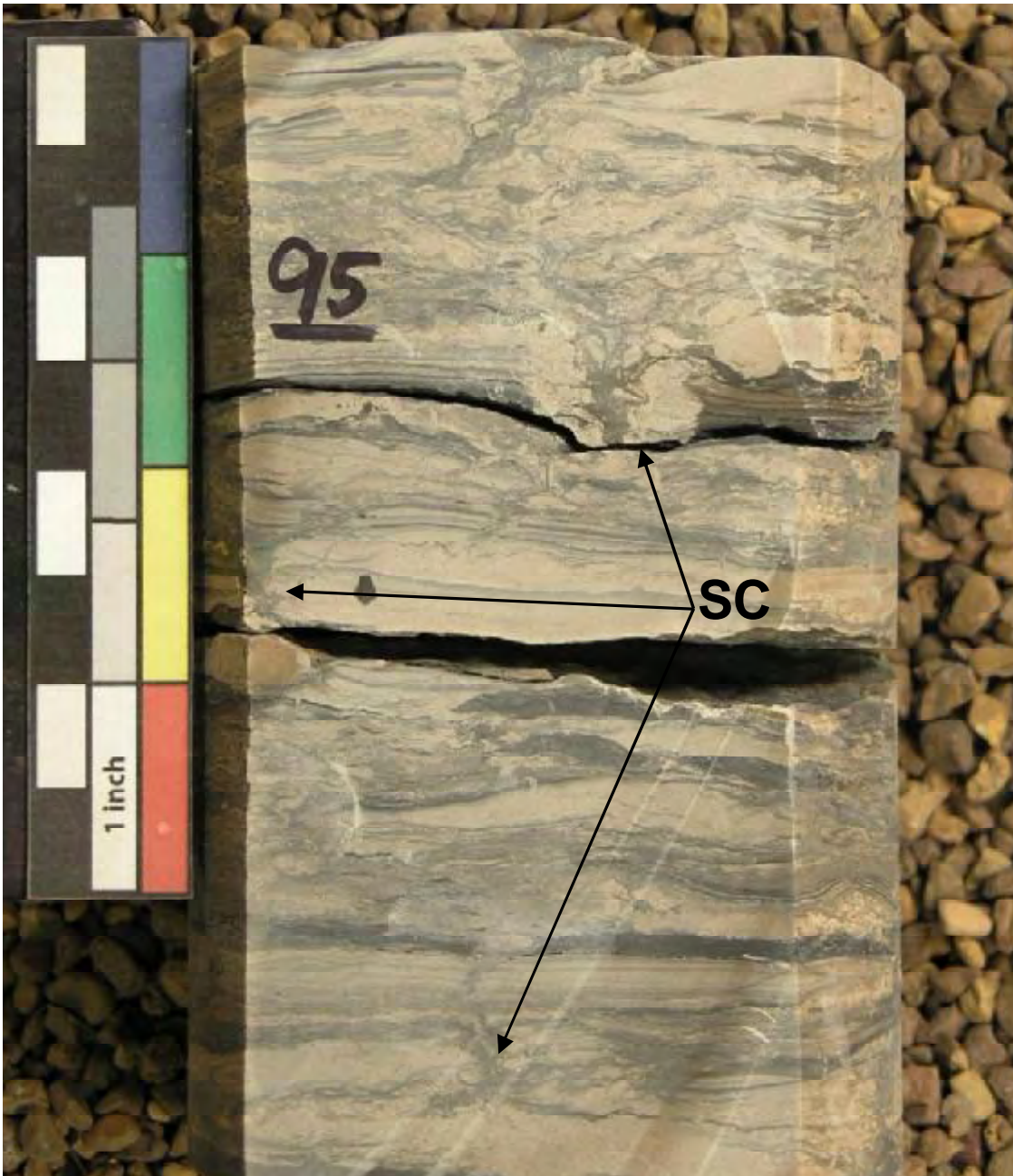


Figure 3.14. Facies D. Core #2. 10,695 feet. Examples of syneresis cracks (SC) are shown in this core sample.



Figure 3.15. Facies E. Core #9. 10,757 feet. Extensive burrowing and bioturbation in Facies E.



Figure 3.16. Facies LBS. Core # 12. 10,214 feet. Facies LBS is a grayish black (N2) to dark black (N1) shale, with parallel-laminations, very thin sandstone and calcite stringers, pyrite nodules.

3.4 Facies Occurrences in Core Samples

Table 3.5.1 summarizes the occurrence of facies in each core in the study area.

Appendix A contains detailed core descriptions.

Core	Facies LBS	Facies E	Facies D	Facies C	Facies B	Facies A
#1	X		X	X	X	
#2	X		X			X
#3	X		X	X	X	
#4	X		X			
#5	X		X			
#6	X		X			
#7	X		X			
#8	X		X			
#9	X	X	X	X	X	
#10	X		X	X	X	
#11	X		X			
#12	X		X			
#13	X		X	X	X	
#14	X		X	X	X	
#15	X		X			
#16	X		X	X	X	
Occurrence %	100%	6%	100%	44%	44%	6%

Table 3.5.1. Facies identified in cores. The percentage of each facies relative to all facies is shown at the bottom of each column.

3.5 Single and Additional Diagnostic Criteria

Described cores yielded several types of primary and secondary sedimentary structures not restricted to a particular depositional environment. Laminations, uni-direction reactivation surfaces, scour-surfaces, loading features (type 2 flame structures), and soft-sediment deformation may be associated with deep marine deposits to fluvial channels (Emery et al.1996; Walker et al.1992). Table 3.5.2 presents these types of primary and secondary sedimentary structures which could be included in many depositional environments.

Table 3.5.3 summarizes the single and additional diagnostic criteria's for the interpretation of the depositional environment (Nao et al.1989; Tucker et al.1990; Kendall 1992; James et al. 1992; Jones et al.1992; Pratt et al. 1992).

3.6 Facies Associations

Table 3.5.4 is an overview of each facies with sedimentary structures that characterize the depositional environment of the Sanish member of the Upper Three Forks Formation. These diagnostic features and structures are critical in interpreting depositional environments.

Non-Specific Criteria (Additional Diagnostic Criteria)	Facies LBS	Facies E	Facies D	Facies C	Facies B	Facies A
Cross-Laminations			X	X		
Parallel-Laminations	X		X	X		
Uni-directional reactivation surfaces			X	X		
Soft-Sediment Deformation			X	X		
Scour Surfaces			X	X		
Loading Features			X	X		
Structureless	X			X	X	X
Burrowing-Bioturbation	X	X				

Table 3.5.2. Sedimentary structures found in the Upper Three Forks Formation that could occur in several depositional environments.

Single Diagnostic Criteria	Facies LBS	Facies E	Facies D	Facies C	Facies B	Facies A
Desiccation Features			X	X		
Mud Drapes			X	X		
Bi-directional Reactivation Surfaces			X	X		
Bottom Sets			X	X		
Flame Structures (Type 1)			X	X		
Flaser-Bedding			X	X		
Herringbone Cross-Bedding			X	X		
Tidal Bundles-Rhythmites			X	X		

Table 3.5.3. Sedimentary structures found in the Upper Three Forks and Sanish member that are diagnostic for intertidal depositional environments.

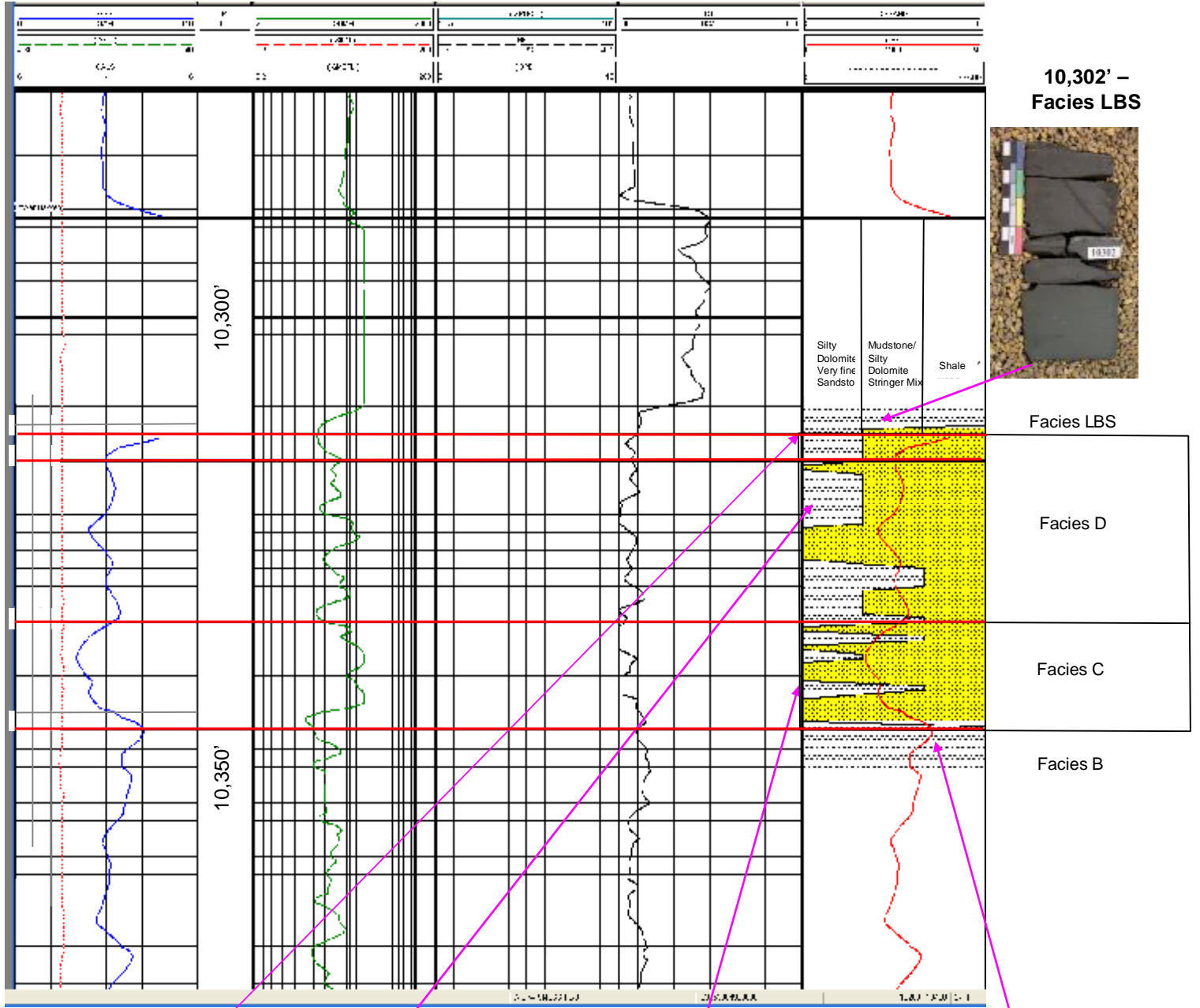
Facies Name	Label	Sedimentary structures	Single-Additional Diagnostic Criteria	Depositional Environment
Dark Black Shale	LBS	Thin, vague, parallel-laminations		Open marine
Burrowed and Slightly Silty Dolomite	E	Burrowed to extensively bioturbated. Sedimentary structures were obscured		Lower Shoreface
Silty Dolomite and Shale	D	Parallel laminations, cross-laminations, soft-sediment deformation, desiccation cracks, scour surfaces, energy-decrease features, loading features, brecciation, and syneresis cracks	Mud drapes, uni- and bidirectional reactivation surfaces, bottom sets, flame structures, flaser bedding, herringbone cross-bedding	Inter-tidal – Supratidal
Highly Deformed and Brecciated Silty Dolomite	C	Soft sediment deformation and brecciation of laminated siltstone clasts		Saline Tidal flat - Sabkha
Calcareous and Very Slightly Silty Dolomite	B	Varying sizes of rip-up clasts in a dolomite matrix		Tidal flat, very shallow marine reworking
Dolomitic and Slightly Silty Shale	A	Varying sizes of rip-up clasts in a shale matrix (Oxidized)		Coastal Plain Sabkha

Table 3.5.4. Facies associations with specific criteria for depositional environments.

3.7 Lithological Chart and Facies Related to Open-Hole Logs

To show the relationship between open-hole logs and the lithological component of the Sanish member, Powerlog© was used to generate a lithological column for each facies. This created an optimum “core to log” presentation (Figures 3.17 – 3.21). The lithological column was categorized as follows: 0 - 1 (mudstone-shale), 1 – 2 (shale-dolomite mix), and 2-3 (dominant siltstone to very fine-grained sandstone component). The lithological column was filled from left to right with shale and from right to left with sand. The sand symbol was used for dolomite. This filling shows the percentage of dolomite and shale in the Upper Three Forks. Finally, the gamma ray curve was overlain on the lithological column to show the relationship between gamma ray and the lithology.

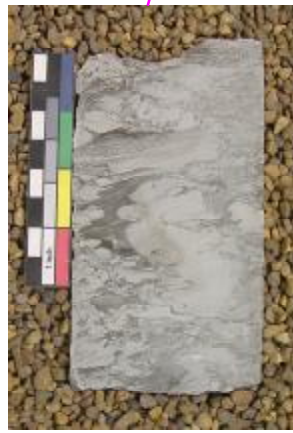
Figure 3.17
Core #1
A.S. Wisness #2 Core Description
152N 96W Sec 3
Core to Log = -12'



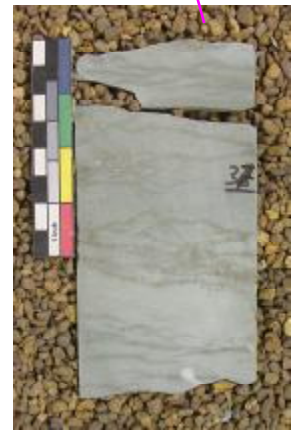
10,304' – Facies D



10,310.2' – Facies D

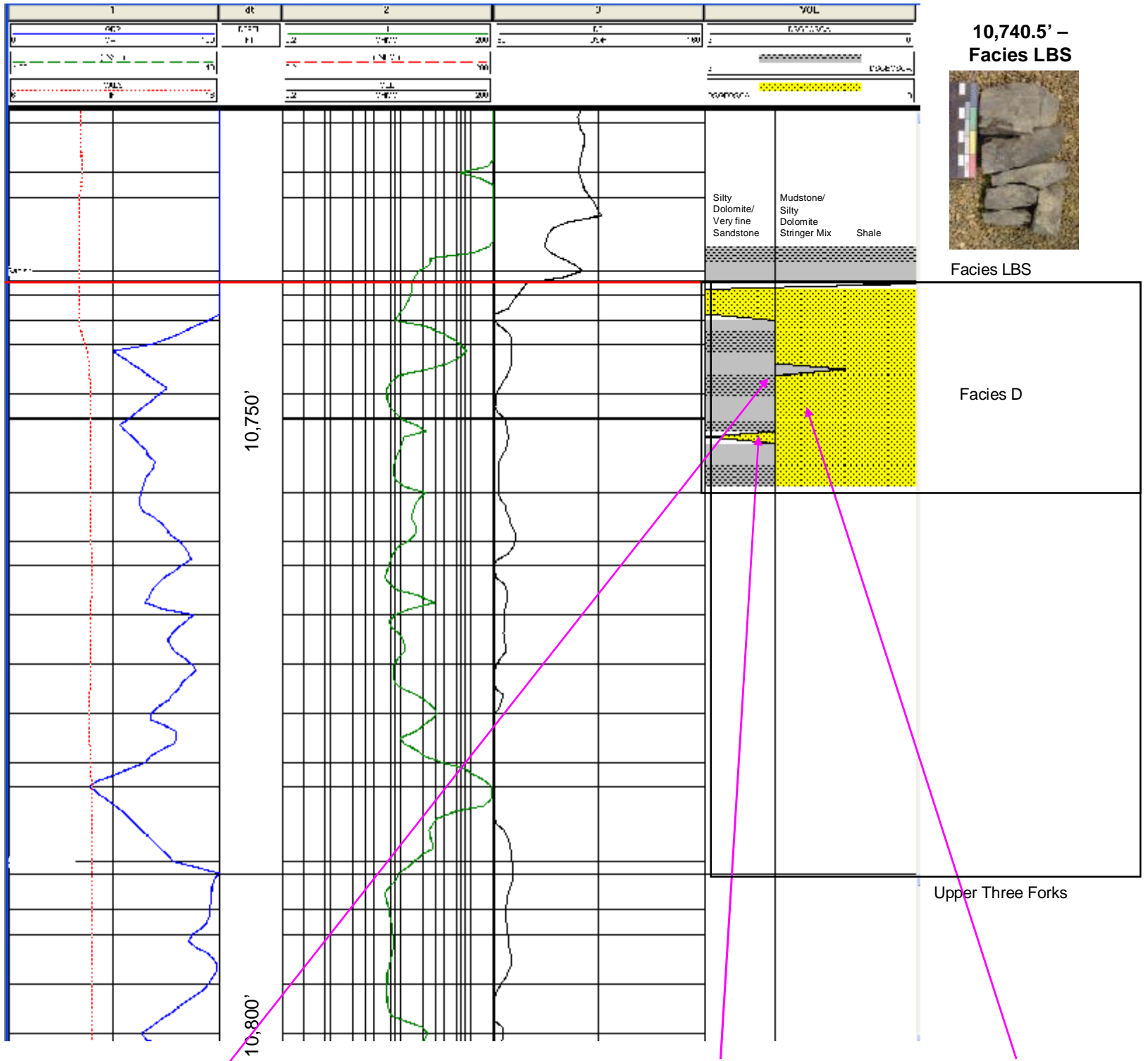


10,333.2' – Facies C



10,337' – Facies B

Figure 3.18
 Core #5
 Fort Berthold – Allottees #1-A Core Descriptions
 150N 93W Sec 4
 Core to Log = -6.8'



10,740.5' – Facies LBS

Facies LBS

Facies D

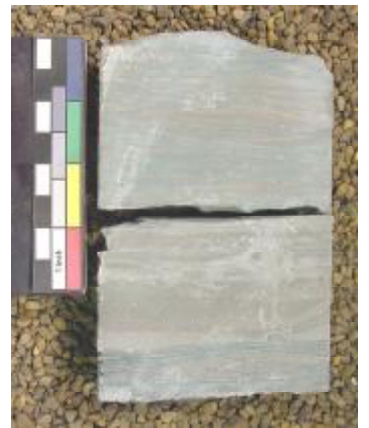
Upper Three Forks



10,750' – Facies D

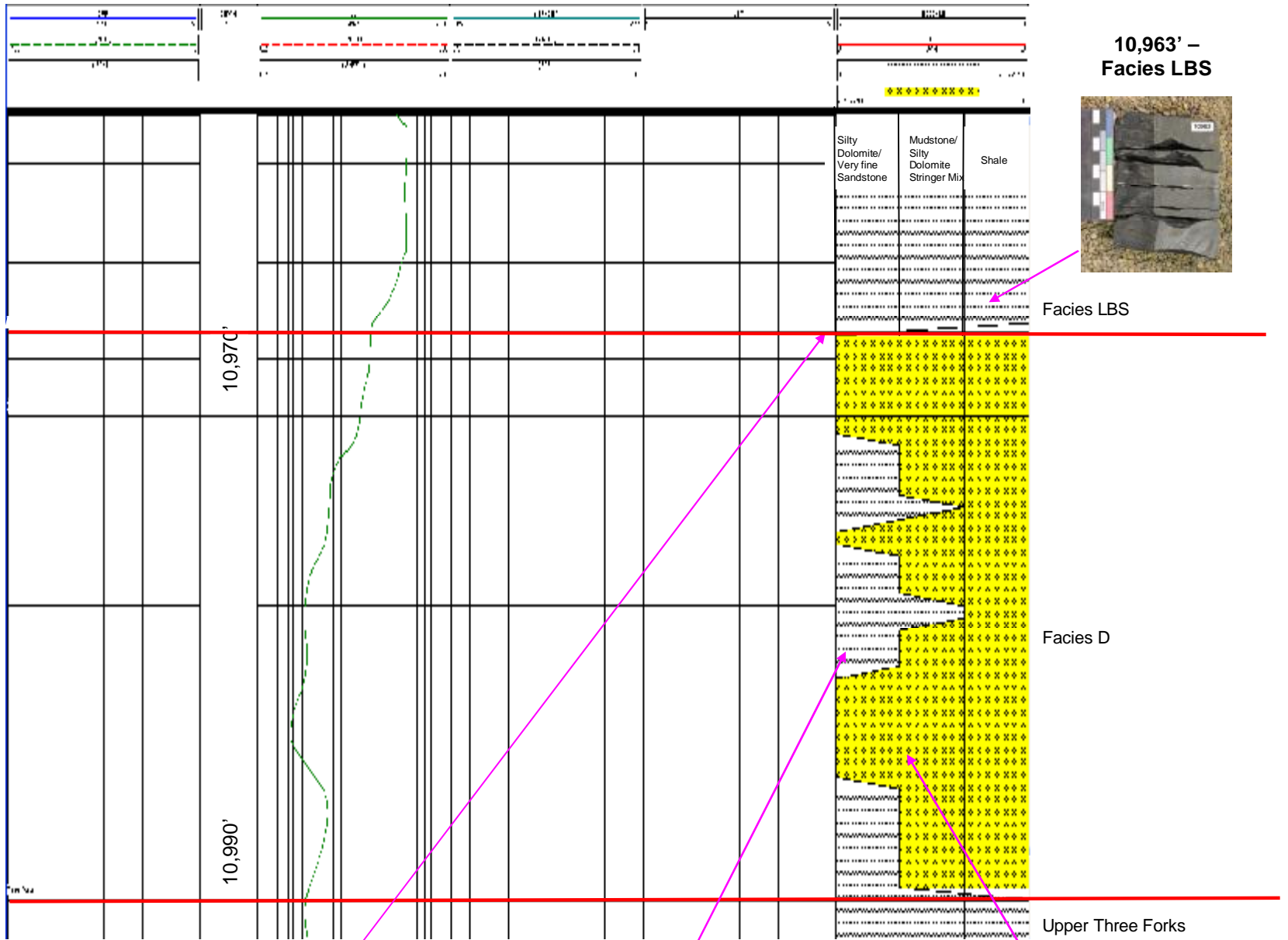


10,755.3' – Facies D



10,751.3' – Facies D

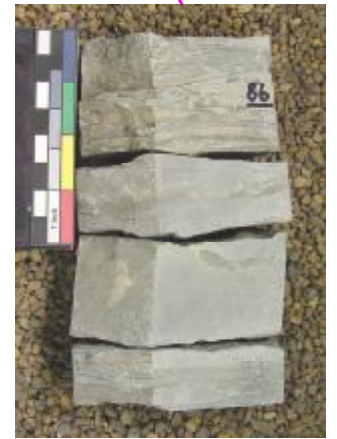
Figure 3.19
Core #11
Minnie Kummer Tract 1 # 1-25 Core Description
150N 96W Sec 25
Core to Log = -1'



10,969' - Contact between Facies LBS and Facies D

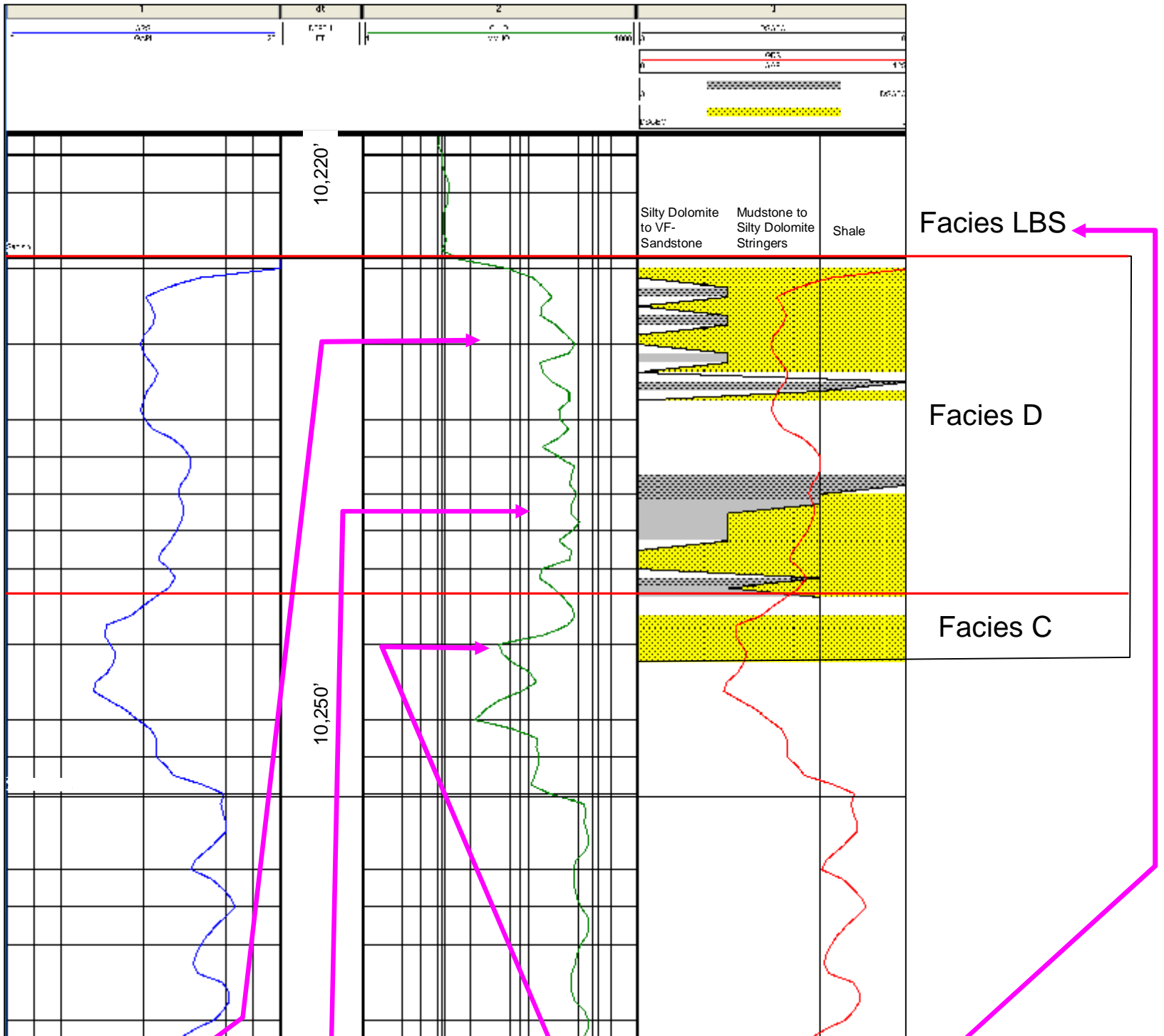


10,982' - Facies D



10,986' - Facies D

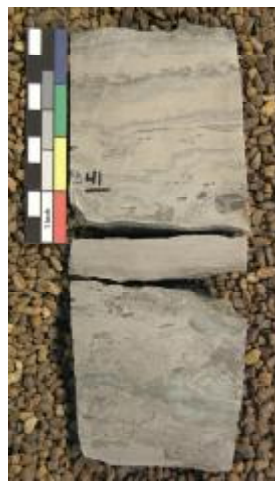
Figure 3.20
 Core #12
 Clarence Pederson (NCT-1)#1-19 Core Description
 157N 96W Sec 19
 Core to log = +6'



10,224' Facies D



10,235' Facies D



10,241' Facies C



10,213' Facies LBS

3.8 Interpretation of Depositional Environments

Primary and secondary sedimentary structures in Table 3.5.2 and diagnostic sedimentary structures in Table 3.5.3 were used to identify Three Forks Formation and Lower Bakken Shale depositional environments. Lithofacies and their interpreted depositional environments are discussed below.

3.8.1 Facies A

Three Forks Facies A occurs in the same stratigraphic position as Facies B, directly below the Sanish member (Figure 3.2). The facies differ in lithology. Facies A is red, dolomitic and slightly silty shale with thin dolomite lenses. Facies B is calcareous and very slightly silty dolomite. The red color of Facies A suggests oxidation in subaerial environments (Figure 3.3). This facies was observed in only one core, core #2. This core was in the southwestern part of the study area and within a Three Forks Formation isopach thin (Figure 3.22) indicating that this facies may occur along the rim of the ancient Upper Three Forks Basin. Furthermore, Facies C is absent in this same core (core # 2) confirming the interpretation that deposition along the edge of the Three Forks Basin affected facies occurrence and distribution. Facies A was deposited in a sabkha where subaerial exposure produced sediment oxidation. (Nao et al.1989; Prothero et al.1996; Scoffin 1987 ; Tucker et al.1990, Walker et al.1992,).

3.8.2 Facies B

Facies B is present at the contact of the Upper Three Forks – Sanish member. (Figure 3.1). This contact is interpreted to be a significant bounding surface which is discussed in detail in Chapter 5.

Several interpretations were made regarding Facies B. Facies B is widespread throughout the study area. It is limey dolomite with angular rip-up clasts of varying size. In the northern part of the study area near the Canadian border (cores #10 and #16 in Figures 3.22; 3.23), rip-up clasts are much larger than those in southern part of the study area. The large clasts are silty dolomite clasts of older tidal-flat deposits

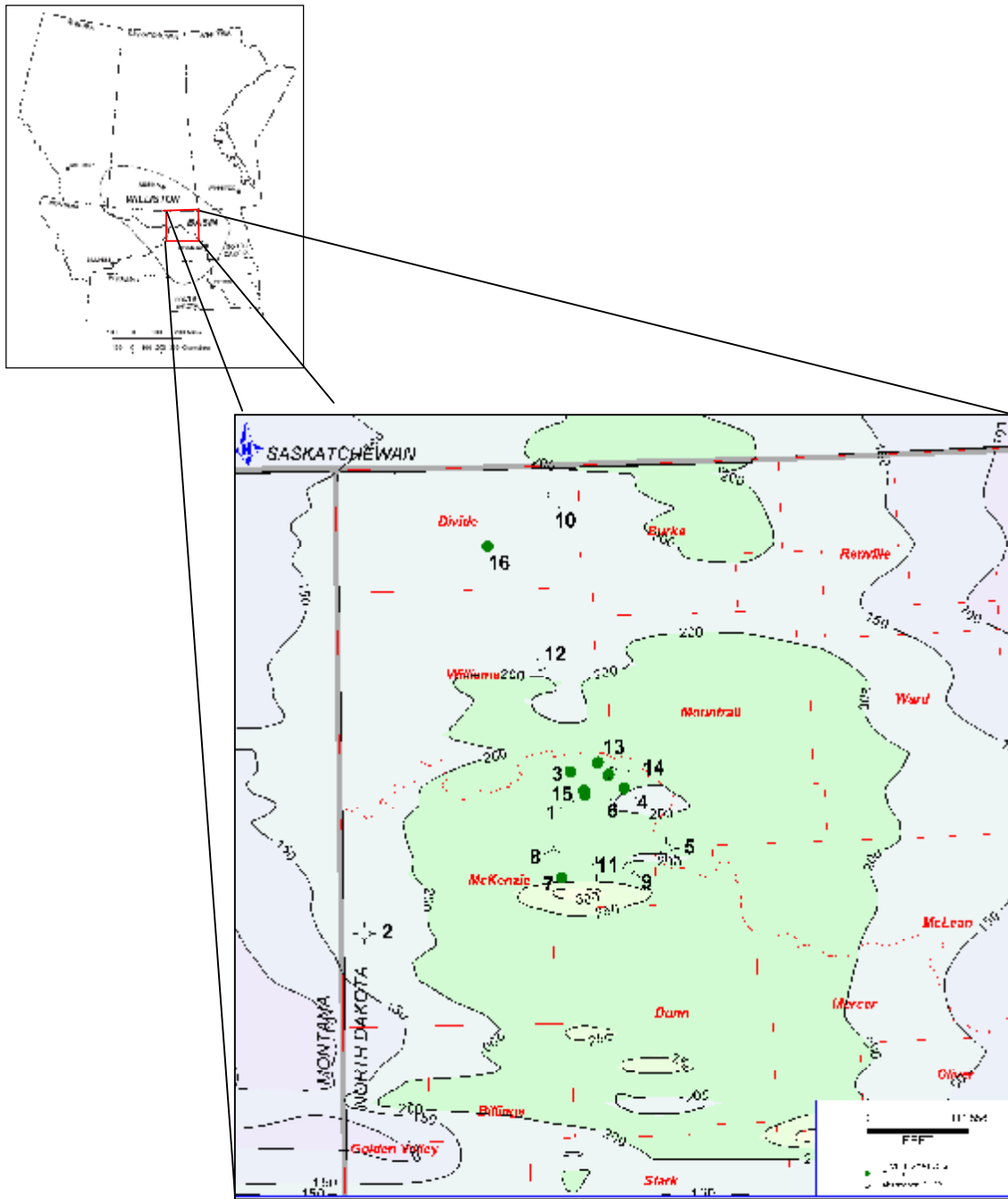


Figure 3.22. An isopach map of the Late Devonian Three Forks Formation shows that most of the cores in this evaluation lie within the thicker portions of the formation. The contour interval is 50 feet. Modified from Pitman et al. (2001).

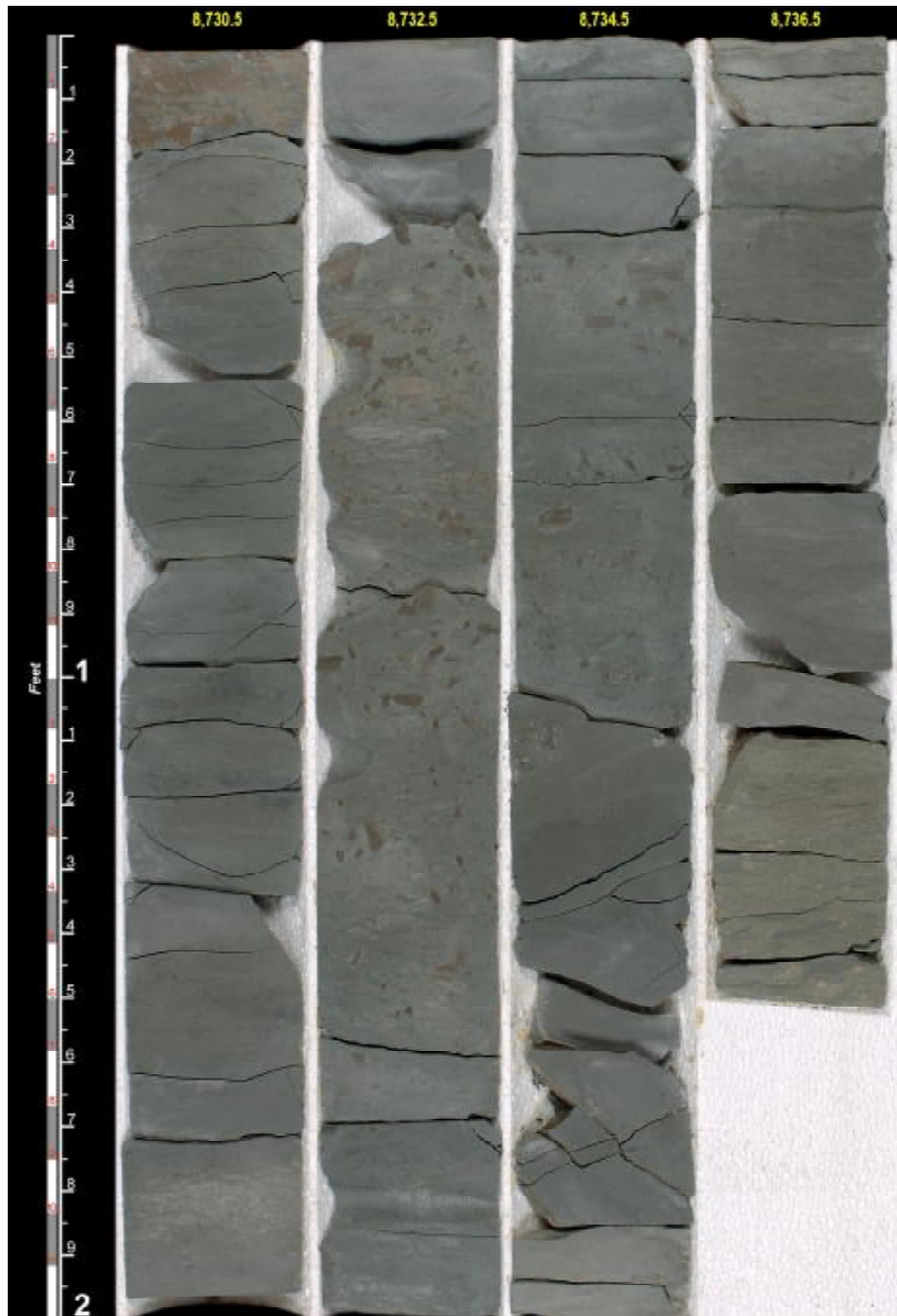


Figure 3.23. Facies B. Core #16., 8,370.5 to 8735.5 feet. Facies B in northern portion of the study area exhibits large rip-up clasts. Used with the permission of Samson Resources.

which were observed in core #16. The core extended below this facies. Smaller clasts in the central and southern portions of the study area may indicate better reworking of clasts or less erosion associated with Facies B.

Throughout the study area, rip-up clasts are not imbricated or ordered. There are no indications of gravity flow or turbidity currents. Likewise, there are no indications of deep water deposition, such as finely laminated beds or thin shale laminations. Therefore, Facies B is interpreted to be shallow restricted marine with storm deposits (Tucker et al.1990; Walker et al.1992). During storms, broken pieces of tidal flat sediments were eroded and redeposited in shallow subtidal environments (Tucker et al.1990; Walker et al.1992).

3.8.3 Facies C

Where present, Facies C is the basal lithofacies of the Sanish member (Figure 3.1). Facies C is highly contorted with significant amounts of soft-sediment deformation and brecciation. Sedimentary structures are sparse (Figure 3.5; 3.24). Limited data indicate that cyanobacteria, hardgrounds, and saline-dry crusts developed on a saline tidal flat and sabkha environment. Desiccation, expansion features, polygons, and tee-pee structures (Figures 3.25; 3.26; 3.27; 3.28; 3.29; 3.30) indicate subaerial exposure in an arid climate. Sediment that later flooded onto this saline tidal flat-sabkha environment was trapped and bound by cyanobacteria and repeated growth of evaporite crystals. Dissolution of the evaporites occurred as a result of upward movement of less-brine-rich groundwater or dissolved by less-brine-rich rain and flood waters. As the cycle repeated, hardgrounds and desiccation features were eroded, reworked, and redeposited as brecciation and rip-up clasts. Desiccation features, such as tee-pee structures, continued to expand, break a part, shrivel and buckle on themselves by the repeated growth and dissolution of evaporites and prolonged exposure (Figures 3.26; 3.27). Void space in the desiccation features were subsequently filled with either evaporites and-or lime mud cements, along with trapped brecciated clasts (Nao et al.1989, Scoffin 1987, Tucker et al.1990, Walker et al.1992). Because energy on the saline tidal flat-sabkha was very low during times of flooding, most of the desiccation features were preserved in-situ (Figure 3.29).



Figure 3.24. Core #16. 8,726.5 to 8729.5 feet. Facies C in northern North Dakota. Used with the permission of Samson Resource.



Figure 3.25. Supratidal flat environment at Fisherman Bay, Spencer Gulf Australia. Tee-pee structures are created at the surface from the lithified polygonal crusts being thrust up by the episodic groundwater recharge. From Kendall (1992).



Figure 3.26. Large, 0.5m, upthrown polygons and tee-pee structures. Devil's Golf Course, Death Valley, U.S.A. From Kendall (1992).



Figure 3.27. Example of desiccation cracks that show buckling effect of polygon edges due to the shriveling of the original microbial (cyanobacteria) mats from prolonged exposure. Hammer is 30 cm long; East Arm Formation, Upper Cambrian, Bonne Bay, western Newfoundland. From Kendall (1992).



Figure 3.28. Cyanobacteria (microbial) mats are wrinkled, shriveled, and are 1-2mm long. These are encrusted with gypsum crystals that are later dissolved. Hyeres salt lagoons, Southern France. From Kendall (1992).

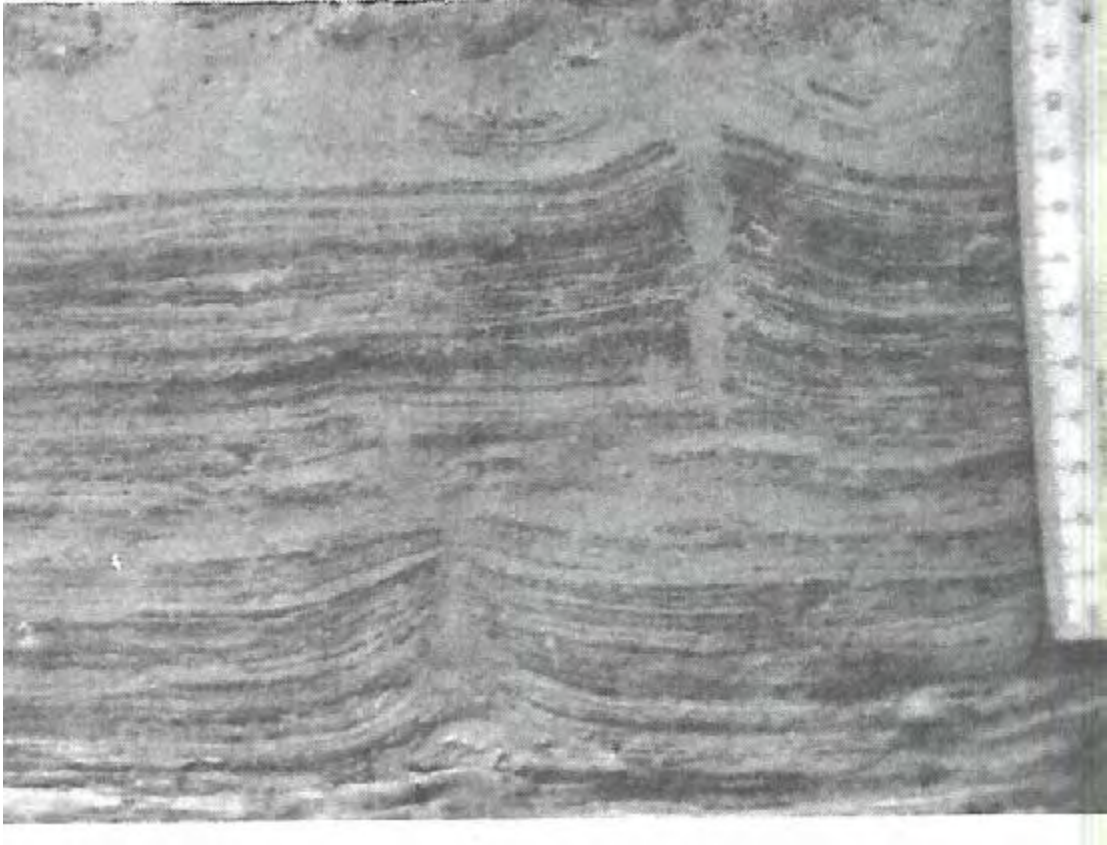


Figure 3.29. Preserved desiccation cracks in a microbial (cyanobacteria) parallel-laminated dolomite. Providence Island Dolomite, Middle Ordovician, Lake Champlain, New York State. From Kendall (1992).



Figure 3.30. Deposited as a laminated silty dolomite, internal sedimentary structures have been destroyed by the repeated growth and dissolution of evaporites and desiccation. Paradox Formation (Pennsylvanian), Utah. From Kendall (1992).

3.8.4 Facies D

Facies D has a variety of sedimentary structures that aid in interpretation. Facies D was deposited in inter-tidal to supratidal environments. This facies has shallowing upward cycles capped by tidal ripples and exposure surfaces with mud and desiccation cracks (Figures 3.9; 3.10; 3.12). The reactivation surfaces are both uni-directional and bi-directional, which is indicative of tidally influenced environments. Bi-directional cross-stratification is an end product of this type of flow (Figures 3.9; 3.9; 3.10; 3.11; 3.12) (Nao et al.1989; Scoffin 1987; Tucker et al.1990; Walker et al.1992). Parallel-laminations are preserved remnants of cyanobacteria that were trapped and shaped into sediment as hardgrounds (Nao et al.1989; Scoffin 1987; Tucker et al.1990; Walker et al.1992). Common breccia fragments are from repeated exposure and tidal current reworking. These clasts were deposited in-situ (Figures 3.8; 3.9; 3.10; 3.11) (Nao et al.1989; Scoffin 1987; Tucker et al.1990; Walker et al.1992).

Mud drapes and type 1 flame structures are abundant in Facies D (Figures 3.12). Sediment was deposited along a migrating ripple. If no instability occurred, a mud-drape was deposited and preserved. If instability occurred during the dominant current stage, the mud drape slid down and along with the newly deposited lamination and formed type 1 flame structures (Nao et al.1989). Type II flame structures formed when dense sediment was deposited on top of less dense sediment. This produced upward narrowing wisps and wedges of mud that were projected into silty dolomite (Figure 3.13) (Compton 1985).

Syneresis cracks are also common in this facies. Unlike desiccation cracks that formed due to desiccation and shrinkage (subaerial), syneresis cracks formed in subaqueous settings. Syneresis cracks display an irregular pattern that pinch out in either direction and can be several inches long (Figures 3.13; 3.14). Syneresis cracks formed within highly porous clays by colloidal suspension, flocculation, and changes in salinity (brines). These syneresis cracks were probably produced by mud layers in Facies D coming in contact with higher salinity waters that were produced by evaporation. In all likelihood, this change in salinity within the mud layers caused dewatering and shrinkage, ultimately resulting in the formation of syneresis cracks (Figures 3.13; 3.14) (Soster 1998).

3.8.5 **Facies E**

Facies E is characterized by extensive burrowing and bioturbation. This facies has no direct indicators of deposition in tidally influenced environments like Facies C and Facies D. The subvertical burrow structures and extensive bioturbation indicate deposition in restricted or stressed marine conditions similar to the lower shoreface environments (Figure 3.15).

3.8.6 **Facies LBS**

Facies LBS is named for the Lower Bakken Shale member of the Bakken Formation (Figure 3.16). To date, numerous publications and studies have been done on this facies and this work agrees with the current interpretation of the Lower Bakken Shale as an anoxic, open marine deposit (Pitman et al.2001; Smith et al. 1995)

3.9 **Summary of the Depositional Environment Interpretation**

Figure 3.31 is a model that depicts the depositional setting of the Sanish member. This diagram shows the relationship between the intertidal environments of Facies D and the saline tidal flat-sabkha environments of Facies C. Sedimentary structures were better preserved in intertidal environments than in the saline tidal flat-sabkha environment where precipitation and dissolution of evaporites destroys most internal sedimentary structure of Facies C (Figure 3.31) (Compton, 1985; Nao et al.1989; Scoffin 1987; Tucker et al.1990; Walker et al.1992).

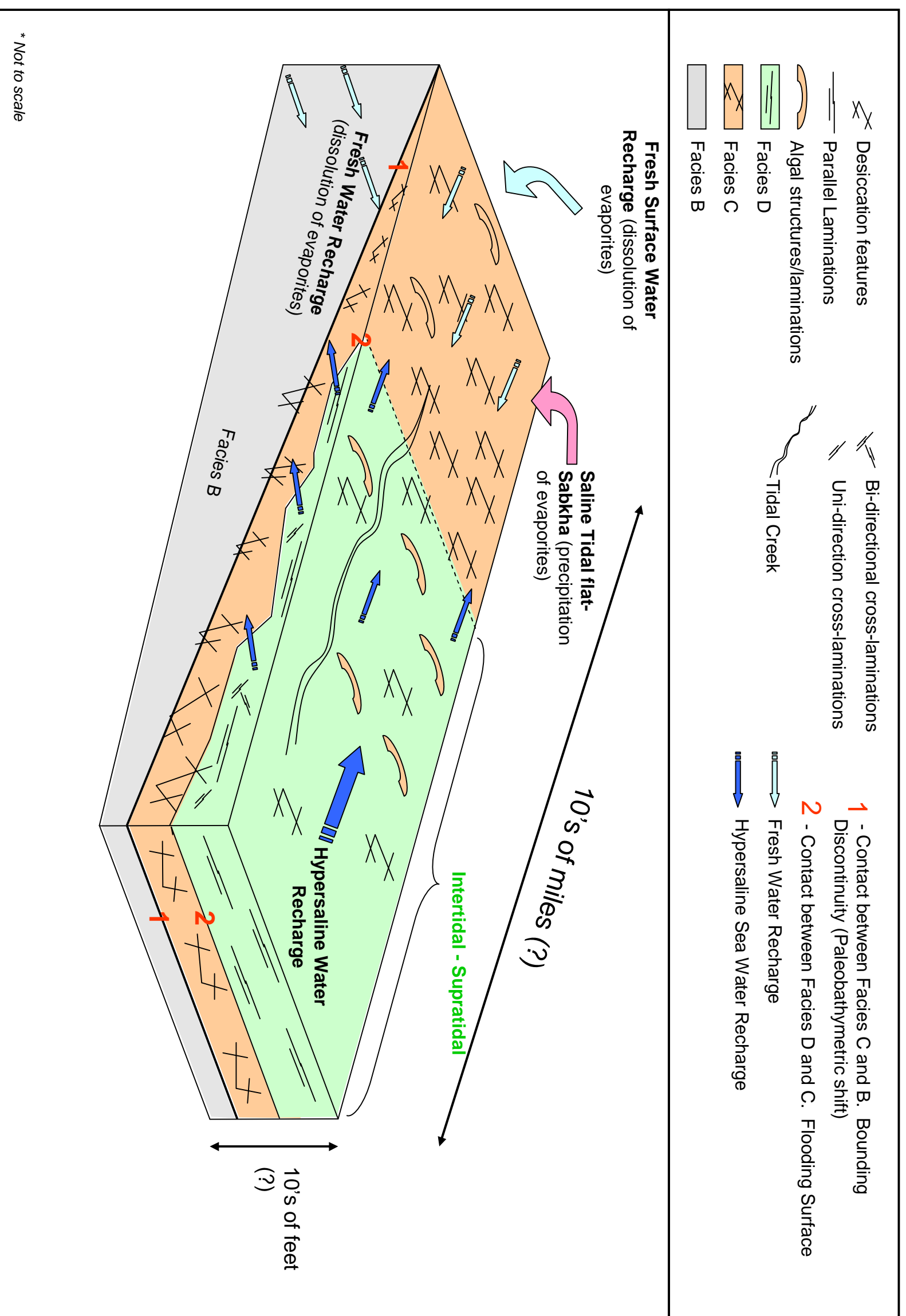


Figure 3.31. Diagram illustrating the typical depositional environments of the Sanish member and associated facies of the Upper Three Forks Formation.

CHAPTER 4

FACIES MINERALOGY

4.1 Introduction

Upper Three Forks (Sanish) and Lower Bakken lithofacies were samples for mineralogy. Facies mineralogy was obtained in the following three ways: 1) X-Ray Diffraction (XRD); 2) Scanning Electron Microscopy with Energy Dispersive X-ray Spectroscopy (SEM-EDS); and 3) Thin-Section analysis. A representative sample of each facies was taken from select cores throughout the study area (Figure 1.1). A total of ten samples were taken from the six lithofacies. If more than one lithology was present in a particular lithofacies, each lithology was sampled.

4.2 XRD Methods

XRD sampling and sample preparation followed procedures in Moore et al. (1997). Facies sampling was designed to evaluate the total mineralogy of a particular sample. To achieve this, a crushing machine was used to crush each sample into a fine powder. The powder of each facies was then placed into the XRD aluminum sample holder using the “random-packed powder mount” method. Each sample was analyzed at 4 degrees to 40 degrees, two theta (4° - 40° 2θ) in order to identify the entire mineral assemblage including the clay fraction.

After the “random-packed powder mount” was performed, it was determined that mixed layered clays of chlorite, kaolinite, and illite were possibly present. Three tests were chosen to identify the clay fraction for each of the samples: 1) orientated – millipore filter transfer method (MFTM) or evaporation-air-dried method; 2) ethanol glycolation; and 3) heat treatment at 550 degrees Centigrade for one hour.

4.3 XRD Results

Appendices B.1 – B.40 show the XRD results for each facies. These data include the random-packed powder, orientated – millipore filter transfer (MFTM) or evaporation-air-dried method, glycolation, and heat treatment tests. All samples detected a mixture of illite, kaolinite and chlorite clays. Smectite was not identified. Table 4.3.1 shows a list of all facies with the minerals identified from the four XRD testing methods.

4.4 SEM-EDS Methods

To further investigate the mineralogy and paragenesis of lithofacies in this evaluation, SEM-EDS analyses were performed. Each lithofacies was broken into a small fragment. The broken side of the sample was placed upright for optimal analysis. Each sample was then affixed to the SEM-EDS sample holder. A carbon coat was continuously applied with an applicator along one edge and onto the SEM-EDS sample holder. (This carbon coat allows for current to run between the sample and the sample holder.) Each sample was then placed into a vacuum and sprayed with a gold coating.

4.5 SEM-EDS Results

Appendices C.1 – C.47 show images of rock constituents for each facies. Table 4.5.1 summarized the data obtained through SEM-EDS analyses. This includes detrital grains and clays, diagenetic cements, authigenic minerals, and authigenic clays.

4.6 Thin-Section Methods

Oversized thin-sections of each facies were prepared by *Wagner Petrographics*, Provo, Utah. Thin-section analyses described the following: lithology, allochems, matrix, grain size, grain shape, sorting, cements, paragenesis, neomorphism and replacement, reservoir potential, and terrigenous components found in each facies. Thin sections are now stored at the North Dakota Geological Survey Core Depository. The following is a summary of thin section analyses.

Facies	Random – Packed Powder	Evaporation-Millipore – Air Dried	Glycolation	Heat Treatment	Appendix
<u>Sample 1</u> Facies D	I, Kspar, D, Qz, Ortho	I, Kao, Chl	PI, Kao, Chl	PI, Chl, Kao?	B.1 - B.4
<u>Sample 2</u> Facies B	I, Kspar, D, Qz, Kao and Py	I, Kao, Chl	PI, Kao, Chl	PI, Chl, Kao?	B.5 - B.8
<u>Sample 3</u> Facies C	I, Kspar, D, Kao and Qz	I, Kao, Chl	PI, Kao, Chl	PI, Chl, Kao?	B.9 - B.12
<u>Sample 4</u> Facies D	I, Kspar, D, Qz, Kao, Chl and Py	I, Kao, Chl	PI and Chl	PI and Chl?	B.13 – B.16
<u>Sample 5</u> Facies A	I, Kspar, D, Qz, Kao and Py	I, Kao, Chl and Kspar	PI, Kao, Chl	PI, Chl, (Kao?)	B.17 – B.20
<u>Sample 6</u> Facies D	I, Kspar, D, Qz, Ca and Py	I, Kao, Chl	PI, Kao, Chl	PI, Chl, (Kao?)	B.21 – B.24
<u>Sample 7 & 8</u> Facies D	I, Kspar, D, Qz, Kao, Chl and Py	I, Kao, Chl and Kspar	PI, Kao and Chl	PI, Chl, (Kao?)	B.25 – B.28
<u>Sample 9</u> Facies D(MD)	I, Kspar, D, Qz, Kao, Chl, Ortho and Py	I, Kao, Chl and Kspar (Ortho)	PI, Kao, Chl	PI, Chl, (Kao?)	B.29 – B.32
<u>Sample 10</u> Facies D(SD)	I, Kspar, D, Qz, Kao and Py	I, Kao and Kspar	PI and Kao	PI, Chl, (Kao?)	B.33 – B.36
<u>Sample 11</u> Facies LBS	I, Kspar, D, Qz, Kao, Chl, Ortho, Musc and Py	I, Kao, Chl and Kspar	PI and Kao	PI, Chl, (Kao?)	B.37 – B.40

Table 4.3.1. XRD Data: Lithofacies and corresponding mineral assemblages for the different XRD procedures. Explanation: I – illite, PI – pure illite, Kspar – potassium feldspar, D – dolomite, Qz – quartz, Kao – kaolinite, Chl – chlorite, Ortho – orthoclase, Ca – calcite, Musc – muscovite, Py – pyrite, and (Kao?) – questionable kaolinite. Heating at 550 °C for one hour makes the kaolinite family of minerals amorphous to x-rays.

Sample	Facies	Authigenic Minerals	Detrital Grains	Clay Matrix	Identified by XRD only	Appendix
1	D	Kspar, D, Py	Kspar, Qz	Kspar, Dolo	I	C.1 – C.4
2	B	D, Chl	D, Kspar	Kspar, Dolo	Kao, Qz	C.5 – C.9
3	C	D, Kspar, Biotite	Qz, Kspar	Kspar, Dolo	I, Chl, Kao	C.10 – C.14
4	D	Qz, D	Ca, Qz	Kspar	I, Chl, Kao, Py	C.15 – C.19
5	A	I, O – Kspar O - I	I, Qz	D, Kspar, I	Chl, Kao	C.20 – C.24
6	D	GC – Kspar GC – Py, GC – Musc	Ca, Qz, Py	??	??	C.25 – C.31
7	D (Mudstone)	O – Kspar, D Py O – Py O – Plag	Kspar, Qz	Kspar (high Fe)		C.32 – C.37
8	D (Siltstone)	D, GC – I GC – Kspar	Qz, Biotite	D-Qz	Chl, Kao Microporosity	C.38 – C.41
9	D (DM)	Py	I, Kspar	I, Kspar	D, Qz	C.42 – C.44
10	D (DS)	D	Qz	D Kspar	Si Cement, Amorphous Fe component Kao, Chl, I	C.45
11	LBS	Framboidal Pyrite	D, Bio Py, Kspar, I	I	Chl, Kao, Qz	C.46 – C.48

Table 4.5.1. SEM Data: Lithofacies with corresponding detrital grains, authigenic minerals and authigenic clay, and depositional clay. If minerals were not found through SEM-EDS but identified in XRD, they are listed in the identified by XRD category. Explanation: I – illite, PI – pure illite, Kspar – potassium feldspar, D – dolomite, Qz – quartz, Kao – kaolinite, Chl – chlorite, Ortho – orthoclase, Ca – calcite, Musc – muscovite, Bio – biotite, Py – pyrite, O – overgrowths, and GC – grain coating.

4.7 Thin-Section Descriptions

The following contains a list of the petrographic analysis and photomicrographs of the interpreted facies.

4.7.1 Facies: A

Microfacies Description: Dolomitic and slightly silty shale

Lithology: Dolomitic and slightly silty shale

Allochems: None

Matrix: Clay (illite)

Crystal Size: Very fine to fine-crystalline dolomite

Crystal Shape: Euhedral to subhedral

Grain Size: Silt

Grain Shape: Angular to subrounded

Sorting: Poor

Cement: Dolomite

Paragenesis: Dolomitization of micrite and shale

Neomorphism and Replacement: Pyrite replacement

Reservoir Potential: None

Terrigenous Component: Detrital quartz

Appendix: D.1

4.7.2 Facies: B

Microfacies Description: Calcareous and very slightly silty and sandy dolomite

Lithology: Limey and silty dolomite

Allochems: None

Matrix: Clay (illite) and micrite

Crystal Size: Very fine to medium-crystalline dolomite

Crystal Shape: Euhedral to subhedral

Grain Size: Silt to very-fine grained sand ($< 125\mu$; $\geq 3.0 \text{ } \emptyset$)

Grain Shape: Angular to subrounded

Sorting: Poor

Cement: Dolomite

Paragenesis: Dolomitization of micrite and recrystallization of dolomite to dolospar

Neomorphism and Replacement: Pyrite replacement of dolomite

Reservoir Potential: Poor to none – microfractures may enhance permeability

Terrigenous Component: Detrital quartz

Appendix: D.2

4.7.3 Facies: C

Microfacies Description: Silty dolomite

Lithology: Silty dolomite

Allochems: None

Matrix: Clay (illite)

Crystal Size: Very fine to medium-crystalline dolomite

Crystal Shape: Euhedral to subhedral

Grain Size: Silt

Grain Shape: Angular to subrounded

Sorting: Poor

Cement: Dolomite

Paragenesis: Probable dolomitization of micrite and recrystallization of dolomite to dolospar

Neomorphism and Replacement: Pyrite replacement of dolomite and matrix

Reservoir Potential: Poor to Good – locally porous and microfractures enhance permeability

Terrigenous Component: Detrital quartz

Appendix: D.3

4.7.4 Facies D

Microfacies Description: Silty and sandy dolomite and shale

Lithology: Silty dolomitic and shale

Allochems: None

Matrix: Shale, illite, and chlorite

Crystal Size: Very fine to medium-crystalline dolomite

Crystal Shape: Euhedral to subhedral

Grain Size: Silt to very-fine sand ($< 125\mu$; $\geq 3.0 \text{ } \emptyset$)

Grain Shape: Angular to subrounded

Sorting: Poor

Cement: Dolomite

Paragenesis: Probable dolomitization of micrite and recrystallization of dolomite to dolospar

Neomorphism and Replacement: Pyrite replacement of matrix and dolomite

Reservoir Potential: Poor to fair – microfractures may enhance the permeability

Terrigenous Component: Detrital quartz

Appendix: D.4 – D.11

4.7.5 Facies E

Microfacies Description: Silty burrow mottled dolomite

Lithology: Silty dolomitic

Allochems: None

Matrix: Illite

Crystal Size: Very fine to medium-crystalline dolomite

Crystal Shape: Euhedral to subhedral

Grain Size: Silt

Grain Shape: Angular to subrounded

Sorting: Poor

Cement: Dolomite

Paragenesis: Probable dolomitization of micrite and recrystallization of dolomite to dolospar

Neomorphism and Replacement: Pyrite replacement of matrix and dolomite

Reservoir Potential: Poor to fair – microfractures may enhance the permeability

Terrigenous Component: Detrital quartz

Appendix: D.4 – D.11

4.7.6 Facies: LBS (Lower Bakken Shale)

Microfacies Description: Silty and calcareous, organic-rich shale

Lithology: Shale

Allochems: Fossil shell fragments (brachiopod)

Matrix: Clay (illite)

Crystal Size: Very fine to fine-crystalline dolomite

Crystal Shape: Euhedral to subhedral

Grain Size: Silt

Grain Shape: Angular to rounded

Sorting: Poor

Cement: Dolomite

Paragenesis: Minor dolomitization of matrix

Neomorphism and Replacement: Pyrite replacement of shale and dolomite

Reservoir Potential: None to poor – microfractures may enhance permeability

Terrigenous Component: Detrital quartz

Appendix: D.12 – D.13

4.8 Comparison of XRD, SEM-EDS, and Thin-Section Results

The XRD, SEM-EDS, and thin-section analyses produced similar results. Each facies has minor amounts of detrital quartz, orthoclase and plagioclase feldspar, muscovite and biotite mica, detrital and authigenic dolomite, and authigenic pyrite. Clay minerals are a mixture of chlorite, kaolinite and illite. The “glycolation” method detected pure illite, while the “heating” method detected chlorite. It was not determined whether kaolinite and chlorite occur together.

4.8.1 Illite Problem

Illite, $(K,Na,Ca)(Al,Mg,Fe)_2(Si,Al)_4O_{10}(OH,F)_2$ was identified in XRD and inferred in thin-sections as clay matrix. Illite was difficult to detect with SEM-EDS. This difficulty was most likely a result of illite’s small crystal size. All samples contained varying proportions of potassium (K), aluminum (Al), and silica (Si). Potassium (K) and aluminum (Al) peaks that are of similar intensity and could be orthoclase (potassium feldspar). Recognition of illite with the SEM-EDS is difficult because the electron beam targets not only the small illite crystals but also the surrounding grains and matrix producing ambiguous readings. However, SEM-EDS and thin-section analysis confirmed the presence of pure illite as a major part of the clay matrix.

4.8.2 Kaolinite Problem

Kaolinite, $Al_4Si_4O_{10}(OH)_8$, was detected in the XRD plots, but kaolinite was not detected in either SEM-EDS or thin section analysis. With SEM-EDS analyses, kaolinite may be present, but the electron beam was possibly overshadowed by the chemical composition of kaolinite. Kaolinite contains both aluminum (Al) and silica (Si), which are also present in potassium feldspar and illite.

4.9 Interpretation of the Mineralogical Results

All lithofacies exhibited many similar and non-similar characteristics which are discussed and interpreted below.

4.9.1 Sheet Silicate Minerals – Biotite and Muscovite

Biotite, $K(\text{Mg, Fe})_3(\text{AlSi}_3\text{O}_{10})(\text{OH})_2$, is a silicate mineral with sheet structures that occurs in igneous rocks rich in feldspars, such as granite, and in certain metamorphic rocks such as schist. During weathering, biotite becomes leached of its alkalis (Na and K). This weathering action of biotite may have played a major role in the formation of secondary minerals, especially chlorite, as described below (Blatt et al.1996; Dietrich et al.1979; Klein 2002).

Muscovite, $\text{KAl}_2(\text{AlSi}_3\text{O}_{10})(\text{OH})_2$, is another common sheet silicate mineral that occurs in igneous and metamorphic rocks. The (001) peak of illite near $8.8^\circ 2\theta$ in all samples was interpreted to be pure illite. Muscovite has the same XRD (001) signature and can easily be confused with pure illite (Moore et al.1997). The only XRD sample that contained detrital muscovite was sample #11 which is from the Lower Bakken Shale (LBS).

4.9.2 Silicate Minerals with Framework Structures – Feldspar

Potassium feldspar, $\text{K}(\text{AlSi}_3\text{O}_8)$, can occur in all types of rocks and is one of the most widely distributed and abundant minerals in the earth's crust (Dietrich et al.1979; Klein 2002). When surface and subsurface waters act upon feldspars, silica is liberated as free silica. Along with K and Al, this free silica forms clay minerals. Examples of clay minerals that can be formed by the free alkali process include smectite-illite and chlorite, which were both found to be abundant in the Sanish member (Blatt et al.1996; Dietrich et al.1979; Klein 2002; Moore et al.1997).

All six facies analyzed with XRD have detrital potassium feldspar, with a consistent potassium feldspar peak around $27.5^\circ 2\theta$ (Moore et al.1997). Potassium feldspar minerals include: 1) orthoclase, which crystallizes from plutonic rocks; 2) microcline, which is the invert of orthoclase as the rock cools; and 3) sanidine, which is typical of very high temperature minerals related to volcanic rocks (Blatt et al.1996).

Samples 9, 10, and 11 had XRD peaks that indicated an orthoclase component (Moore et al.1997). For the remaining samples, XRD data were inconclusive for orthoclase identification.

4.9.3 Smectite-Illite – Smectite Illitization

Smectite $(Ca,Na)_x(Al,Mg,Fe)_4(Si,Al)_8O_{20}(OH,F)_4 \cdot nH_2O$ has been a subject of high interest in clay mineralogy. Smectite forms in various ways: 1) the alteration of volcanic glass; 2) alteration of potassic-rich minerals by slow-moving water in various surface environments; 3) directly from illite, kaolinite, and chlorite (Moore et al.1997). This study infers that smectite initially formed near the surface as a result of feldspar alteration. It was then converted to illite through smectite illitization.

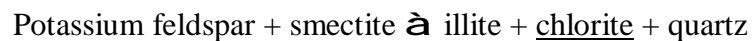
The three most important factors involved with the conversion of smectite to illite are burial temperature, time, and availability of potassium (figure 4.1) (Moore et al.1997). All facies in this evaluation are from cores within the Thee Forks-Bakken oil window in the Williston Basin (Meissner 1978). Rocks were buried deeply enough to initiate illitization. As smectite was buried with potassium feldspar, potassium, aluminum, and silica were liberated. These elements, combined with temperature and time, drove the system to illitization.

XRD results confirm that smectite was converted to illite. Pure illite occurred at a sharp (001) peak at $8.8^\circ 2\theta$ (Moore et al.1997). This sharp peak was consistent with all four of the XRD methods indicating that the illite conversion occurred from either muscovite, smectite, or both. Muscovite was only found in Facies A as a grain coating and not as a detrital grain. Smectite was not identified in any samples. However, because less than 10 percent of interstratified material is difficult to detect through XRD, it is assumed that at least 10 percent of the “pure” illite was mixed with interstratified clays such as smectite and-or chlorite (Moore et al.1997).

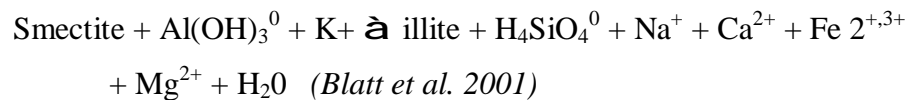
4.9.4 Sheet Silicate Mineral – Chlorite

Chlorite, $(Mg, Fe, Al)_6[(Si, Al)_4O_{10}](OH)_8$, is another common silicate mineral that owes its origin to diagenetic processes associated with minerals that contain iron, aluminum, and magnesium (Blatt et al.1996; Dietrich et al.1979; Klein 2002; Moore et

al.1997). As described above, free potassium is used to create illite during smectite illitization. Chlorite is formed at the expense of remaining potassium feldspar and smectite (Figure 4.1) (Moore et al.1997). With XRD testing, chlorite occurred in all the samples with a (001) peak increase, while the (002), (003), and (004) peaks were suppressed (Moore et al.1997). The green shale beds of Facies D are chloritic and had high Fe content in chlorite with a very low (001) peak. Other facies with chlorite did not indicate high Fe content. These results suggest that, in the Sanish member, chlorite was formed through two types of secondary geological processes (Moore et al.1997). The first was the alteration of iron-magnesium silicates from biotite. The second process was smectite illitization. Hower et al. (1981) argues that during smectite illitization:



(Moore et al. 1997)



Because chlorite is present in the Sanish member, it could be the other clay for the less than 10 percent intrastratified mineral mixed with illite as described by Moore et al.(1997). The liberated silicate minerals from K-spar could have enabled the formation of chlorite. Thus, the interstratified material was interpreted to be chlorite rather than smectite.

Though chlorites have six-sided plates and tablets that are usually recognizable in SEM-EDS (Moore et al.1997), chlorite was not identified with SEM-EDS and thin-section analysis. Chlorite's mineralogical make-up is very similar to potassium feldspar and illite (Moore et al.1997). The clay matrix of every lithofacies contained potassium feldspar, dolomite, and illite. Chlorite was probably not identified because the EDS spectrum identified surrounding grains and clays. In addition, chlorite was most likely in the less than 10 percent mixture with illite, making it amorphous to SEM-EDS, but recognizable in XRD.

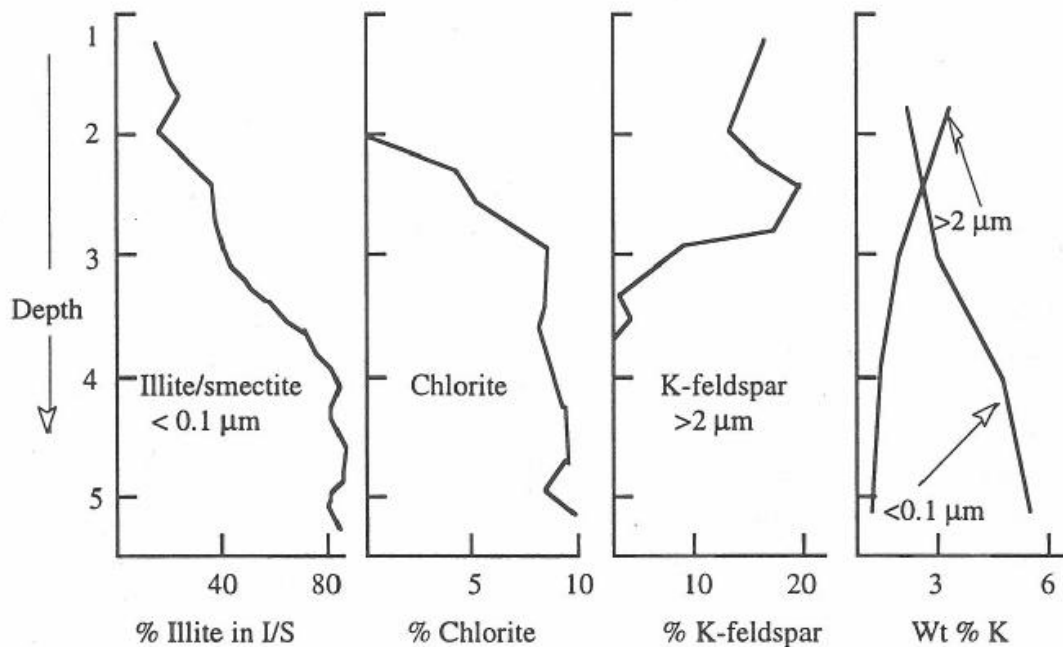


Figure 4.1. During the process of smectite illitization, potassium is liberated from K-spar. This “freeing” of potassium from K-spar enables the conversion of smectite to illite. Other free silicates are liberated from k-spar and these aid in the creation of secondary minerals such as chlorite and quartz. From Moore et al.(1997, p. 176).

4.9.5 Quartz

The two most abundant elements in the earth’s crust are silicon and oxygen (Dietrich et al.1979). When these two minerals combine to form $(\text{SiO}_4)^{4-}$, they comprise a major structural unit and the most abundant group of rock-forming minerals – silica (quartz) and the silicate mineral group (feldspars). Unlike feldspar, which uses Al^{+3} to substitute some of the Si^{+4} during its formation, quartz charges balance by sharing each of its four oxygens of the silica tetrahedron with adjacent tetrahedrons. Quartz, (SiO_2) , follows feldspar as the second most abundant mineral in the earth’s crust (Blatt et al.1996; Dietrich et al.1979; Klein 2002).

Quartz occurs in the Sanish as angular to rounded, silt to fine-grained detritus, and it was observed in every SEM-EDS and thin-section. Quartz also occurs as sparse authigenic quartz overgrowths (Appendix C.16). The quartz overgrowths formed in two

ways: 1) fluids moving through the rock became saturated with respect to silica 2) potassium feldspar combined with smectite to yield illite, chlorite, and quartz (including quartz overgrowths) (Blatt et al.1996; Dietrich et al.1979; Klein 2002; Moore et al.1997). It is inferred that smectite illitization was probably the mechanism for authigenic quartz formation.

4.9.6 Dolomite

Three types of dolomite, $\text{Ca}(\text{Mg,Fe})(\text{CO}_3)_2$ were found in the Sanish member: primary, detrital, and secondary. Primary dolomite was created at or near the surface of tidal flat environments in hardgrounds or crusts. These were eventually brecciated and redeposited as the next major tidal flood swept across the tidal flats (Blatt et al.1996; Dietrich et al.1979; Klein 2002; Nao et al.1989; Tucker et al.1990; Walker et al.1992).

Detrital dolomite grains were eroded from dolomitic strata that surrounded the basin and were transported and deposited as detritus. These grains tend to be subrounded to rounded and differ from in situ fragments associated with brecciated crusts and hardgrounds.

Dolomite also occurs in the Sanish member as authigenic dolomite. Authigenic dolomite is created during burial when dolomitizing fluids move through pore space and selectively replace limestone or other minerals (Blatt et al.1996; Dietrich et al.1979; Klein 2002; Tucker et al.1990; Walker et al.1992). Authigenic dolomitizing fluids most likely created the clay-grain-size particles and cement in the Sanish member.

Thin section analyses indicate that at least two episodes of dolomitization occurred (Appendix's D.5; D.7; D.9). Early (shallow burial) dolomitization is characterized by very fine-crystalline rhombohedra. Late (deeper burial) dolomitization produced larger crystals (fine to medium-crystalline). This type of dolomitization could be related to recrystallization. Also, coarser-crystalline dolomite commonly occurred at or near microfractures.

4.9.7 **Pyrite**

Pyrite, FeS_2 , is common within all lithofacies. It occurs as a replacive mineral and probably formed during shallow burial as free iron from the weathering of biotite and other iron bearing minerals combined with sulfur in strongly reducing environments. The strongly reducing conditions (abundant hydrogen sulfide) associated with the preservation of organic material in the Lower Bakken Shale probably contributed to the precipitation of pyrite in the Lower Bakken Shale and the underlying Upper Three Forks.

4.10 **Provenance**

The Upper Three Forks, Sanish, and Lower Bakken Shale contain detritus from a plutonic and-or metamorphic provenance. Potassium feldspar grains, muscovite, and biotite are minerals associated with these types of rocks. The angularity of grains and the near absence of potassium feldspar corrosion and abrasion indicate that the source area was relatively close. The North American Shield (craton) was northeast of the Williston Basin, and erosion of this area supplied detritus.

Subrounded to rounded dolomite grains in Sanish tidal flat environments probably came from older Paleozoic rocks that may have been exposed along the edges of the ancient Williston Basin. Travel distance is inferred to be short.

CHAPTER 5

SIGNIFICANT SURFACES AND SEQUENCE STRATIGRAPHY OF THE UPPER THREE FORKS FORMATION (SANISH MEMBER)

5.1 **Methods**

The methods used to define significant surfaces and evaluate the sequence stratigraphy of the Upper Three Forks and Sanish member were modeled after Walker et al. (1992). Significant stratigraphic surfaces were defined using detailed lithofacies descriptions. Inferred depositional environments were then assigned to lithofacies and their significant surfaces. Finally, depositional environments were placed into an overall depositional system and evaluated using sequence stratigraphy. The placement of the Sanish member within the Upper Three Forks-Lower Bakken sequence stratigraphic system was determined.

5.2 **Previous Sequence Stratigraphic Interpretation**

Smith et al. (1995) detailed the sequence stratigraphy of the Bakken and Exshaw Formation in Canada and the United States. In his work, he divided the Bakken-Exshaw Formation into three major stratigraphic sequences: the Lower and Upper Bakken Shales are a transgressive systems tracts, and the Middle Bakken is both a low-stand systems tract and also part of the Upper Bakken Shale transgressive systems tract. Each member of the Bakken Formation is separated by a sequence boundary (Figure 5.1). Smith's interpretation suggests that the Williston Basin experienced major eustatic or tectonic changes during Upper Three Forks and Bakken deposition.

Of importance to this investigation is the sequence boundary at the base of the Lower Bakken Shale. Erosion of the top of the Sanish member was observed in every core in this investigation, and the wireline cross section (Figure 5.11) shows this beveling at the top of the Sanish. Sea-level rise buried the unconformity as deposition and onlap of the Lower Bakken Shale occurred.

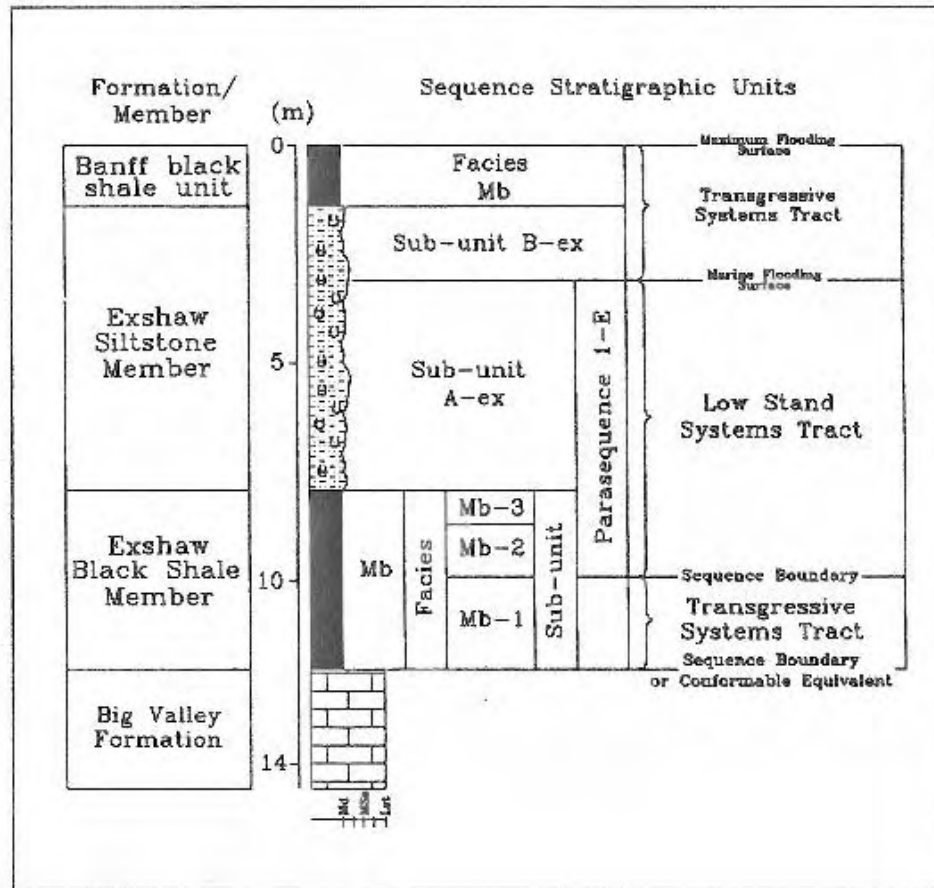


Figure 5.1. Sequence stratigraphic interpretation of the Bakken and Exshaw Formations with associated significant surfaces and interpreted facies in Canada and the United States. From Smith et al. (1995).

5.3 Significant Stratigraphic Surfaces

Significant stratigraphic surfaces include: unconformities, marine flooding surfaces, and bounding discontinuities (Walker et al. 1992; Van Wagoner et al. 1990). By identifying significant surfaces within the Upper Three Forks Formation, placement of the Sanish member can then be determined within the overall depositional system.

It was found that the Sanish member contains three significant surfaces. The first significant surface identified was the *bounding discontinuity* at the base of the Sanish member. This *bounding discontinuity* was correlated Basin-wide in the United States portion of the Williston Basin using nearly 10,000 wireline logs. The authors correlation tops along with IHS[®] tops were used to interpret a paleo-bathymetric shift (discussed below). Within the study area, the base of the Sanish member is Facies C. In the westernmost portion of the study area, the base of the Sanish is Facies A because of facies change or stratigraphic convergence (core #2 Figure 5.3).

The second significant surface identified throughout the study area was at the top of Facies C. This surface was interpreted to be a *flooding surface* that was also correlated Basin-wide in the United States portion of the Basin using nearly 10,000 wireline logs and IHS[®] tops. This flooding surface separates Facies C (tidal mud flat-sabkha) from overlying Facies D (intertidal – sabkha-supratidal).

In addition, a major significant surface (sequence boundary) separates the top of Facies D and Facies E (where present) from Facies LBS (Lower Bakken Shale). This surface is a *marine flooding surface* and a *transgressive surface of erosion*, and this surface was also correlated throughout the United States portion of the Williston Basin using wireline logs.

Bakken Formation	Lower Bakken Shale	<i>Facies LBS</i>		Transgressive Systems Tract
?	Sanish member	<i>Facies D</i>	Sequence Boundary Marine Flooding Surface	?
		<i>Facies C</i>	Flooding Surface	?
Three Forks Formation		<i>Facies B</i>	Bounding Discontinuity Paleobathymetric Shift	

Figure 5.2. Significant surfaces and associated facies of the Upper Three Forks, Sanish member, and Lower Bakken Shale for 15 of the 16 cores.

Bakken Formation	Lower Bakken Shale	<i>Facies LBS</i>		Transgressive Systems Tract
?	Sanish member	<i>Facies D</i>	Sequence Boundary Marine Flooding Surface	?
Three Forks Formation		<i>Facies A</i>	Bounding Discontinuity Paleobathymetric Shift	

Figure 5.3. Significant surfaces and associated facies of the of the Upper Three Forks, Sanish member, and Lower Bakken Shale for core # 2 only.

5.4 Depositional Systems

This study investigated Late Devonian and Early Mississippian depositional systems in the Williston Basin: 1) Upper Three Forks Formation; 2) Sanish member of the Upper Three Forks Formation; and 3) Lower Bakken Shale. The Three Forks Formation depositional system consist of Facies A, a shallow marine deposit with reworked tidal flat clasts, or Facies B, a coastal plain deposit (only present in core #2). The Sanish member includes Facies C, D, and E. Facies C and D are Late Devonian tidal flat deposits that range from shallow inter-tidal to tidal mud flat-sabkha. Facies E is a transitional unit that was deposited in shallow subtidal environments. The Lower Bakken Shale, Facies LBS, is an organic-rich, open-marine deposit that unconformably overlies the Sanish member.

5.5 Sequence Stratigraphy of the Sanish Member and Associated Facies

To understand the sequence stratigraphy of the Sanish member and its associated facies, the overall Late Devonian and Early Mississippian system was analyzed. Figures 2.5 and 2.6 show paleo-reconstructions of the lower Kaskaskia (entire Devonian), including the Three Forks Formation. During the Devonian, the Williston Basin was connected to the northwest with the Alberta Basin (Smith et al. 1995). Figures 2.7 and 2.8 show the paleo-reconstructions of the upper Kaskaskia (Mississippian), indicating the separation of the intracratonic sag of the Williston Basin from the Alberta Foreland Basin.

A series of isopach maps were constructed to investigate the development of the United States portion of the Williston Basin during the Devonian (lower Kaskaskia and upper Kaskaskia). Figure 5.4 is an isopach of the lower Kaskaskia (Ashern through the Niksu formations). This isopach map illustrates continuous connection of the Williston Basin to the Alberta Basin during the Devonian. During most of the Devonian, the Basin center was in Burke and Mountrail counties, North Dakota.

Figure 5.5 is an isopach map of the Three Forks Formation that shows a shift in the Basin axis to the southwest. Thinning near the United States and Canadian borders indicates initial separation of the Alberta Basin from the Williston Basin, and the effects of truncation at the top of the Three Forks Formation.

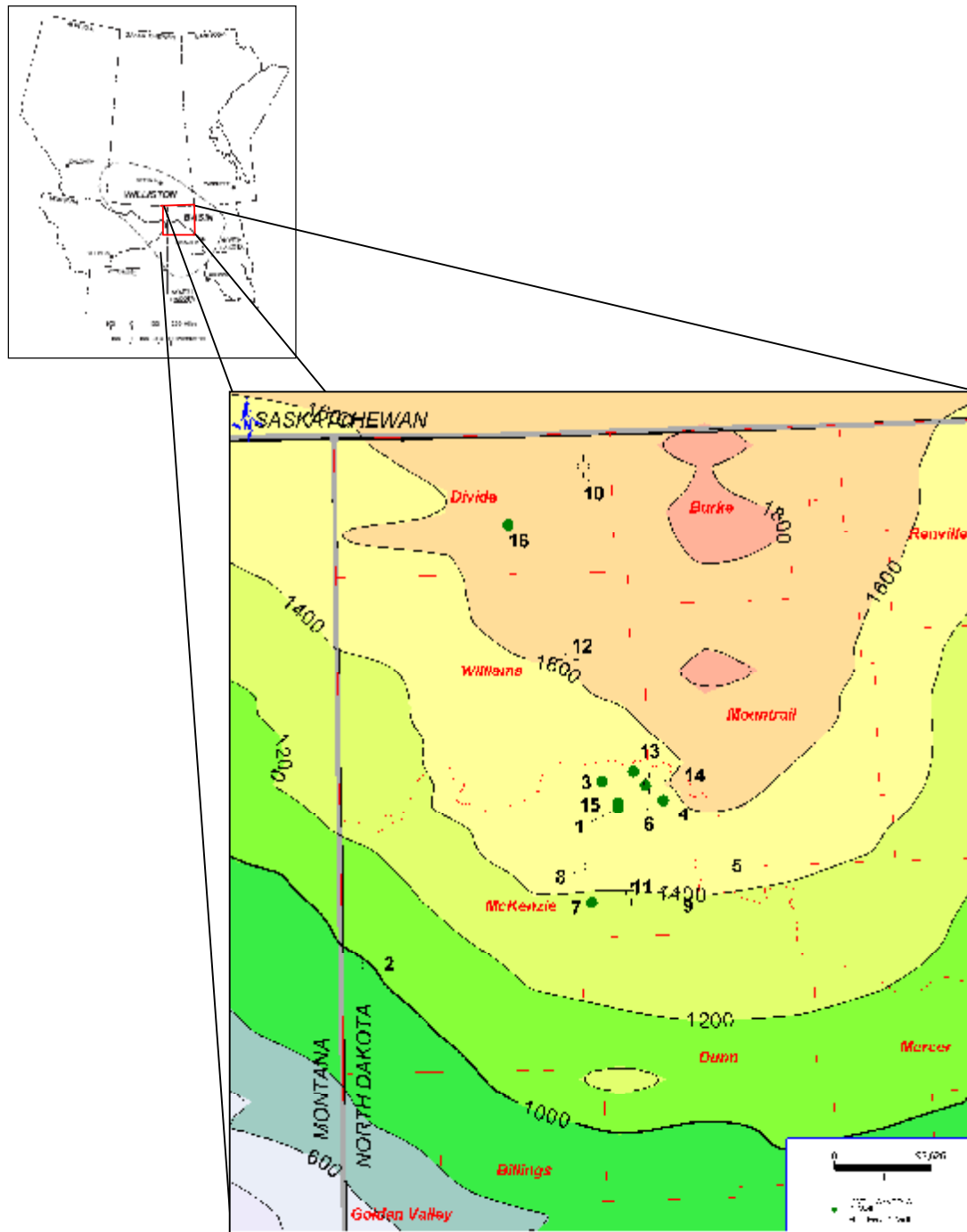


Figure 5.4. Isopach map of the Devonian Ashern through Nisku formations (lower Kaskaskia) prior to Three Forks Formation deposition, U. S. Williston Basin. This isopach map shows the continuous thickening to the north into Saskatchewan, Canada. Well spots indicate study cores and assigned numbers. Contour interval is 200 feet.

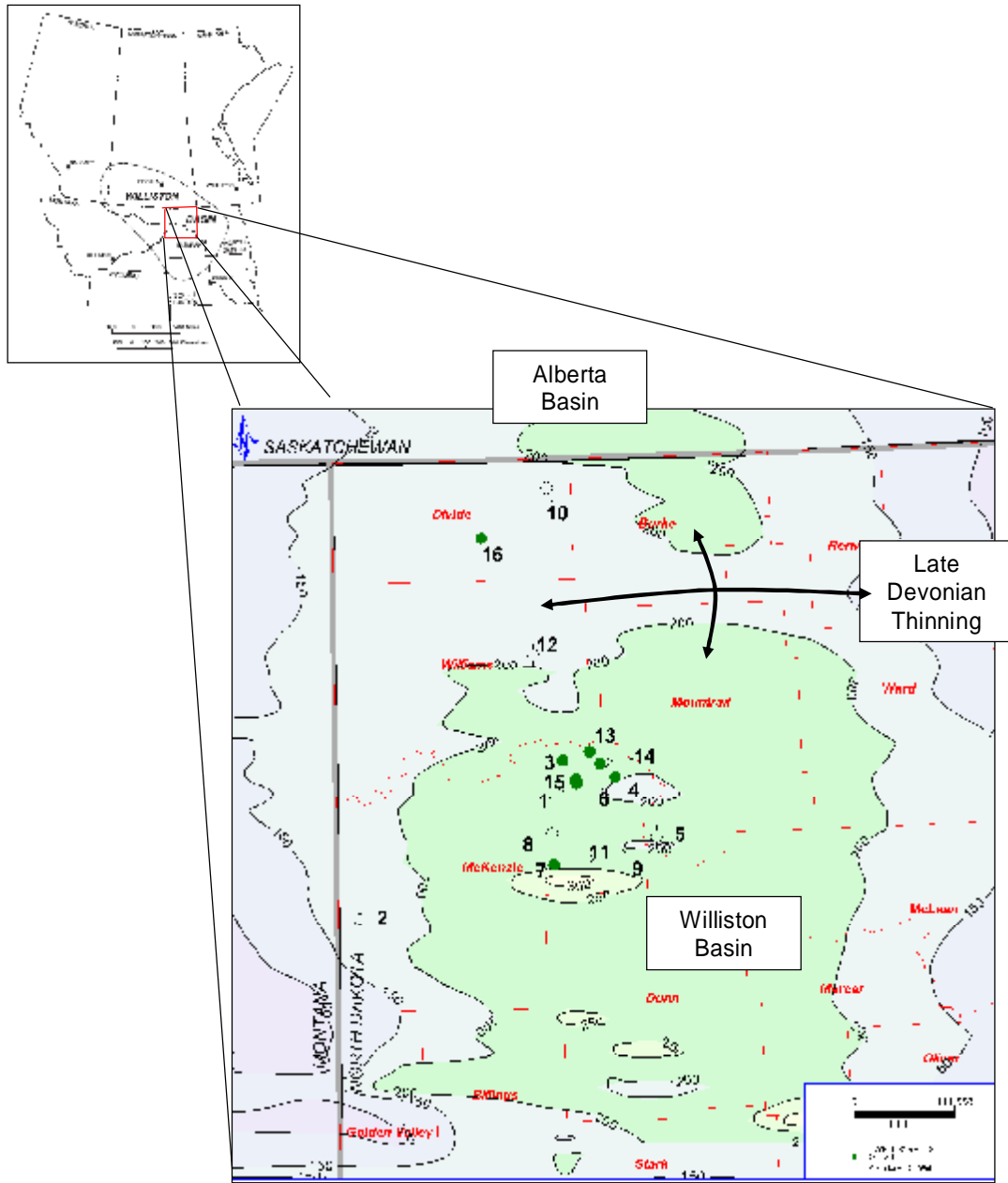


Figure 5.5. Isopach map of the Three Forks Formation (including the Sanish member). The Basin center shifted from Burke and Mountrail counties, ND, to McKenzie County, ND. Late Devonian thinning between Burke and Mountrail counties, which were previously within the Basin center, indicates early separation of the Alberta Basin from the Williston Basin. Well spots are study cores and assigned numbers. Contour interval is 50 feet.

Figure 5.6 displays three Devonian and Early Mississippian Basin center maps: 1) Devonian Ashern through the Nisku; 2) Late Devonian Three Forks Formation; and 3) Late Devonian and Early Mississippian Bakken Formation. The Basin center reconstruction map shows depositional shifts that occurred from the Devonian into the Early Mississippian in western North Dakota. The Basin axis shift from north to south from Devonian to Early Mississippian time coincides with the initiation of the Montana Trough. Variations in depositional environments in the Upper Three Forks (Sanish) are related to this depositional change.

The isopach thin in the northern part of the study area in the Three Forks Formation persisted during deposition of the Lower Bakken Shale. (Figure 5.7). The Lower Bakken Shale thins across this Three Forks trend.

In the study area, a major bathymetric shift occurred at the base of the Sanish member resulting in the deposition of Facies C. Facies C is a saline, tidal mud flat-sabkha deposit found throughout most of the study area. This facies represent a major drop in sea level, that resulted in widespread progradation and exposure.

Facies D is part of a deepening or transgression. These intertidal tidal-flat-sabkha deposits were found to be thickest at Basin center and thinnest at the western and northern edges of the study area (isopach map of facies D, Figure 5.8).

The contact between Facies D and Facies E (both at the top Sanish member) and Facies LBS (Lower Bakken Shale) is a sequence boundary (TSE). A significant stratigraphic change from tidal flat deposits of Facies D and shallow subtidal deposits of Facies E to open-marine deposits of Facies LBS occurred at this contact. Two models are proposed for the formation of the sequence boundary at the top of the Sanish (base of the Lower Bakken Shale). 1) Erosion at the top of the Sanish member occurred because of widespread and prolonged exposure of the Sanish member. These erosional surfaces were subsequently reworked by flooding associated with Lower Bakken Shale deposition. 2) Erosion occurred by transgression of the Lower Bakken depositional system, and lag deposits and rip-up clasts (Figure 5.9) observed throughout the study area indicate ravinement.

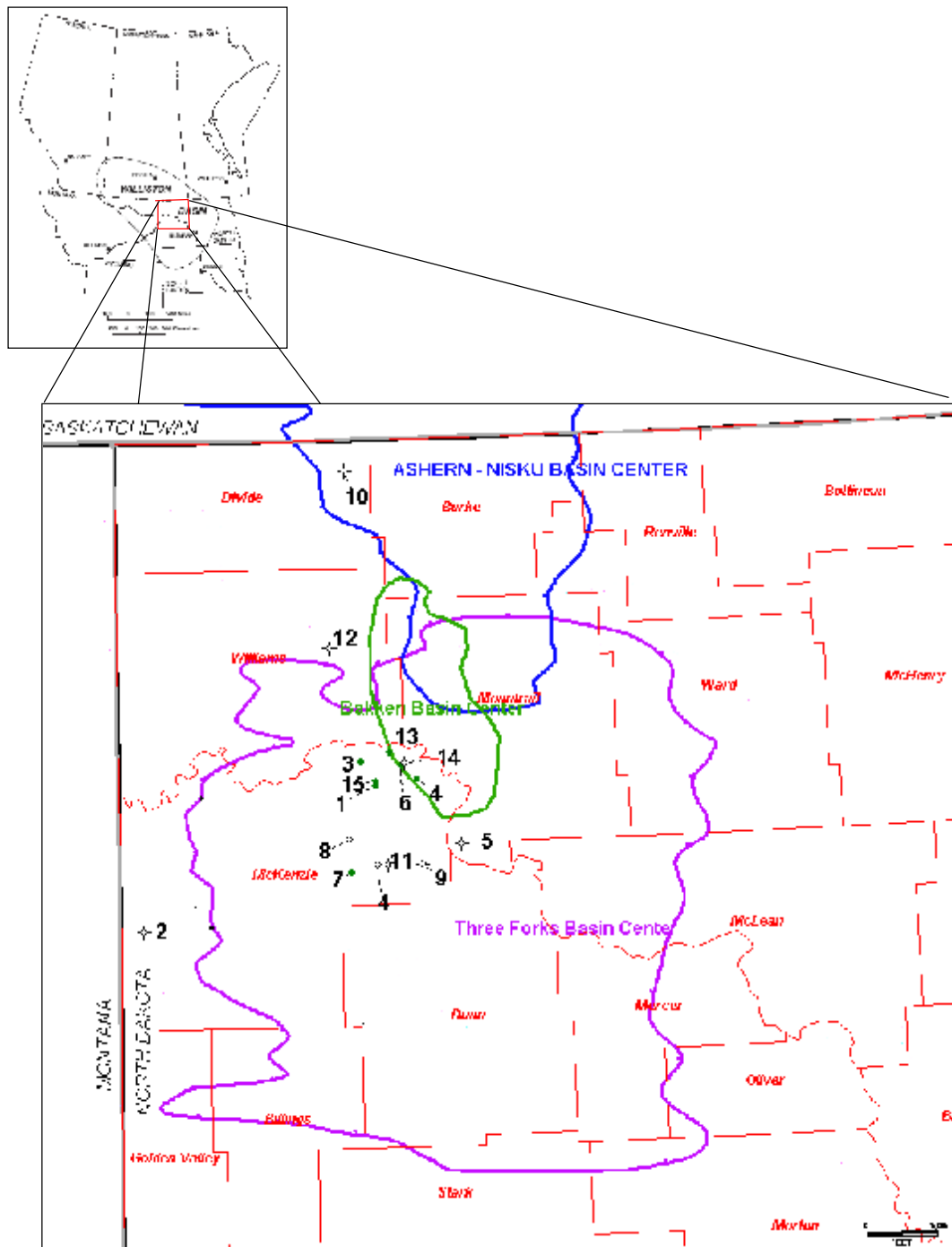


Figure 5.6. Shifting depositional centers during the Devonian and Early Mississippian are shown in this map. The shift occurred from north to south across western North Dakota. The blue outline is the Devonian Basin center (Ashern through Nisku formations). The purple outline is the Late Devonian Three Forks Basin center, and the green outline is the Late Devonian and Early Mississippian Bakken Formation Basin center.

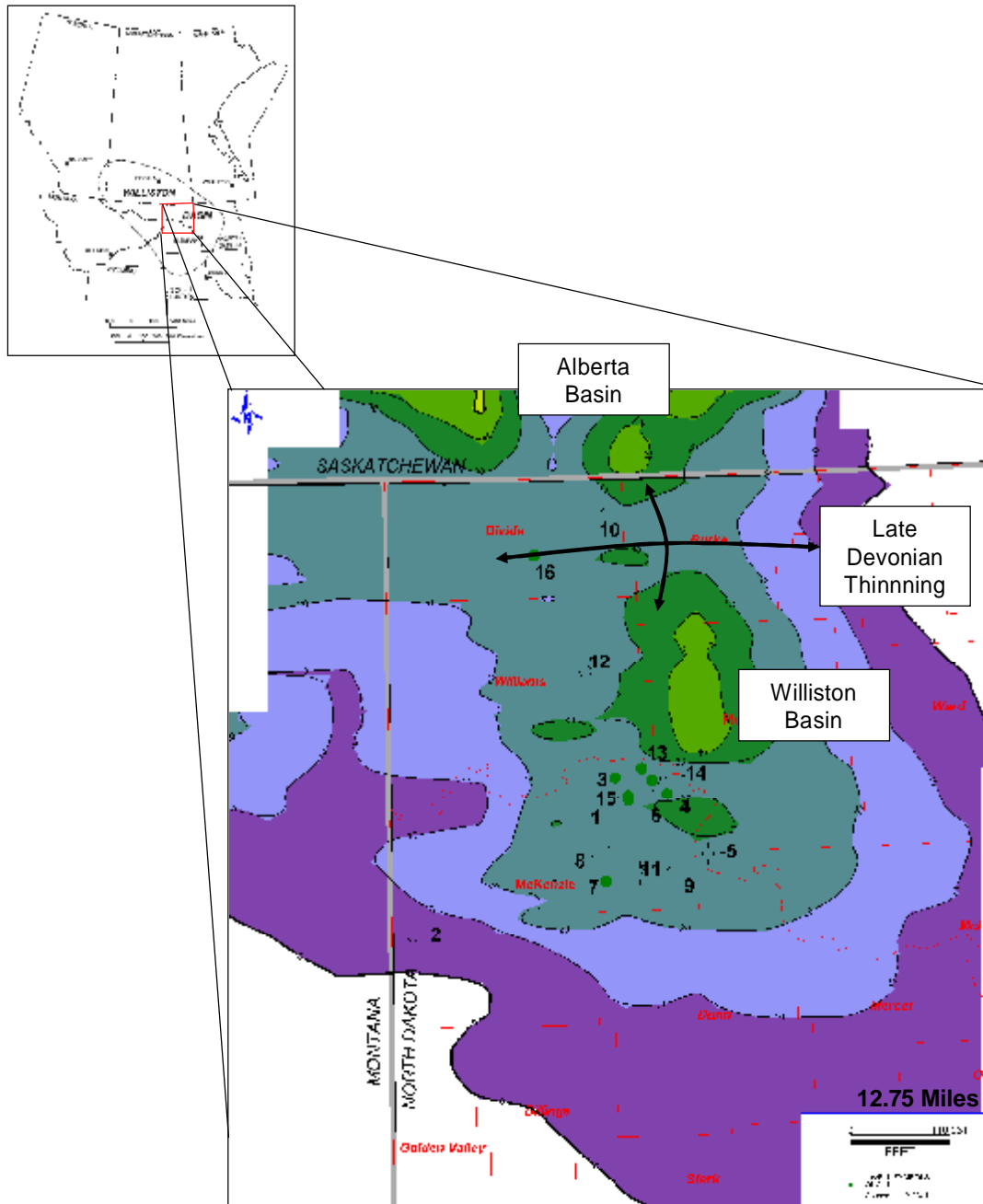


Figure 5.7. Isopach map of the Lower Bakken Shale. Thinning near the United States and Canadian borders that was present during Three Forks deposition continued during Lower Bakken Shale deposition. C.I.= 10 feet.

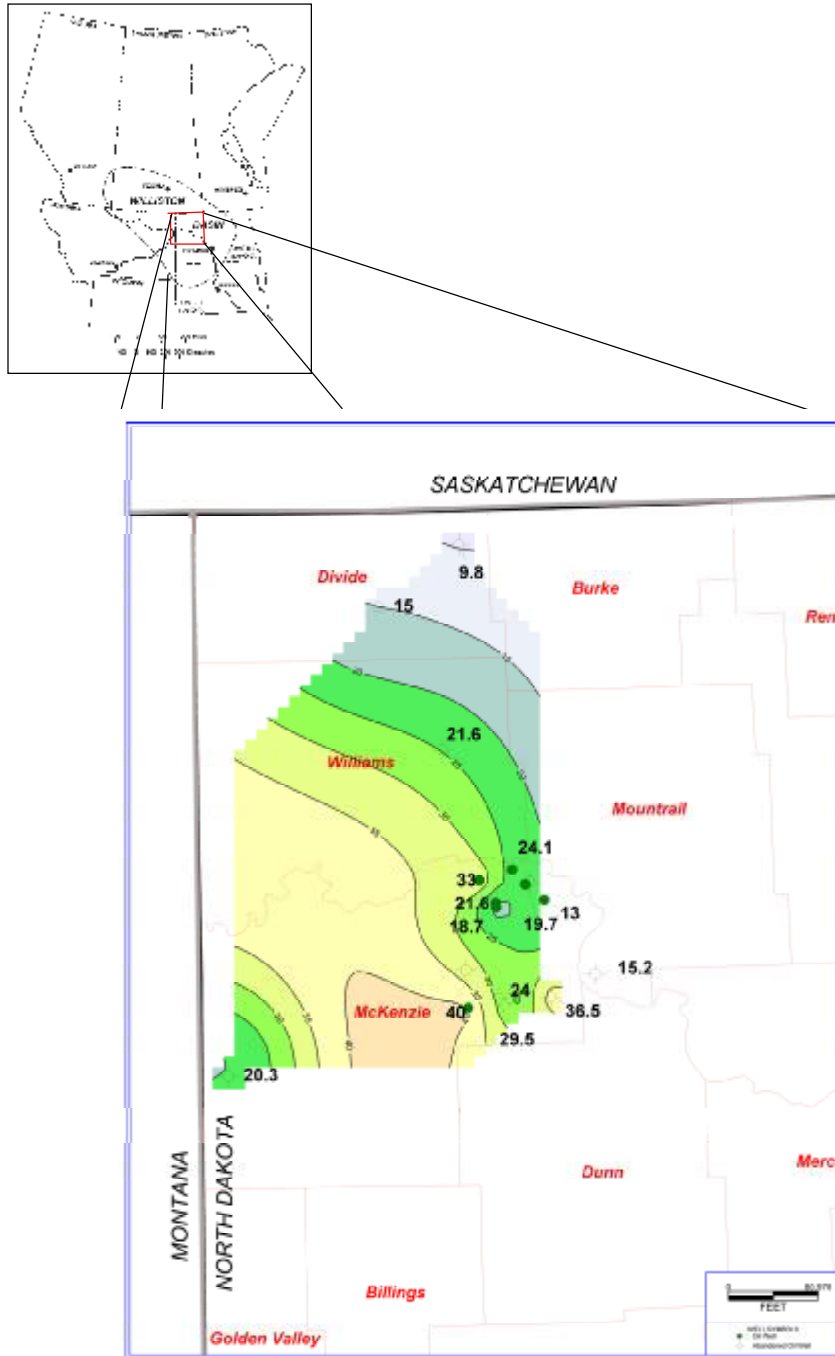


Figure 5.8. Isopach map of Facies D. Thickness values are from cores interpretations which indicate thinning to the north. The northward thinning is associated with the unconformity at the top of the Sanish member. Contour interval is 5 feet. Note cores 2, 4, 5, 6, 7, 8, 11, 12 and 15 did not penetrate Facies D entirely are not used in the creation of the isopach.

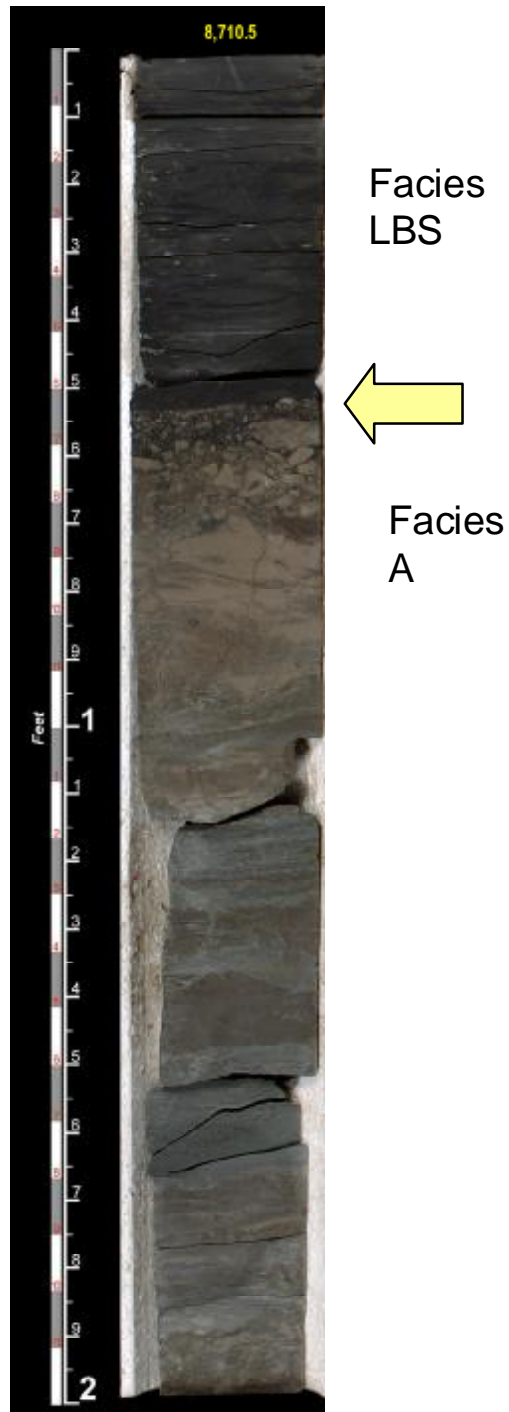


Figure 5.9. Core #17 - 8710.5 – 8,711.5. The contact (yellow arrow) between Facies D (top of Sanish member) and facies LBS (Lower Bakken Shale) is shown. Rip-up clasts and lag deposits occur at the contact, and the contact is interpreted to be an unconformity and a marine flooding surface.

This thesis confirms transgression at the Lower Bakken contact and the formation of a sequence boundary. Evidence for extended subaerial exposure before the transgression was not identified in cores. Reworking associated with transgression may have obscured any evidence of prolonged exposure and erosion. Detailed wireline correlations and cross section A-A' (Figures 5.10 and 5.11) show truncation at the top of the Sanish. This truncation is interpreted to be an angular unconformity. An isopach map of Facies D shows wedge-shaped thinning to the north associated with the unconformity.

5.6 Stratigraphic Placement of the Sanish Member

The Sanish member is a part of the Late Devonian Three Forks Formation and is a separate systems tract from the Late Devonian and Early Mississippian Lower Bakken Formation. Segregating the top of the Three Forks into a separate member, the Sanish member, is useful in modeling and depicting stratigraphic changes associated with the sequence boundary at the top of the Three Forks Formation (Figures 5.13; 5.14; 5.15).

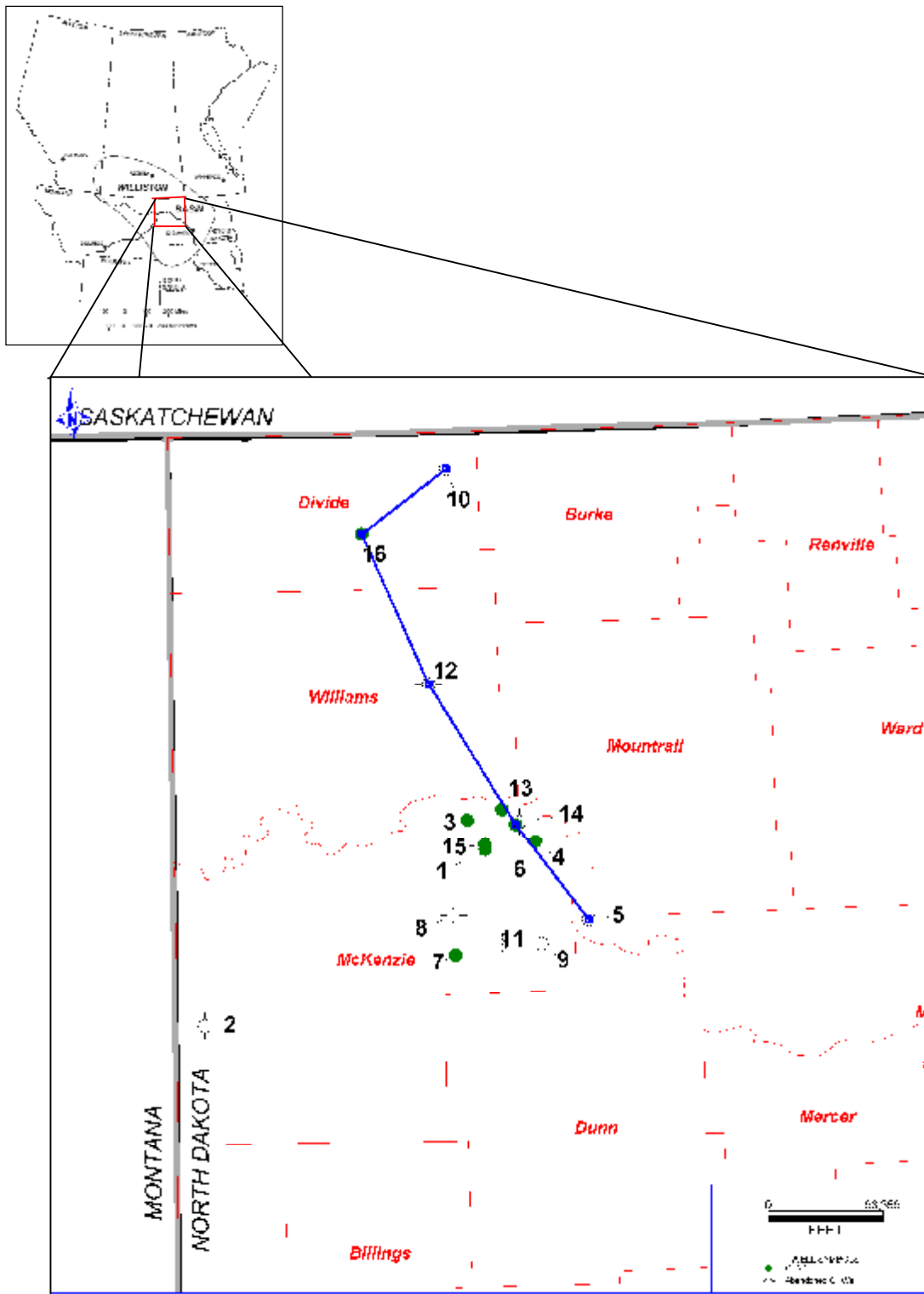


Figure 5.10. Location map of cross-section A-A'. Cores used in this study are identified by numbers.

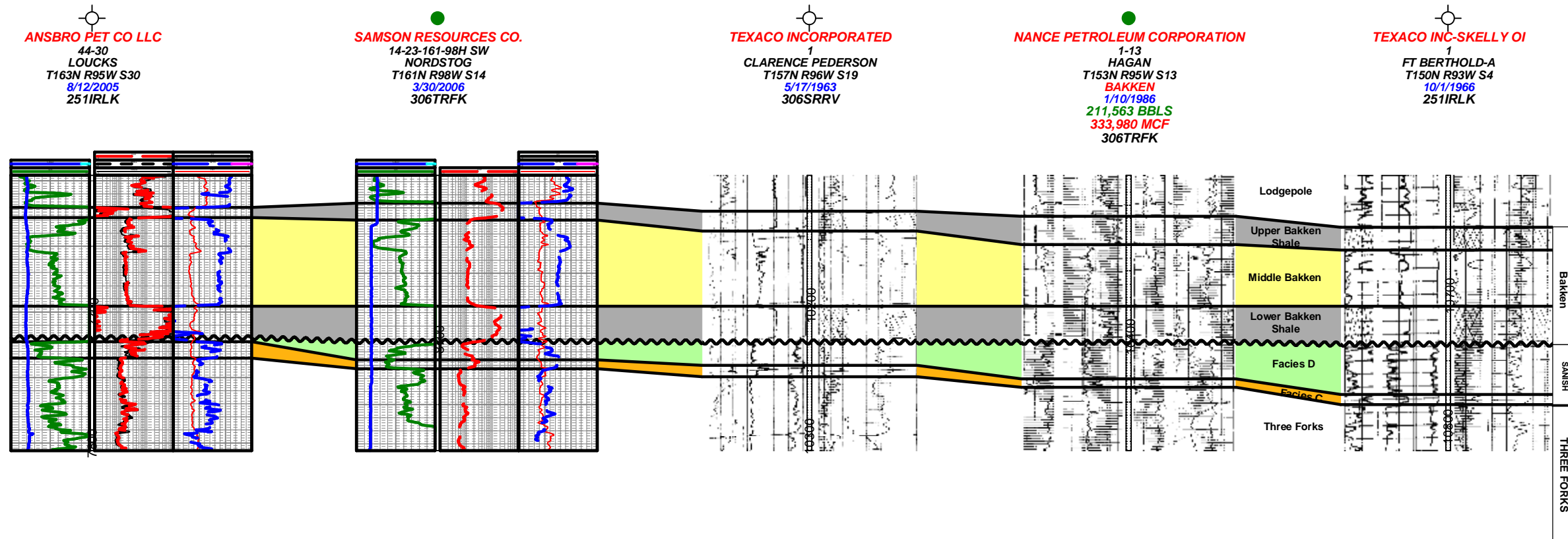


Figure 5.11. Cross section A-A' showing the erosional unconformity that exists at the top of Facies D and possibly Facies C. This unconformity occurs across the study area. The thickness of Facies D increases toward present day basin-center and is truncated along the basin-edges. Location map for the cross-section is figure 5.11. Note the Three Forks Formation includes both Facies A and B. The Lower Bakken Shale is Facies LBS.

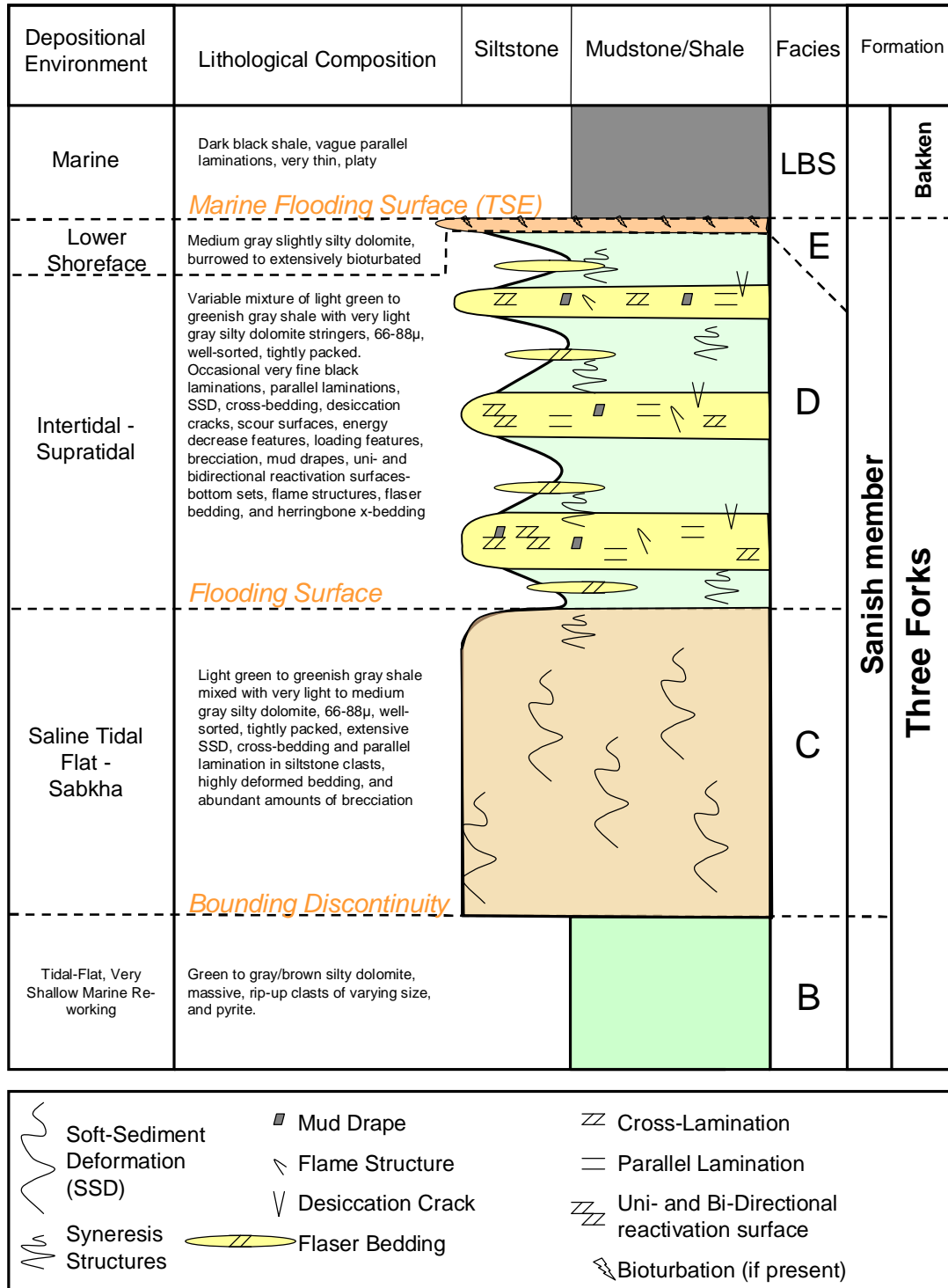


Figure 5.12. General stratigraphic column for the individual facies derived from 15 of the 16 core descriptions within the study area. This stratigraphic column includes depositional environment and significant surface interpretations. Thickness of each facies varies throughout the study area.

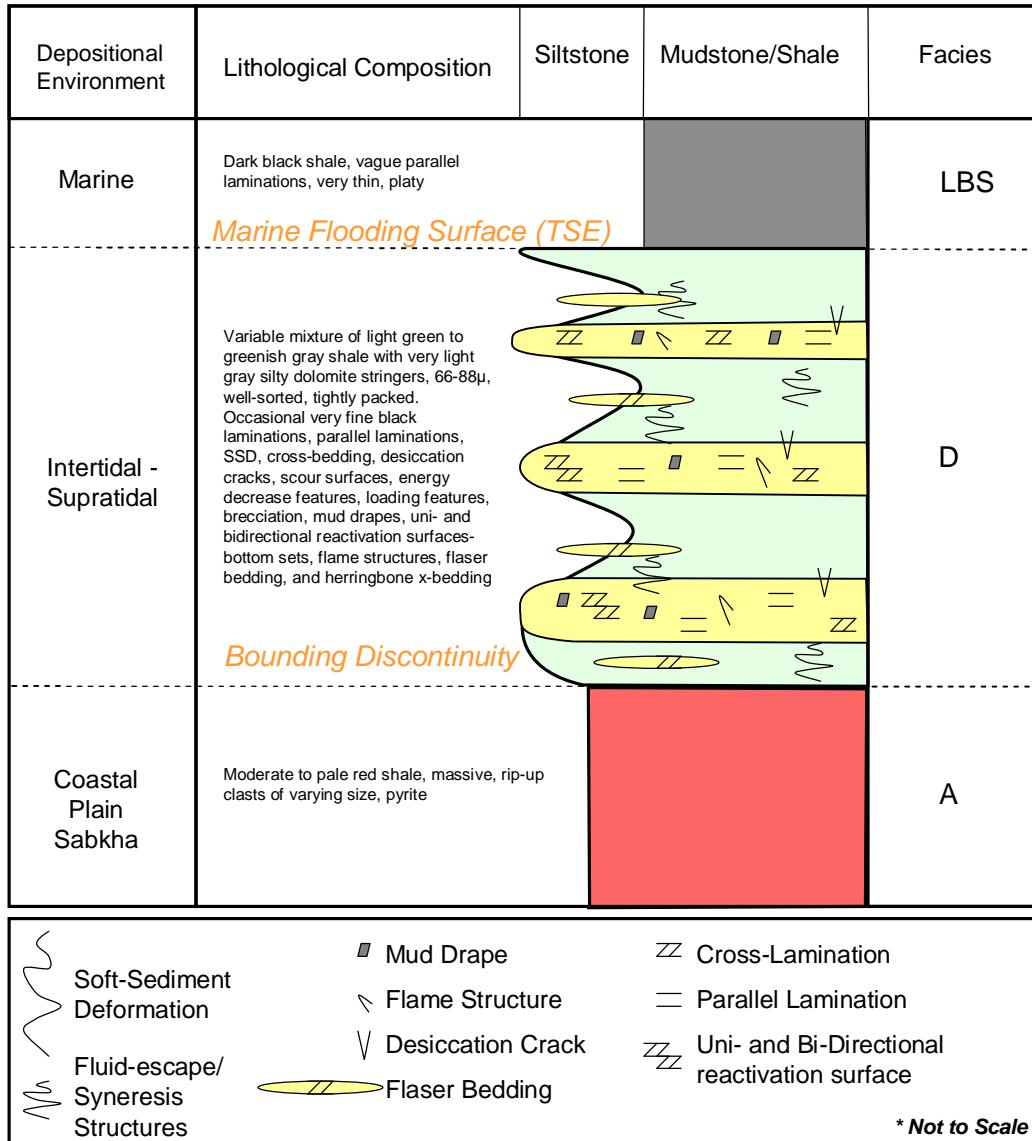


Figure 5.13. The stratigraphic column of facies observed in core #2; includes the depositional environment and significant surfaces.

Three Forks Formation	Bakken Formation	Lower Bakken Shale	<i>Facies LBS</i>		Transgressive Systems Tract
	Sanish member		<i>Angular Unconformity</i>	Sequence Boundary Marine Flooding Surface	<i>Angular Unconformity</i>
			<i>Facies D</i>		Transgressive Depositional Systems
			<i>Facies C</i>	Flooding Surface	
		<i>Facies B</i>	Bounding Discontinuity Paleobathymetric Shift		

Figure 5.14. Sequence stratigraphic placement of the Sanish member with associated facies and significant surfaces.

Bakken Formation	Lower Bakken Shale	<i>Facies LBS</i>		Transgressive Systems Tract	
	Three Forks Formation	Sanish member	<i>Angular Unconformity</i>	Sequence Boundary Marine Flooding Surface	<i>Angular Unconformity</i>
			<i>Facies D</i>		Transgressive Depositional Systems
		<i>Facies A</i>	Bounding Discontinuity Paleobathymetric Shift		

Figure 5.15. Sequence stratigraphic placement of the Sanish member with associated facies and significant surfaces within core #2.

CHAPTER 6

CONCLUSIONS AND RECOMMENDATIONS

The main purpose and scope of this thesis was to do a reconnaissance interpretation of depositional environments, mineralogy, and sequence stratigraphy of the Sanish member of the Upper Three Forks Formation.

6.1 Conclusions

The following are study conclusions:

6.1.1 Core Lithofacies

- Two lithofacies are present in the Upper Three Forks and these directly underlie the Sanish member. Facies A: pale red, dolomitic shale with common shale clasts and discontinuous lenses of very fine to fine-crystalline dolomite; and Facies B: gray, calcareous (limey) dolomite. Both Facies A and B are recognized on wireline logs and are widespread in the study area.
- Facies A and B contain rip-up clasts that are larger in size in the northern portion of the study area.
- Three lithofacies were identified from core descriptions of the Sanish member: 1) Facies C: highly deformed and brecciated, silty dolomite and gray-green shale; 2) Facies D: silty dolomite and shale; and 3) Facies E: slightly silty dolomite that is burrowed to extensively bioturbated.
- Facies C and Facies D exhibit cross-laminations, parallel-laminations, uni-directional reactivation surfaces, soft-sediment deformation, scour surfaces and loading features.
- Locally, Facies C and D are petroleum reservoirs.

- The base of the Bakken Formation contains an organic-rich black shale member named the Lower Bakken Shale (LBS). This shale is widespread in the study area.
- Facies D was present in every core, Facies E in one core, and Facies A, B, and C were present only if the operator cored far enough into the Upper Three Forks. Facies C was not present in core # 2.
- A general stratigraphic column illustrates facies similarities in cores throughout the study area. A second stratigraphic column was constructed for core # 2 because Facies C is absent in this core and Facies D rests on Facies A.

6.1.2 Mineralogy

- The minerals identified in each lithofacies using four x-ray diffraction methods (XRD) include: illite, potassium-feldspar, dolomite, quartz, chlorite, pyrite, calcite, muscovite, biotite and possibly kaolinite.
- Detrital and authigenic minerals were identified with scanning electron microscopy and energy dispersive spectroscopy (SEM-EDS). Detrital grains include: potassium feldspar, dolomite, quartz, illite, calcite, muscovite and biotite. Authigenic grains include: potassium feldspar, dolomite, chlorite, quartz, biotite and pyrite.
- The clay-sized fractions identified with XRD, SEM-EDS and thin-section analyses include: potassium feldspar, dolomite, illite and chlorite.
- Smectite-illitization is interpreted to be responsible for the formation of authigenic minerals such as illite, dolomite, quartz, and chlorite.
- Detritus in the Upper Three Forks Formation was eroded and transported from the North American Craton that was northeast of the study area. Carbonate grains were derived from Paleozoic rocks that were exposed northeast of the study area.

- Dolomite is both syndepositional and diagenetic.
- Abundant microfractures were observed in each lithofacies utilizing both a binocular microscope and a petrographic microscope.
- Differing sizes of dolomite crystals along microfractures indicate potential recrystallization or burial dolomitization.

6.1.3 Depositional Environments

- Primary and secondary sedimentary structures were used to identify depositional facies. These sedimentary structures include: desiccation features, mud drapes, bi-directional reactivation surfaces, bottom sets, flame structures, flaser bedding, and herringbone cross-bedding.
- Using lithology and sedimentary structures, depositional environments were inferred. Facies A – sabkha; Facies B – highly restricted subtidal to tidal flat; Facies C – tidal flat and sabkha; Facies D – tidal flat and supratidal; Facies E – restricted subtidal; Facies LBS – open marine anoxic basin.

6.1.4 Sequence Stratigraphy

- The Upper Three Forks beds that directly underlie the Lower Bakken Shale have been informally named in literature as the Sanish member. This terminology was applied throughout this study in both core descriptions and wireline correlations.
- During the Late Devonian and Early Mississippian, thinning occurred near the United States-Canadian border in present-day Divide and Burke counties, ND. This thinning may indicate initial separation of the Williston Basin from the Alberta Basin.

- Significant surfaces were identified in cores. These include: an unconformity at the top of the Sanish member (base of the Lower Bakken Shale), a marine flooding surface at the same stratigraphic position, flooding surfaces at the base of Facies D, and a bounding discontinuity at the base of Facies C.
- A cross-section was constructed using wireline logs from described cores to show an angular unconformity that occurs at the top of Sanish (base of the Lower Bakken Shale).
- Exposure and erosion of the Upper Three Forks (Sanish) occurred either before transgression of the Lower Bakken or by ravinement associated with the transgression.
- Prolonged subaerial exposure and erosion of Facies D and Facies E were not identified in cores.
- Sequence stratigraphy shows the top of the Sanish member to be genetically related to deepening of the upper Three Forks depositional system. Truncation at the top of the Sanish is a sequence boundary, and placement of the Sanish in the Upper Three Forks is confirmed.

6.2 Recommendations for Further Study

The following are recommendations for further study:

- Additional cores need to be described in other parts of the Williston Basin to better understand the regional distribution of facies in the Upper Three Forks Formation.
- Additional core description and mapping should show the degree and extent of the unconformity at the top of the Sanish member.

- Additional work on mineralogy and diagenesis is needed, especially in understanding the timing of dolomitization and smectite-illitization.

REFERENCES CITED

- <http://en.wikipedia.org/wiki/Image:WillistonStratCol.jpg> Last accessed January 31, 2008).
- <http://jan.ucc.nau.edu/rcb7/namD360.jpg>. (Last accessed on January 2nd, 2008)
- <http://jan.ucc.nau.edu/rcb7/namM345.jpg>. (Last accessed on January 2nd, 2008)
- <https://www.dmr.nd.gov/oilgas/>. (Last accessed on February 12^d, 2008)
- Bally, A.W., 1989, Phanerozoic basins of North America. Chapter 15: *in* The Geology of North America – An Overview. The Geological Society of America. Pp. 397 – 446.
- Burrus, J., K. Osadetz, S. Wolf., B. Doligez., K. Visser., and O. Dearborn, 1996, A two-dimensional regional model of the Williston Basin hydrocarbon systems: American Association of Petroleum Geologists Bulletin, v. 80, p. 265-291.
- Collinson, J.D., 1969, The Sedimentology of the Grindslow Shales and the Kinderscout Grit: a Deltaic Complex in the Namurian of Northern England: Journal of Sedimentary Petrology, v. 39, p. 194 – 221.
- Compton, R.R., 1995, Geology in the Field: John Wiley and Sons, 398 p.
- Dow, W.G., 1974, Application of oil-correlation and source-rock data to exploration in Williston Basin: AAPG Bulletin, v.58, p. 1253-1262.
- Emery D., and K.J. Myers, 1996, Sequence Stratigraphy: Blackwell Science Ltd, 297 pp.
- Gerhard, L.C., D.W. Fischer, and S.B. Anderson, 1990, Petroleum Geology of the Williston Basin. Interior Cratonic Basins: AAPG Memoir 51; Chapter 29, p.507-559.
- Green, A.G., W. Weber, and Z. Hajnal, Z., 1985, Evolution of Proterozoic terrains beneath the Williston Basin: Geology, v. 13, p. 624-628.
- Goddard, E.N., P.D. Trask, R.K. De Ford, O.N. Rove, J.T. Singewald Jr., and R.M. Overbeck, 1970, Rock Color Chart: The Geological Society of America, Boulder, Colorado.
- Hunt, J.M., 1996, Petroleum Geochemistry and Geology, *in* J.M.Hunt eds., Petroleum Geochemistry and Geology: 2nd edition, 743 p.

- James, N.P. and A.C. Kendall, 1992, Introduction to Carbonate and Evaporite Facies, Chapter 14, *in* R.G. Walker ed., Facies Models: Geosciences Canada Reprint Series 1, 454 p.
- Jones, B. and A. Desrochers, 1992, Shallow Platform Carbonates, Chapter 15, *in* R.G. Walker ed., Facies Models: Geosciences Canada Reprint Series 1, 454 p.
- Kendall, A.C., 1992, Evaporites, Chapter 19, *in* R.G. Walker ed., Facies Models: Geosciences Canada Reprint Series 1, 454 p.
- Kerr Jr., S. D, 1988, Overview: Williston Basin Carbonate Reservoirs.: *in* Goolsby, S.M., and M.W. Longman, eds., Occurrence and Petrophysical Properties of Carbonate Reservoirs in the Rocky Mountain Region: RMAG Guidebook, p. 251-274.
- Meissner, F.F., 1978, Petroleum Geology of the Bakken Formation Williston Basin, North Dakota and Montana.: *in* D. Estelle and R. Miller, eds., The Economic Geology of the Williston Basin, 1978 Williston Basin Symposium: Billings, Montana, Montana Geological Society, p. 207-230.
- Moore, D.M and Reynolds, R.C. Jr, 1997, X-Ray Diffraction and the Identification and Analysis of Clay Minerals: 2nd Edition: p. 1 – 373.
- Murray, Jr. G.H., 1968, Quantitative Fracture Study – Sanish Pool, McKenzie County, North Dakota: AAPG Bulletin, v. 52, p. 57-65.
- Nio, S.D., and C.S. Yan, 1989, Recognition of Tidally-Influenced Facies and Environments: Second International Research Symposium on Clastic Tidal Deposits, International Geoservices, Short Course Series; 1.
- Pitman, J.K., L.C. Price and J.A. LeFever, 2001, Diagenesis and Fracture Development in the Bakken Formation, Williston Basin: Implications for Reservoir Quality in the Middle Member: U.S. Geological Survey Professional Paper 1653, U.S. Department of the Interior and U.S. Geological Survey, 19 p.
- Pratt, B.R., and N.P. James, 1992, Peritidal Carbonates Chapter 16, *in* R.G. Walker ed., Facies Models: Geosciences Canada Reprint Series 1, 454 p.
- Prothero, D.R., and F. Schwab, 2001, An Introduction to Sedimentary and Rocks and Stratigraphy, Sedimentary Geology: W.H. Freeman and Company, Fourth Printing, 559 p.
- Scoffin, T.P., 1987, An Introduction to Carbonate Sediments and Rocks: Blackie, London, 274 p.

- Sloss, L.L., 1963, Sequences in the cratonic interior of North America: Geological Society America Bulletin, v. 74, p, 93 – 114.
- _____, 1988, Tectonic evolution of the craton in Phanerozoic time, *in* Sloss, L.L., ed., Sedimentary cover-North American craton, U.S: Boulder, Colorado, Geological Society of America, Geology of North America, v. D-2, p. 25-52.
- Smith, M.G., R.M. Bustin and M.L. Caplan., 1995, Sequence Stratigraphy of the Bakken and Exshaw Formations: A Continuum of Black Shale Formations in the Western Canadian Sedimentary Basin: *in* Hunter, L.D.V., and R.A. Schalla, eds., 1995 Guidebook: Seventh International Williston Basin Symposium.: Montana Geological Society, p. 399 – 409.
- Smith, M.G., and Bustin, R.M., 1995, Sedimentology of the Late Devonian and Early Mississippian Bakken Formation, Williston Basin, *in* Vern Hunter, L.D., and Schalla, R.A., eds., Seventh International Williston Basin Symposium 1995 Guidebook: Montana Geological Society, North Dakota Geological Society, and Saskatchewan Geological Society, p. 103-114.
- Smith, M.G., and Bustin, R.M., 2000, Late Devonian and Early Mississippian Bakken and Exshaw Black Shale Source Rocks, Western Canada Sedimentary Basin: A Sequence Stratigraphic Interpretation: AAPG Bulletin, v.84, No. 7 (July (2000) p. 940 -960.
- Soster, F.M., 1998, Mudcracks: Department of Geology and Geography, Depauw University. <http://www.depauw.edu/acad/geosciences/fsoster/Mudcracks.htm>. (Last accessed January 2008)
- Tucker, M.E. and .P. Wright, 1992, Carbonate Sedimentology: Blackwell Scientific Publications, Oxford, 496 p.
- Van Wagoner, J.C., Mitchum, R.M., Campion, K.M., and V.D. Rahmanian, 1990, Siliciclastic Sequence Stratigraphy in Well Logs, Cores and Outcrops: American Association of Petroleum Geologist, Methods in Exploration Series, No. 7, 55 p.
- Walker, R.G., 1992, Facies Models: Response to Sea Level Change: *in* Walker, R.G. and N.P. James, eds., Facies Models (2nd Edition), 2004 Seventh Printing, Geological Association of Canada, Geosciences Canada Reprint Series 1, 454 p.
- Webster, R.W., 1982, Analysis of petroleum source rocks of the Bakken Formation (Devonian and Mississippian) in North Dakota: Grand Forks, N. Dakota, University of North Dakota, M.S. thesis, 150 p.

Webster, R.W., 1984, Petroleum source rocks and Stratigraphy of the Bakken Formation in North Dakota, *in* Woodward, J., Meissner, F.F., and Clayton, J.L., eds., Hydrocarbon Source Rocks of the Greater Rocky Mountain Region: Rocky Mountain Association of Geologists, p. 57-81.